PERIDOTITE AND PYROXENITE XENOLITHS FROM THE MUSKOX KIMBERLITE, NORTHERN SLAVE CRATON, CANADA

by

David Edward Newton

BSc. The University of Massachusetts Amherst, 2007

A THESIS SUBMITTED IN PARTIAL FULFILLMENT OF THE REQUIREMENTS FOR THE DEGREE OF

MASTER OF SCIENCE

in

The Faculty of Graduate and Postdoctoral Studies

(Geological Sciences)

THE UNIVERSITY OF BRITISH COLUMBIA

(Vancouver)

August 2015

Abstract

Petrography, mineralogy and thermobarometry are reported for 53 mantle-derived xenoliths from the Muskox kimberlite pipe in the northern Slave craton. The xenolith suite includes 15% coarse spinel peridotite, 4% coarse spinel-garnet peridotite, 4% coarse garnet peridotite, 9% porphyroclastic peridotite, 60% websterite and 8% orthopyroxenite. Peridotites are composed primarily of forsteritic olivine (Fo 89-94), enstatite (En 89-94), Cr-diopside, Cr-pyrope garnet and chromite spinel. Pyroxenites are composed primarily of enstatite (En 90-92), Cr-diopside and Cr-pyrope garnet. Thermobarometric estimates were made using two-pyroxene, garnet-clinopyroxene and Ca-in-orthopyroxene thermometers and garnet-orthopyroxene barometer. Results suggest that coarse peridotites equilibrated at 650-1220 °C and 23-63 kbar; porphyroclastic peridotites equilibrated at 1200-1350 °C and 57-70 kbar; pyroxenites equilibrated at 1030-1230 °C and 50-63 kbar. Muskox xenoliths are compared with xenoliths recovered from the neighboring Jericho kimberlite, erupted 15 km away from and at the same time as Muskox. Contrasts in the characteristics of these two suites of mantle samples include: 1) higher levels of depletion throughout the Muskox mantle column based on the contents of MgO in olivine and orthopyroxene and Cr_2O_3 in garnet; 2) the presence of a shallow zone of metasomatism in the spinel stability field in the Muskox mantle; 3) a higher proportion of pyroxenitic versus peridotitic rock types at the base of the mantle column beneath the Muskox kimberlite and higher Cr_2O_3 in all minerals in pyroxenites; and 4) lower levels of deformation in the Muskox mantle. We interpret these contrasts as representing small scale heterogeneities in the bulk composition of the mantle, as well as the local effects of kimberlite formation and ascent. If percolation of asthenosphere-derived pre-kimberlitic fluids in the less permeable

Muskox mantle was impeded, localization of this fluid may have resulted in higher proportions of pyroxenitic rock types here, as well as lower degrees of deformation of the peridotitic mantle.

Preface

This thesis is original, unpublished, independent work by the author, D. Newton.

Table of Contents

List of Tables

List of Figures

Acknowledgments

I would like to thank my supervisor Maya Kopylova, and my committee members Jim Mortensen, Mati Raudsepp and Lori Kennedy for their support and guidance. Thanks to my labmates for putting up with me, especially to Amy Ryan, Luke Hilchie and Dr. Evan Smith for assistance and advice. Thanks also to my family and friends for helping me get this far.

Chapter 1 Introduction

1.1 Background and Objective

Kimberlite pipes provide rare samples of the subcontinental lithospheric mantle beneath cratons. These mantle samples are critical to our understanding of the composition and structure of sub-cratonic mantle and can provide clues about the evolution of early earth and the nature of the present day mantle processes (Nixon and Boyd, 1973; Gurney and Harte, 1980; Boyd et al., 1997a). Study of mantle-derived xenoliths has found that cratonic crust is underlain by deep (>200 km) keels of lithospheric mantle, having stabilized by the Late Archean and since modified by processes of continent building and destruction (e.g., Griffin et al., 1999a). Cratonic mantle has been found to be heterogeneous on small and large scales, both laterally and vertically (Griffin et al., 1999b; Grutter et al.,1999; Carbno and Canil, 2002; Davis et al., 2003). However, kimberlite sampling of the mantle is highly restricted spatially and temporally, providing only a snapshot of a narrow window of the mantle at the time of kimberlite emplacement. Moreover, kimberlites are not just passive carriers of mantle fragments, as kimberlite-generating processes may alter the mantle in the vicinity of melt extraction and transport (Goetze, 1975; Doyle et al., 2004; Kopylova et al., 2008; Artemieva, 2009) Thus, differences found in the mantle sample in kimberlites erupted in two different places at two different times may reflect spatial compositional heterogeneities, temporal differences in mantle modification processes, or the varying effects of kimberlite formation and ascent. Geochronological studies of mantle-derived minerals can shed some light on the timing of mantle modification processes (Walker et al., 1989; Irvine et al., 1999; Pearson et al., 2003; Carlson et al., 2005), but commonly the

resolution of such data is not fine enough to accurately relfect time transient processes. Our objective in this study is to compare two suites of mantle samples removed from ambient mantle conditions at the same time by adjacent kimberlite pipes, and in so doing elucidate time-independent contrasts to highlight spatial variability on small scales in the Slave mantle. The Muskox kimberlite was emplaced contemporaneously and within 15 km of the well studied Jericho kimberlite (Kopylova et al., 1999). In this work, mantle samples from the Muskox pipe are described and compared with those from Jericho.

We find distinct compositional and mineralogical characteristics in the mantle column beneath these two pipes, which we interpret as resulting from mantle heterogeneity as well as differences in local permeability and fluid flow over distances as small as 15 km. Differences in the proportion of rock types and the extent of deformation of peridotite near the lithosphere-asthenosphere boundary suggests lower permeability of the Muskox peridotitic mantle and higher levels of pooling and crystallization of asthenosphere-derived mafic melts. The presence of a zone of modal and cryptic metasomatism and strain localization at a shallow depth in the spinel stability field at Muskox suggests at least one event of hydrous metasomatism that is absent beneath Jericho.

1.2 Geological Setting

The Slave Province, located in northwestern Canada, is a small Archean cratonic block of the larger North American craton. It covers approximately 170,000 km^2 and is bounded in the east and west by the Proterozoic Thelon and Wopmay orogens respectively (Hoffman, 1989). The Great Slave Lake shear zone marks the southern

boundary whereas the northern boundary is less certain, but possibly continues beneath Coronation Gulf and Victoria Island (Griffin et al., 1998). The craton is subdivided into five accreted terranes of varying age, the Central Slave superterrane being the oldest and containing some of the oldest exposed rocks on earth (Helmstead et al., 2012). Kimberlites were first discovered on the Slave craton in the early 1990's, with more than 150 found in the following decade (Pell, 1997). Some of these pipes are diamondiferous and have been exploited by mineral resource companies, but overall few have been drilled and even fewer studied extensively. Mantle xenoliths have been found in some pipes, brought to surface from great depths by kimberlite volcanism providing information on the composition and thermal state of the mantle (Pell, 1997).

The Muskox kimberlite (172.1+/−2.4 Ma; Hayman, 2009) is located in the northern part of the Slave craton, ~400 km NE of Yellowknife near the northern end of Contwoyto Lake, and was emplaced into the Archean granite-granodiorite Contwoyto batholith (2589 ± 5 Ma; Van Breemen et al., 1987). It is part of a cluster of 15 kimberlites, including the Jericho kimberlite, which were emplaced during the mid-Jurassic (Hayman et al., 2008). The Muskox kimberlite is made up of volcaniclastic kimberlite (VK), accounting for 60% of the pipe infill, and 40% coherent kimberlite. Both phases contain 2-4% mantle xenoliths, including eclogites, peridotites and pyroxenites.

The Jericho kimberlite (172 ± 2 Ma; Heaman et al., 1997) is also located 400 km NE of Yellowknife near the northern end of Contwoyto Lake. It intrudes Archean granitoids of the Contwoyto Batholith (Bowie, 1994), and is a multiphase intrusion comprising 3 separate pipes (Cookenboo, 1998). The mantle sample recovered from the

Jericho kimberlite includes coarse peridotite, porphyroclastic peridotite, eclogite, megacrystalline pyroxenite and ilmenite-garnet wehrlite and clinopyroxenite (Kopylova et al., 1999). The types and proportions of mantle-derived xenoliths from Jericho are mainly consistent with those from other cratons and include high- and low-temperature suites of peridotites, defining a disturbed geotherm at the base of the sample suite related to the proximal lithosphere-asthenosphere boundary (Kopylova et al., 1999). Jericho peridotites show unique chemical characteristics including Cr-enrichment of minerals in high-temperature peridotites and a high proportion of chemically unequilibrated samples; the mantle beneath Jericho contains a high proportion of magmatic-textured megacrystalline pyroxenites and ilmenite-bearing rocks (Kopylova et al., 1999).

Chapter 2 Petrography

This work is based on a suite of 53 mantle peridotite and pyroxenite xenoliths recovered from kimberlite drill core (Appendices A,B). Based on macroscopic examination of sample cores, 70% of the mantle samples used in this study were recovered from the coherent kimberlite facies with the remaining 30% from the volcaniclastic facies. Samples are 2-8 cm in size and rock types are found in the following proportions: 15% coarse spinel peridotite, 4% coarse spinel-garnet peridotite, 4% coarse garnet peridotite, 9% porphyroclastic peridotite, 60% websterite and 8% orthopyroxenite. The rock texture classification into coarse and porphyroclastic follows Harte (1977).

2.1 Coarse peridotite

Coarse peridotite xenoliths are primarily composed of olivine (40-70%) and orthopyroxene (10-40%), with lesser amounts of clinopyroxene (0-5%), garnet (0-10%) and/or spinel (0-10%). These xenoliths come from the spinel, spinel/garnet and garnet facies and are mostly classified as harzburgites with rare dunite. Coarse peridotites are characterized by subhedral, equant olivine and orthopyroxene (Fig. 1A). Grain size is correlated with the facies of the sample. Spinel facies samples generally contain olivine and orthopyroxene in the size range 0.5-2.5 mm. Grains are slightly larger in spinel-garnet peridotites, in the 1-4 mm range (Fig. 1B). In garnet facies samples olivine continue to increase in size, to between 1-10 mm (Fig. 1C), wheras orthopyroxene become both smaller and less abundant (up to 2 mm).

2.1.1 Coarse spinel peridotite

Coarse spinel peridotite contains 30-40% olivine, 30-40% orthopyroxene, ≤10% spinel and amphibole, and minor amounts of clinopyroxene, phlogopite and serpentine. Olivine (0.5-2.5 mm) is equant and polygonal with rounded corners. Samples are fresh with minor fracturing of grains, minimal serpentinization along these fractures and minor undulatory extinction and subgrain development (Fig. 1A). Orthopyroxene is found in a similar size range with slightly more fracturing and serpentinization than olivine. Spinel is small with a tight grain size distribution between 200-600 μm. Grains are irregularly shaped with curvilinear boundaries, are translucent brown to opaque black and are often minimally to extensively replaced by a black, opaque aggregate of cryptocrystalline spinel (Fig. 2A). Clinopyroxene, where present, is found as small anhedral grains fitting between larger olivine and orthopyroxene grains. Yellow-green amphibole is present in some samples (5-10%), is up to 2 mm in size and can have prominent orthopyroxene rims (Fig. 2B). Phlogopite is rare, with one exceptional sample containing 10-15% phlogopite, infiltrating the xenolith via a set of parallel veins replacing orthopyroxene and olivine (Fig. 2C). Coarse spinel peridotite also contains minor amounts of serpentine and magnetite replacing primary minerals along fractures and grain boundaries, and carbonate infiltrating as veins through both xenolith and kimberlite.

One amphibole-bearing coarse spinel peridotite (MOX7 62.38) shows recrystallization of olivine and orthopyroxene into smaller grains and a fabric defined by lattice-preferred orientation of elongate grains. This fabric is developed in areas of

recrystallization, and is absent in coarse domains that have not been recrystallized. These coarse domains also lack amphibole.

2.1.2 Coarse spinel-garnet peridotite

Coarse spinel-garnet peridotite contains roughly equal proportions of olivine and orthopyroxene (30-40%) with lesser garnet, spinel and clinopyroxene (5%) and minor amphibole and serpentine. Olivine (40 µm-4 mm) is coarse, equant and subhedral with rounded corners and straight grain boundaries (Fig 1B). Orthopyroxene (800 µm-3.5 mm) is subhedral to anhedral with straight to slightly curved grain boundaries and contain extensive fracturing and thin rod-like clinopyroxene exsolution lamellae. Samples contain ~5% garnet (600 µm-2 mm), which is subhedral-anhedral with curved grain boundaries, and fit into interstices and triple junctions between larger olivine and orthopyroxene grains, or rarely is wispy, anhedral films on primary minerals (Fig. 2D). Garnets have a variable thickness, coarse to fine kelyphite rim of small euhedral phlogopite and spinel. Some grains appear to be partially consumed by a finer grained aggregate of similar composition. Spinel (100-800 µm) occurs as small opaque black to translucent dark brown anhedral grains with generally curvilinear grain boundaries (Fig 2E) or rarely is wispy, anhedral films on primary minerals (Fig. 2D). Both anhedral and subhedral varieties of garnet can have central inclusions of spinel (Fig. 2D, 2E). Clinopyroxene (1-3 mm) is rare (0-5%) anhedral grains and fits into interstices of larger olivine and orthopyroxene grains. Samples are minimally serpentinized (10%) along grain boundaries

and fractures of all primary phases, especially orthopyroxene, and in small interstitial patches. Veins and patches appear to contain a fine aggregate of serpentine, phlogopite and carbonate. Magnetite is found as small (10 μm) rounded black grains along with serpentine. Carbonate is often present as infiltrating veins and as small patches of small equigranular rounded-hexagonal grains.

2.1.3 Coarse garnet peridotite

Coarse garnet peridotite is made up of olivine (50-70%) and lesser orthopyroxene (10-20%) with garnet (10%) and clinopyroxene (5%). Olivine (1 mm-10 mm) is subhedral with mostly straight grain boundaries, shows undulatory extinction and deformation lamellae, are fractured and 10-40% serpentinized along these fractures (Fig. 1C). Orthopyroxene (<2 mm) fits into interstices between larger olivine and garnet grains or forms small rounded inclusions inside olivine, are fractured and 30-70% serpentinized along these fractures. Garnets are large in this sample group (1 mm-4 mm), are subhedral and rounded (Fig. 1C). Garnet has ragged edges and appear resorbed or altered, and has thick coarse kelyphite rims of phlogopite and spinel, but seem to be more robust against serpentinization compared to orthopyroxene. Clinopyroxene is rare in coarse garnet peridotites and is found mostly as small irregularly shaped grains filling interstices between larger olivine and orthopyroxene grains (Fig. 2F), and rarely as small rounded inclusions inside orthopyroxene.

2.2 Porphyroclastic Peridotite

Porphyroclastic peridotite is classified as mostly harzburgite with rare dunite. Samples contain garnet and lack spinel; clinopyroxene is rare. Samples are composed

mostly of olivine porphyroclasts (60-70%) with olivine neoblasts (5-20%) and lesser orthopyroxene (0-10%) garnet (5%) and clinopyroxene (0-5%). Olivine porphyroclasts are large (8-20 mm) grains (Fig. 1D) with undulatory extinction, deformation lamellae and development of non-deformed subgrains. Porphyroclasts are subhedral to anhedral. Grains are fractured and 10-100% replaced with serpentine, magnetite and carbonate and locally contain inclusions of subhedral orthopyroxene and garnet. Olivine neoblasts (10-150 μm) are polygonal isometric or tabular (Fig. 2G) and rarely fully envelope olivine porphyroclasts. They are variably replaced (0-100%) by serpentine or a cryptocrystalline aggregate of serpentine + phlogopite + magnetite ± carbonate ±spinel, especially near borders with kimberlite. Orthopyroxene is rare in porphyroclastic peridotites (≤10%), and are large euhedral rectangles (2-4 mm), smaller subhedral rounded inclusions in olivine porphyroclasts (1 mm), or anhedral grains filling interstices between olivine porphyroclasts (<1 mm). Orthopyroxene is serpentinized along rims and replacement of fractures inside grains and show varying degrees of undulatory extinction. Garnet is large (1-4 mm), euhedral-subhedral rounded grains and occur in triple junctions of olivine porphyroclasts and orthopyroxene (Fig. 1D), and rarely as inclusions or partial inclusions in olivine porphyroclasts. Garnet grains are fractured and filled with small dark inclusions which we interpret to be partial melt, and show some undulatory extinction and development of subgrains. Rims of garnets are commonly ragged, variably resorbed and replaced by phlogopite + spinel kelyphite. The thickness of these rims (≤200 μm) and grain size of constituent minerals seem to increase with proximity to host kimberlite and degree of serpentinization of surrounding xenolith. Garnets included in olivine porphyroclasts lack kelyphite rims, instead having a thin serpentine rim or a thick halo of

olivine neoblasts. Clinopyroxene (0.2-1 mm) is rare, and occurs as small anhedral-subhedral grains found in interstices and triple junctions of larger olivine porphyroclasts, orthopyroxenes and garnets. Serpentine is found in cryptocrystalline aggregates between grains and within fractures in primary phases. It is found along with clusters of small (5-10 μm) rounded magnetite. Phlogopite (200 μm-0.5 mm) and spinel (10-80 μm) is found in kelyphite rims around garnets, often in euhedral cubic grains. Cryptocrystalline carbonate is rare in porphyroclastic peridotites (~1%) and forms 100 μm grains in small interstitial patches and as replacement along fractures in olivine.

2.3 Pyroxenite

Pyroxenitic rock types in the Muskox suite include websterites and rare orthopyroxenites, divided based on the modal proportion of clinopyroxene and mineral chemistry (discussed in next chapter).

2.3.1 *Websterite*

Websterite xenoliths are composed of orthopyroxene (20-70%) and clinopyroxene (5-40%) with olivine (0-40%), garnet (5-20%) and rarely spinel (2-5%). Rock types are dominantly pure websterites with rare olivine websterites. Websterites are characterized by large (0.5mm-4cm) subhedral to euhedral orthopyroxene hosting monogranular networks of anhedral wormlike clinopyroxene (100 μm-1 cm) with highly irregular habit and curvilinear grain boundaries crystallizing along lattices of host orthopyroxene (Fig. 1E). Clinopyroxene also contains numerous dark dusty rounded inclusions along grain boundaries, internal fractures and often in patches in centers of grains. These are

interpreted to be melt inclusions and therefore the clinopyroxene was interpreted as having been subjected partial melting. Garnet (100 μm-1 cm) and is found either as anhedral grains having similar texture to clinopyroxene or rarely as subhedral grains. Subhedral grains are generally fractured and either altered or partially melted, often more so than pyroxenes, and have variable thickness rims of either tabular pleochroic phlogopite (up to 200 μm) and cubic spinel (10-40 μm) or opaque cryptocrystalline aggregates of presumably similar composition. Olivine is found in some websterites, with one rare sample hosting 40% olivine as a single large grain (1 cm) irregularly intergrown with orthopyroxene. Olivine is also locally found as irregular grains with curvilinear grain boundaries growing in a similar fashion to clinopyroxene. Websterites have patches and veins of a dark brown to opaque black cryptocrystalline aggregate probably composed of serpentine, magnetite, carbonate and spinel (Fig. 1E). They are commonly zoned, with either magnetite or carbonate dominant in the centers, with a zone of serpentine and then phlogopite developing towards margins. These patches commonly appear to be the approximate size and shape of garnet and could possibly be fully replaced garnet grains. This material makes up 5-10% of websterite samples. Websterites are texturally classified as “magmatic” as an interpretation of allotriomorphic rock textures resulting from highly anhedral clinopyroxene grains with curvilinear grain boundaries simultaneously crystallized and intergrown with orthopyroxene and olivine. Those pyroxenites with higher modal orthopyroxene are texturally classified as hypidiomorphic, due to the dominant effect of subhedral orthopyroxene rock texture.

2.3.2 *Orthopyroxenite*

Orthopyroxenite is composed almost entirely of orthopyroxene porphyroclasts (90%) and neoblasts (5%) with minor olivine (<1%), serpentine (5%) phlogopite <1%) and secondary spinel (<1%). Orthopyroxene porphyroclasts make up most of the sample and are found as large, euhedral to anhedral grains with straight grain boundaries in the size range 200 µm-1 cm. This broad grain size distribution may be the result of deformation, as smaller grains may be fully developed subgrains of larger porphyroclasts (Fig. 1F). Grains show undulatory extinction and development of subgrains and most are surrounded by tiny neoblasts (Fig. 2H). Grains are fractured and 10-60% serpentinized along these fractures. Small (10-20 µm) rounded orthopyroxene neoblasts are found in clusters and interstices surrounding orthopyroxene. Olivine is present in interstices of orthopyroxene porphyroclasts, is up to 200 µm in size, and is anhedral with straight grain boundaries. Serpentine, phlogopite and spinel is found replacing groups of orthopyroxene neoblasts.

3.0 Mineral Chemistry

3.1 Analytical Methods

Mineral compositions were analyzed using a fully automated Cameca SX-50 electron microprobe at the Dept. of Earth and Ocean and Atmospheric Science at the University of British Columbia. Samples were analyzed in wavelength dispersion mode at accelerating voltage of 15 mV and beam current of 20 mA. On-peak counting times were 10 s for major and 20 s for minor elements. Raw data were treated with the 'PAP' $\phi(\rho Z)$ on-line correction program. Individual phases in samples were analyzed as 15-20 points in cores and rims over 3-5 grains. Homogenous analyses were averaged, zoned mineral analyses were averaged separately as cores and rims. All analyses available in Appendix C and Electronic Supplementary Material 1. Precision (2σ, relative %) and minimum detection limits (absolute wt.%) are as follows: SiO_2 (0.7, 0.03); Na_2O (3, 0.02); MgO (1, 0.05), Al_2O_3 (2, 0.08); CaO (1.5, 0.02); TiO_2 (22, 0.03); Cr_2O_3 (9, 0.04); MnO (27, 0.03); FeO (3, 0.04); NiO (20, 0.03).

3.2 Mineral Chemistry

3.2.1 Olivine

Olivine is forsterite, and range in Mg# (Mg/(Mg+Fe) cpfu) from 88-94 (Fig. 3A, Fig. 3C). Olivine Mg# is highest in coarse spinel and coarse spinel-garnet peridotite, with values of 92-94. Values are lower for coarse garnet and porphyroclastic peridotite, with values of 89-91. Olivine pyroxenite shows a wide distribution of Mg# (88-93) with higher values for orthopyroxenites. Olivine is homogenous within grains, both core-rim in porphyroclasts and between porphyroclasts and neoblasts. NiO contents in peridotitic

olivines are 0.25-0.45 wt.% across all types and calculated depth ranges. NiO contents in pyroxenitic olivine is 0.15-0.45 wt.% and decrease with depth.

3.2.2 Orthopyroxene

Orthopyroxene is enstatite, with Mg# ranging from 89 to 94 (Fig. 3B, Fig. 3D). Values are generally more restricted than those in olivine, however, and are mostly in the range of 91-94 in peridotites and 90-92 in pyroxenites. Mg# in peridotitic orthopyroxene generally decreases with depth facies, ranging from ~92-93 wt.% in coarse spinel and spinel-garnet peridotites, and around 91-92 in coarse garnet and porphyroclastic peridotites. Orthopyroxene in orthopyroxenites ranges to higher Mg# of 92. In all depth ranges and rock types, the calculated Mg# is generally higher in orthopyroxene than in coexisting olivine. Al_2O_3, Cr_2O_3 and CaO in orthopyroxene in coarse peridotite are widely varied, but show little correlation with rock type.

Al_2O_3 content in orthopyroxene in all rock types ranges from 0.3 to 3.0 wt.%; Cr_2O_3 ranges 0.2-1.0 wt.% (Fig. 4A); CaO ranges 0.1-2.0 wt.%. Values for websterites are far more restricted for Al_2O_3 (0.4-0.7 wt.%), Cr_2O_3 (0.2-0.6 wt.%) and CaO (0.5-1.0 wt.%). Values for orthopyroxenites are high and variable for Al_2O_3 (0.3-1.3 wt.%) Cr_2O_3 (0.1-1.3 wt.%) and CaO (0.5-1.2 wt.%). Zoning is observed in orthopyroxenes in all rock types except coarse garnet peridotite. This zoning is associated with a rimward decrease in Al_2O_3 (2 wt.%), Cr_2O_3 (0.5 wt.%) and CaO (2 wt.%) and an increase in MgO (3 wt.%). Exceptions to these ranges exist for metasomatized samples, where values can be variably raised or lowered in tandem or separately.

Aluminum content of orthopyroxene was used to determine the depth facies of the peridotites where garnet or spinel could not be found. This is based on lower Al_2O_3 content of orthopyroxenes in equilibrium with garnet (Boyd et al., 1997), but with a minor variation in absolute concentrations of the threshold. For example, orthopyroxene from spinel peridotites contains 0.9-2.2 wt. % Al_2O_3, whereas orthopyroxene from garnet peridotites contains 0.5-0.6 wt. % Al_2O_3. Jericho spinel peridotites show 0.8-1.9 wt. % Al_2O_3 in orthopyroxene (McCammon and Kopylova 2004) and 0.6 wt. % and lower Al_2O_3 for garnet-bearing peridotites (Kopylova et al., 1999). Gahcho Kue spinel peridotites host orthopyroxene with 0.6-2.5 wt. % Al_2O_3, whilst spinel-garnet peridotites have orthopyroxene with 0.3-0.5 wt. % Al_2O_3 (Kopylova et al., 2004). We assigned the garnet facies to Muskox peridotites that contained orthopyroxenes cores with less than 0.9 wt.% of Al_2O_3.

3.2.3 Clinopyroxene

Clinopyroxene in all rock types is Cr-diopside. Cr_2O_3 contents are high (~1.0-3.0 wt.%) and are correlated with high Na, with the highest values of Cr_2O_3 in websterites and the lowest in coarse spinel peridotites (Fig. 4B). Mg# ranges from 89-96, are highest in coarse peridotites (90-96) and decrease in pyroxenites (Fig. 4B). Values are lowest for pyroxenites (89-91), porphyroclastic peridotites lie between this range (90-93). Al_2O_3 is higher in peridotitic clinopyroxene (2.0-5.0 wt. %) and lower and more restricted in pyroxenites (~2.0 wt. %). Zoning is observed in clinopyroxene in all rock types except for coarse garnet peridotite, expressed as rimward decreases in Al_2O_3 (2.5 wt. %), Cr_2O_3

(0.25 wt. %) and Na_2O (0.6 wt. %) and increases in MgO (1 wt. %), CaO (3 wt. %), FeO (0.9 wt. %).

3.2.4 Garnet and Spinel

Garnet in Muskox xenoliths is pyrope, and contains high Cr_2O_3 (Fig. 4C), high MgO and low CaO. All garnets plot within the 'G9' field in the Cr_2O_3 – CaO diagram (Fig. 5). Cr_2O_3 is highest for porphyroclastic peridotites (4.0-12.0 wt. %) and lowest for coarse spinel-garnet peridotites (1.5-4.0 wt. %). Values for websterites show a wide range in Cr_2O_3 contents, between 3.0 and 11.0 wt. %. CaO values are highest for some websterites (<8.0 wt. %) with a tight range shared by all other rock types (4.5-6.5 wt. %). The garnet compositions follow two separate trends. Most data fit on the 'lherzolitic trend' (Sobolev et al., 1973) which closely follows the G9/G10 boundary, while a subset of websterites fits along a different trend of lower Cr_2O_3 enrichment with increasing CaO (Fig. 5). Mg# ranges between 76-82, with the highest values and a wide variation in porphyroclastic peridotites (76-82), and lower values for pyroxenites (76-79). Coarse peridotites straddle this range (77-81) (Fig. 4C). Garnets are often zoned, with rimward increases in Al_2O_3 (<2 wt.%), FeO (1 wt.%) and MgO (1 wt.%) and decreases in Cr_2O_3 (2 wt.%). Zoning is most pronounced in websterites.

Spinel is chromite and contains 0-0.05 wt. % TiO_2, 30-55 wt. % Cr_2O_3, 15-33 wt.% Al_2O_3 and 11-16 wt. % MgO. It occurs only in coarse peridotites and demonstrates the common negative correlation of MgO and Cr_2O_3. One outlying spinel analyses is found in a coarse spinel peridotite with low Cr_2O_3 (~13 wt.%) and high Al_2O_3 (~53

wt.%). The low Cr_2O_3 compositions of Muskox spinel places them below the diamond inclusion field (Gurney and Zweistra, 1995).

3.2.5 Amphibole

Amphibole is pargasite, with MgO (18-20 wt.%), CaO (10-13 wt.%) and Al_2O_3 (10-13 wt.%) and lesser Na_2O (3 wt.%), FeO (3 wt.%), Cr_2O_3 (1 wt.%) with minor K_2O and TiO_2. Grains are homogenous with respect to cores and rims and between grains, and demonstrate higher Al_2O_3 (13 wt.%) in coarse spinel peridotites than garnet peridotites (10 wt.%).

4.0 Thermobarometry

4.1 Methodology

For thermobarometry, we used compositions of homogeneous grains for most samples. In rare samples that showed core-rim heterogeneities, rim compositions were employed. Compositions for lamellae and inclusions were not used for thermobarometry. Because the Muskox mantle xenolith suite is diverse mineralogically, we devised different approaches to deal with rocks that lack different minerals.

For samples containing orthopyroxene, clinopyroxene and garnet, combined Brey and Kohler (1990) two-pyroxene temperature (BK T) and an orthopyroxene-garnet pressure (Brey and Kohler (1990), (BK P) can be computed (Table 1). This thermometer is calibrated in natural lherzolite for the conditions 900-1400 °C and 10-60 kbar, with an accuracy of ± 16 °C and ± 2.2 kbar (Brey and Kohler, 1990). This thermobarometric combination was used because it is recommended for natural lherzolite compositions at P-T conditions comparable to that expected for the shallow mantle beneath the Muskox kimberlite (Smith, 1999), and has been widely applied in similar contexts. This combination also allows us to make comparisons to the geotherm derived from the Jericho xenolith suite, which has also been plotted in BK T/BK P space (Kopylova et al., 1999). When BK P/BK T points are plotted against the Jericho geotherm, it can be seen that there is good agreement between the two data sets (Fig. 6A).

For samples containing two pyroxenes with no garnet and with or without olivine, it was difficult to estimate the equilibrium pressure. Our approach was based on the match between Muskox and Jericho geotherms and therefore the conclusion that these spatially proximal and roughly contemporaneous pipes share the same thermal regime.

For garnet-free samples, we computed Brey and Kohler (1990) two-pyroxene temperature (BK T) at two assumed pressures and projected the resulting univariant P-T line onto the Jericho geotherm for peridotites (Fig. 7; Table 2) and for pyroxenites (Fig. 8; Table 2). The geothermal intercept is the most likely pressure and temperature of the sample equilibrium.

For samples that do not contain clinopyroxene, it is not possible to compute BK T two-pyroxene temperatures and other thermometers consistent with the BK T should be employed. We have tested the match of the Brey and Kohler (1990) Ca-in-Opx thermometer (BK Ca-in-Opx T) against BK T (Fig. 6B, Table 1). While there is consistency between the two methods, it is found that BK Ca-in-Opx values are 40-80 °C cooler than those reported by the BK T method for pyroxenites, but deviate ~30 °C above and below BK T for two spinel-garnet peridotites (Fig. 6B). The match is better than between BK T and O'Neill et al. (1979) olivine-garnet temperatures that deviate up to 200 ^{o}C (Smith, 1999; Kopylova and Caro, 2004). Therefore, we estimated BK Ca-in-Opx temperatures for 2 assumed pressures for each clinopyroxene-free sample in order to derive a line intersecting the Jericho geotherm for peridotites (Fig. 7, Table 3) and pyroxenites (Fig. 8; Table 3)

Table 1. Pressure and temperature estimates of Muskox samples containing two pyroxenes and garnet

Sample #	Rock Type	Combined			
		BK P (kbar)	BK T (°C)	Ca-in-OPX T (°C) @ BK P	Nakamura T (°C) @ BK P
MOX 3 33	Coarse Spinel Garnet Peridotite	42.1	860	824	862
MOX 7 62.38	Coarse Spinel Garnet Peridotite	32.1	739	771	670
MOX 1 45.5	Coarse Garnet Peridotite	61.2	1205	1132	1132
MOX 24 124.00A	Porphyroclastic Peridotite	56.7	1208	1169	1095
MOX 0 157.45	Websterite	58.8	1169	1103	1097
MOX 0 162.80A	Websterite	60.6	1206	1121	1188
MOX 0 162.80B	Websterite	59.6	1198	1122	1176
MOX 0 179.3	Websterite	60.0	1195	1130	1152
MOX 0 197	Websterite	59.6	1163	1085	1164
MOX 0 198.37	Websterite	57.1	1168	1104	1148
MOX 0 216.83	Websterite	61.1	1171	1098	1130
MOX 1 59	Websterite	58.6	1183	1113	1136
MOX 3 42.1	Websterite	59.7	1177	1117	1175
MOX 11 122.2	Websterite	57.9	1172	1114	1174
MOX 11 200.50A	Websterite	61.8	1163	1115	1129
MOX 24 43.35	Websterite	59.1	1183	1102	1195
MOX 24 206.73	Websterite	56.7	1174	1134	1147
MOX 24 240	Websterite	60.8	1193	1135	1086
MOX 31 230.74	Websterite	63.4	1174	1136	1168
MOX 31 281.2	Websterite	59.2	1204	1143	1163

For Tables 1-3: BK P - Brey and Kohler (1990) orthopyroxene-garnet barometer
BK T - Brey and Kohler (1990) two-pyroxene thermometer
BK Ca-in-Opx T- Brey and Kohler (1990) Calcium in orthopyroxene thermometer
Nakamura - Nakamura (2009) clinopyroxene-garnet thermometer
Geothermal Intercept - Intersection of calculated univariant line with geotherm constrained for xenoliths from the Jericho kimberlite (Kopylova, 1999)

For samples without orthopyroxene, but containing coexisting clinopyroxene and garnet, we have investigated the use of the Nakamura (2009) clinopyroxene-garnet thermometer (NK T). Nakamura (2009) thermometer (NK T) is based upon Fe-Mg exchange between coexisting garnet and clinopyroxene for mafic to ultramafic bulk compositions at 800-1820 °C and 15-75 kbar, with an accuracy of ± 74 °C. NK T has been plotted against BK T to check consistency (Fig. 6C; Table 1). The two thermometers are shown to be in good agreement, with NK T reported as 0-80 °C cooler than BK T for the same samples, with the exceptions of two deviating samples with NK T ~100 °C lower than that the BK T (Table 1). We computed the intersection of the univariant P-T line of Nakamura (2009) temperatures at assumed pressures with the Jericho geotherm (Table 3).

Table 2. Pressure and temperature estimates for Muskox samples containing two pyroxenes

Sample #	Rock Type	Combined		Combined		Geothermal Intercept	
		Assumed P_1 (kbar)	BK T (°C) @ P_1	Assumed P_2 (kbar)	BK T (°C) @ P_2	Pressure (kbar)	Temperature (°C)
MOX 3 69.25	Coarse Spinel Peridotite	25	809	40	831	35.6	824
MOX 24 31.10A	Coarse Spinel Peridotite	25	736	35	749	30.0	743
MOX 24 65.16	Coarse Spinel Peridotite	30	798	40	811	34.0	800
MOX 24 124.00B*	Coarse Spinel Peridotite	50	1130	60	1150	58.0	1145
MOX 25 161.52B	Coarse Spinel Peridotite	25	811	40	832	36.0	825
MOX 31 224.5[+]	Coarse Garnet Peridotite	55	1191	65	1217	50-62.8	1178-1213
MOX 3 74.42	Websterite	55	1194	65	1214	62.5	1211
MOX 3 78.85B	Websterite	55	1173	65	1194	61.0	1183
MOX 7 30	Websterite	50	1115	60	1135	57.1	1128
MOX 7 54	Websterite	55	1174	65	1194	60.9	1186
MOX 24 42.6	Websterite	60	1192	70	1214	61.4	1195
MOX 24 105.2	Websterite	60	1207	70	1228	62.9	1213
MOX 25 120.6A	Websterite	55	1162	65	1183	60.0	1170
MOX 25 161.52C	Websterite	60	1196	70	1217	62.0	1200
MOX 31 242.5	Websterite	55	1123	60	1133	56.7	1126
MOX 31 242.6	Websterite	60	1210	65	1221	63.5	1218
MOX 1 48.6	Orthopyroxenite	55	1192	65	1213	62.5	1208
MOX 24 31.1B	Orthopyroxenite	55	1192	65	1213	62.5	1208
MOX 28 269.6	Orthopyroxenite	55	1113	60	1123	55.9	1113

*Coarse Spinel Peridotite MOX24 124.0B is not plotted on Fig. 7, becasue orthopyroxene composition is unusually low-Al and was considered to be re-equilibrated by late processes.

[+] High-T sample, geothemal intercept reported as possible range of intersections with disturbed Jericho geotherm. Here and Table 3.

Table 3. Pressure and temperature estimates for Muskox samples lacking (A) clinopyroxene or (B) orthopyroxene

A.		Combined		Combined		Geothermal Intercept	
Sample #	Rock Type	Assumed P_1 (kbar)	BK Ca-in-Opx T @ P_1	Assumed P_2 (kbar)	BK Ca-in-Opx T @ P_2	Pressure (kbar)	Temperature (°C)
MOX1 107.57	Coarse Spinel Peridotite	35	835	45	876	37	842
MOX7 97.68	Coarse Spinel Peridotite	35	861	45	902	39.5	877
MOX24 84.8	Coarse Spinel Peridotite	20	635	30	670	23	645
MOX11 162.1	Porphyroclastic Peridotite$^+$	55	1161	65	1209	50-61	1135-1190
MOX3 78.85A	Websterite**	45	1013	55	1058	50	1035
MOX25 120.60B	Orthopyroxenite	55	1207	65	1256	65	1256

B.		Combined		Combined		Geothermal Intercept	
Sample #	Rock Type	Assumed P_1 (kbar)	Nakamura T (°C) @ P_1	Assumed P_2 (kbar)	Nakamura T (°C) @ P_2	Pressure (kbar)	Temperature (°C)
DDH2 91.5	Porphyroclastic Peridotite$^+$	50	1228	70	1340	52-70	1250-1340
MOX25 124.8	Porphyroclastic Peridotite$^+$	50	1156	70	1264	50-62	1140-1200
MOX28 320.1	Porphyroclastic Peridotite$^+$	50	1114	70	1217	50-59	1110-1145
MOX0 158.8A	Websterite**	40	986	60	1080	50	1033
MOX0 233.5	Websterite**	40	1050	60	1152	58	1150
MOX11 287.67	Websterite**	40	998	60	1094	52	1050
MOX24 255	Websterite**	40	1099	70	1258	64	1230
MOX25 246.19	Websterite**	40	1063	60	1167	60	1167

**Clinopyroxene or orthopyroxene data not available due to extensive kimberlite alteration of xenolith.

4.2 Results

Results derived by the thermobarometric methods described above are plotted together for peridotites (Fig. 7) and for pyroxenites (Fig. 8). On these plots, samples with independently derived pressures and temperatures are plotted as single symbols, whereas samples that needed to be projected onto the Jericho geotherm to get estimates of pressures or temperatures are shown as lines. Finding the intersection points was straightforward for the steady-state, shallow geotherm that can be approximated as a curve or a short linear segment, but in the thermally-disturbed asthenosphere (Kopylova et al., 1999) this projection is not possible.

Depth positions from Fig. 7 and Fig. 8 constrain the Muskox mantle cross-section (Fig. 9A). Coarse spinel peridotite is found between the top of the sample suite at 75 km down to 135 km. These samples overlap with coarse spinel-garnet peridotite which begin to occur at 95 km and extends down to 150 km. There is a data gap between 150 km and 165 km and a transition to coarse garnet peridotite, the actual transition must lie within the unsampled depth interval. Pyroxenites begin to appear along with peridotites at 165 km and range in depth to 215 km. Porphyroclastic peridotites are found at the deepest levels and extend to 230 km depth. Pyroxenites are found to coexist with both coarse garnet peridotite and porphyroclastic peridotite. This model stratigraphy is compared to the mantle column reported below the Jericho kimberlite (Fig. 9B).

The thermobarometry combined with the mineral chemistry enables conclusions on the presence of low-T and high-T suites of peridotites commonly distinguished in the cratonic mantle (Harte and Hawkesworth, 1989; Pearson et al., 2003). Most coarse peridotites and two porphyroclastic peridotites with magnesian olivines and orthopyroxenes (with Mg#>92 on Fig 4) can be classified as low-T. The rest of porphyroclastic peridotites (2 samples) and two coarse

peridotites that plot together with pyroxenites on Fig. 4 can be considered high-T. The scarcity of high-T samples makes it impossible to comment on the P-T conditions of their formation. The presence of undeformed, coarse peridotites with high-T mineral chemistry suggests that asthenospheric thermal and chemical disturbance has in some cases affected the mineral chemistry of the Muskox peridotitic mantle without causing shear-related recrystallization.

5.0 Discussion

5.1 Depletion of the Muskox peridotitic mantle

Based on Mg# in olivine (Fig. 10A) and orthopyroxene (Fig. 10B) and Cr_2O_3 content in garnet (Fig. 11B), the peridotitic mantle beneath the Muskox kimberlite is more depleted than that below the Jericho kimberlite in all depth facies except within a couple of narrow depth windows (Fig. 10A, 10B). Mg# in peridotitic olivine in Muskox samples has a slightly higher mode (93) and ranges to higher values (94) compared to Jericho samples (Fig. 3A). Mg# in orthopyroxene reflects a similar pattern, with a mode at 93-94 in Muskox samples compared to a slightly lower mode in Jericho samples at 93 (Fig. 3B). This relationship can also be seen in Mg# depth profiles for both olivine (Fig. 10A) and orthopyroxene (Fig. 10B), with Mg#s generally showing higher values at all depths in the Muskox samples except at 130-150 km and >200 km.

Garnet chemistry also shows this trend (Fig. 11B). A histogram of Cr_2O_3 in garnet shows a mode at 5 wt.%, with a secondary mode at 11 wt.%. This mode is slightly higher than that of Jericho at 4 wt.%. The majority of data points in Muskox samples lie at or above 5 wt.%, whereas the majority of data points in Jericho samples lie at or below 5 wt.%.

The Muskox and Jericho kimberlite pipes are close to one another both spatially and temporally, therefore identical mantle compositions for Muskox and Jericho are expected. However, the peridotitic sample suites from these two pipes show differing levels of depletion at the same depth. Observations of contrasting Mg#s of peridotitic olivines and CaO content in garnet have been reported for xenoliths in adjacent kimberlites, (i.e., from Ekati kimberlite pipes; Menzies et al., 2004) and from the main and satellite kimberlite pipes at Letseng (Lock and Dawson, 2004). The distinct average olivine compositions from adjacent pipes in these examples

were ascribed by the authors to distinct lherzolite/harzburgite ratios in the xenolith suites. The proportions of xenolith types entrained by individual kimberlites vary from pipe to pipe, which may relate to the stratified mantle and the preferential sampling of a certain depth interval. To our knowledge, the contrast in the garnet and olivine mineral chemistry of peridotites at the same depth found at Jericho-Muskox has not been reported before, as similar detailed depth profiles of mineral compositions are not available for other clusters of kimberlites sampling adjacent mantle within a very short time period.

5.2 Two depth zones of metasomatism

Several samples of Muskox peridotites stand out from the rest of the samples based on mineralogical and petrographic characteristics. The samples show textural evidence of reequilibration and recrystallization, crystallization of late metasomatic minerals and either zoned or outlying mineral compositions. We interpret all these signs as evidence for mantle metasomatism. Our analysis shows that these anomalous samples are sourced from two depth intervals, a shallow zone at 100-150 km, and a deep zone at >200 km. Below we discuss how metasomatism is expressed in these zones.

5.2.1 Shallow zone of metasomatism

The shallow zone of metasomatism lies in the spinel stability field between 130 km and 150 km. This zone is characterized petrographically by samples showing any of the following: 1) the presence of primary euhedral amphibole that is in textural equilibrium with surrounding minerals (Fig. 2D); 2) secondary anhedral phlogopite that has infiltrated the sample via a network of parallel veins resorbing and replacing orthopyroxene (Fig. 2C); 3) spinel grains

rimmed by garnet (Fig. 2D, 2E); 4) resorption of primary spinel and its recrystallization into finer-grained secondary spinel (Fig. 2A); and 5) dynamic recrystallization of olivine into smaller grains. The mineralogy of these metasomatized samples is characterized by low Cr_2O_3 in spinel, an increase in TiO_2, NaO, Cr_2O_3 and Al_2O_3 in pyroxenes as compared to all other Muskox peridotites, and Mg# in olivine (Fig. 10A) and orthopyroxene (Fig. 10B) that is lower than those for all other Muskox peridotites. Shallow metasomatism at Muskox may also occur at changing pressure or temperature conditions of the mantle. Evidence for this is found in spinel-garnet peridotites in which spinel is enclosed by garnet. The early stage of rock formation is reflected in crystallization of spinel and higher-Al_2O_3 and Cr_2O_3 orthopyroxene cores. Contents of Al_2O_3 above 1.5 wt.% indicates formation of the orthopyroxene in the spinel stability field (Boyd et al., 1997). The later stage of rock formation occurred in the garnet stability field, where spinel was mantled by garnet and orthopyroxene rims with lower Al_2O_3 and Cr_2O_3 formed. Possible explanations for this transition include an increase in ambient pressure, or a decrease in ambient temperature.

These metasomatic fingerprints are observed in sporadic and complex ways (Table 4), possibly suggesting that either 1) there has been more than one metasomatic event affecting different samples in different ways or 2) a single metasomatic event can manifest itself non-uniformly, depending on intensive and kinetic parameters, the composition of original protoliths and the permeability of the mantle. Olivine and orthopyroxene Mg# and Cr_2O_3 in spinel seem to be less affected, with only one sample in this depth range having a significantly lowered value of 89 and extremely low Cr_2O_3 in spinel. The latter may also explain the mode of Cr_2O_3 in Muskox spinel (~40 wt.%) at a lower content than the mode of Jericho spinel (Fig. 11A), where shallow metasomatism is absent. The most easily disturbed compositional variables are TiO_2 and

Na_2O contents in clinopyroxene as they show variations of up to 0.24 wt.% and 1.5 wt.% respectively (Table 4).

Shallow metasomatism in the amphibole stability field is strongly developed on the Kaapvaal craton, but is absent on other cratons. The Kaapvaal peridotites are altered and metasomatically recrystallized to phlogopite–K-richterite-bearing peridotites (terminology of Erlank et al., 1987), which are thought to be formed by interaction of MARID-related hydrous fluids with peridotitic wall rocks (Dawson and Smith, 1977; Jones et al. 1982; Erlank et al. 1987; Waters et al. 1989; Winterburn et. al. 1990; Konzett et al. 2000). Based on the stability field of amphibole, these peridotites probably originate at a maximum of 80-90 km depth under water-undersaturated conditions (Wallace et al., 1991). There are diverging opinions on the origin of the agent of metasomatism. It has been proposed to be related to subduction and orogenesis (Sen et. al. 1994; Koornneef et al., 2009) or to kimberlite melts (Griffin et al., 1996).

Amphibole-producing metasomatism is very common in off-cratonic mantle, where it is observed as clinopyroxene-amphibole veinlets cutting peridotites (Harte and Hawkesworth, 1989). Such veinlets and zones with metasomatic amphibole and phlogopite are ascribed to reaction with fluids released by crystallizing silicate melts (O'Reilly et al., 1991). Amphibole has been experimentally produced by metasomatism of spinel peridotite by an analog slab melt at pressures of 15-20 kbar (Sen et al., 1994).Influx of hydrous fluid into the mantle, inferred as the source of metasomatism on and off cratons, should change the strength of the lithosphere and its rheological properties. So called "hydrous weakening" of the lithosphere should lead to more plastic mantle and enhanced recrystallization of olivine (Mei and Kohlsted, 2000). The weaker mantle should be finer grained (Karato and Wu, 1993).

Table 4. Evidence for metasomatism in Muskox peridotite xenoliths

Shallow Zone

Sample	Rock Type	Depth (km)	Petrographic Features	Chemical Features
MOX7 62.38	Coarse Spinel-Garnet Peridotite	95	Amphibole; garnet-rimmed spinel	
MOX24 31.1A	Coarse Spinel Peridotite	99	Recrystallization of spinel	Low (36.09 wt. %) Cr_2O_3 in spinel High (2.23 wt. %) Na_2O in clinopyroxene
MOX3 69.25	Coarse Spinel Peridotite	117	Amphibole rimmed by orthopyroxene	Low (35.28 wt. %) Cr_2O_3 in spinel; High (2.11 wt. %) Na_2O in clinopyroxene; High (0.22 wt. %) TiO_2 in clinopyroxene;
MOX25 161.5B	Coarse Spinel Peridotite	119	Phlogopite; recrystallization of olivine	High (1.23 wt. %) CaO in orthopyroxene
MOX7 97.68	Coarse Spinel-Garnet Peridotite	130		Low (13.76 wt. %) Cr_2O_3 in spinel; Low Mg# in olivine (89.5) and orthopyroxene (89.8)
MOX3 33.00	Coarse Spinel-Garnet Peridotite	139	Garnet rimmed spinels	Core-rim depletion in Al_2O_3 in orthopyroxene (0.5 wt.%)
MOX24 124.00B	Coarse Spinel Peridotite	153		High (1.23 wt. %) TiO2 in clinopyroxene

Deep Zone

Sample	Rock Type	Depth (km)	Petrographic Features	Chemical Features
MOX1 45.5	Garnet Peridotite	202		High (0.11 wt. %) TiO_2 in orthopyroxene; High (0.24 wt. %) TiO_2 in clinopyroxene; Low (90) Mg# in olivine; Low (91) Mg# in orthopyroxene
MOX31 224.5	Garnet Peridotite	207	Interstitial clinopyroxene and garnet films	High (0.11 wt. %) TiO_2 in orthopyroxene; High (0.23 wt. %) TiO_2 in clinopyroxene; Low (89) Mg# in olivine; Low (91) Mg# in orthopyroxene

In full correspondence with this model, modal and cryptic metasomatism in the shallow Muskox mantle is also associated with 80-90% recrystallization of olivine into finer grains. This recrystallization is accompanied by development of crystal lattice-preferred orientation (LPO). Development of LPO occurs during deformation by dislocation creep (Karato and Wu, 1993), which is the favored process over diffusion creep in the presence of water (Wang, 2010). Thus, LPO may be another indicator of hydrous weakening in the Muskox shallow mantle. Influx of this fluid may have involved transient heating, evidenced by garnet-rimmed spinels suggesting cooling during recrystallization. Heating would act to enhance strain (Karato, 1993).

5.2.2 Deep zone of metasomatism

There is a second, deep region of metasomatism in the Muskox peridotitic mantle, at about 200 km depth in the garnet stability field. We cannot constrain the deeper termination of this zone as the kimberlite did not sample below 220 km. The metasomatism is manifested in development of late garnet and clinopyroxene along olivine-orthopyroxene grain margins (Fig. 2F), low Mg# in olivine (Fig. 10A) and orthopyroxene (Fig. 10B), high TiO_2 contents of pyroxenes, and chemical disequilibrium in zoned garnet with rims enriched in Al_2O_3 and depleted in Cr_2O_3 (Table 4). The metasomatism at this level may relate to the ubiquitous presence of pyroxenites and sheared peridotites (Figs. 7, 8, 9A), and rare high-T coarse peridotites observed at these depths have acquired mineral chemistry typical for the more prevalent websterites found at this depth.

The deep zone of metasomatism is seen in plots of depth vs. Mg# of both olivine (Fig. 10A) and orthopyroxene (Fig. 10B), with a trend decreasing from ~92-93 at shallower depths (100-150km) to ~89 at 200 km depth. These coarse garnet peridotite samples demonstrate even

lower Mg# in olivine and orthopyroxene than do porphyroclastic peridotites derived from a deeper level. Porphyroclastic peridotites are not the most chemically fertile peridotites, but are underlain by and interspersed with metasomatized high-T coarse peridotites containing clinopyroxene with higher Al_2O_3, TiO_2, NaO and FeO and orthopyroxene with higher TiO_2 .

The metasomatized sample with interstitial films of clinopyroxene and garnet contains primary orthopyroxene with higher CaO (compared to the sample without late development of clinopyroxene and garnet). This possibly suggests metasomatic addition of CaO rather than the origin of garnet and clinopyroxene as exsolution phases from a higher-T orthopyroxene in a closed system. The late introduction of clinopyroxene and garnet could relate to refertilizing metasomatism commonly reported in cratonic mantle (Simon et al., 2007; Miller et al., 2014).

Post-craton stabilization metasomatism at the base of the subcontinental lithospheric mantle (SCLM) (>190 km) is common in cratonic mantle, is characterized by an increase with depth in FeO, CaO, Al_2O_3 and TiO_2 in the bulk composition and in the mineral chemistry, and a decrease in olivine Mg#, and may represent infiltration of asthenosphere-derived mafic melts and fluids (O'Reilly et. al., 2010, and references therein). The deep metasomatic zone in the Muskox peridotitic mantle may be a continuation of the "fertile layer" found in the Jericho peridotitic mantle between 160-200 km depth (marked by arrow on Fig. 10) (Kopylova and Russell 2000). This fertility of peridotites at the base of the SCLM sample suite from the Jericho kimberlite may result from the intrusion of and reaction with younger pyroxenitic magmas and related fluids (Kopylova and Russell, 2000). A lower proportion of these fertile coarse peridotites in the Muskox sample suite may suggest a lower degree of penetration and enrichment by these pyroxenitic magmas and fluids.

5.3 Deformation of the Muskox peridotitic mantle

Porphyroclastic or 'sheared' peridotites are found at the deepest levels of the Muskox sample suite, co-existing with coarse peridotites and pyroxenites (Fig. 9A). The deeper origin of sheared Muskox peridotites is also confirmed by higher values of Cr_2O_3 in garnet in porphyroclastic peridotites (Fig. 5) which is a commonly used indicator of the formation depth (O'Neil, 1981; Grutter et al., 2006). The Cr_2O_3 enrichment in deformed cratonic peridotites is a common trait in cratonic mantle and is also seen at Jericho (Kopylova et. al. 1999), in the central Slave craton (MacKenzie et. al. 1999) and in xenoliths from the Udachnaya pipe on the Siberian craton (Boyd et. al. 1997). This suggests that deformed peridotites sit stratigraphically below coarse peridotites and may represent the base of the sub-continental lithospheric mantle. Boyd and Gurney (1987) interpret deformed peridotites as representing the beginning of melting of peridotite in the presence of volatiles at the lithosphere-asthenosphere boundary. Kennedy et al. (2001) suggest that deformed peridotites have accommodated localized shearing along a partially coupled lithosphere-asthenosphere boundary.

The degree of strain may be higher at shallower depths within the suite of sheared peridotites from both Muskox and Jericho. This is suggested by a negative correlation between the degree of shearing and the estimated depth of the samples, and the amount of Cr_2O_3 in garnet and clinopyroxene. The Muskox sample with the highest Cr_2O_3 in garnet (~10 wt.%) is sourced from 187 km and shows 5% olivine neoblasts. A single sample showing 20% neoblasts (the highest degree of deformation in the Muskox sample suite) has only ~6 wt.% Cr_2O_3 in garnet. Minimum depths of equilibration, based on Cr_2O_3 contents (Grutter et al., 2006), are 100 km for the more deformed sample, compared to 142 km minimum depth for the above mentioned, less

deformed sample This pattern fits for the rest of the Muskox porphyroclastic peridotite suite, with less deformed samples reporting Grutter et al. (2006) minimum depths of around 140 km, and more deformed samples reporting minimum depths of around 100 km. In the Jericho sample suite, those peridotites showing extensive recrystallization of olivine and garnet (porphyroclastic disrupted peridotites) derive from depths of 170 km (Table 3 in Kopylova et al., 1999) and have only about 3 wt.% Cr_2O_3 in garnet, while less sheared samples (porphyroclastic non-disrupted peridotites) derive from depths of 165-195 km (Table 3 in Kopylova et al., 1999) and have the highest values of Cr_2O_3 in garnet of all Jericho peridotites with up to ~11 wt.%. A similar pattern is seen in wt.% Cr_2O_3 in clinopyroxene in both sample suites. High Cr_2O_3 in garnet and clinopyroxene is the result of the deep position of samples. An analagous relationship is seen in peridotites from pipes in the Kimberley area on the Kaapvaal craton (Boyd et al., 1987).

We relate this to the fact that deviatoric stress is higher in the shallow mantle due to lower temperature (Chu et al., 2012). This is corroborated by the smaller grain size of Muskox coarse spinel peridotite compared to coarse garnet peridotites (Fig. 1), as grain size will decrease with increasing stress in the regime of dynamic recrystallization (Karato and Wu, 1993). At higher stresses, non-linear dislocation creep is the dominant deformation mechanism in the shallow mantle and can result in the formation of crystal preferred orientation (Karato and Wu, 1993). Effective viscosity of olivine for dislocation creep decreases with depth and reaches a minimum toward the lithosphere-asthenosphere boundary, suggesting that strain may be localized at this minimum at shallower depths in the lithospheric mantle. With increasing depth from this minimum, the effective viscosity for dislocation creep begins to increase, and stresses are lowered due to increased temperature (Chu et al., 2012). At these conditions, grain size reduction caused by dislocation creep allows for increased deformation by diffusion creep and a

rapid weakening of the mantle. This zone of weakening, along with the effects of higher proportions of partial melts at this depth, may represent the rheological lithosphere-asthenosphere boundary (Karato and Wu, 1993). Another factor in the stronger deformation of the shallower Muskox peridotite could be its dunitic mineralogy, as olivine is known to deform more readily than orthopyroxene (Harte, 1977, and references therein).

Muskox peridotites with the most sheared textures contain tabular neoblasts (Fig. 2G) suggesting fluid-assisted grain boundary migration (Drury and Van Roermund, 1989) as the mechanism for static annealing in these samples. Other Muskox sheared peridotites from 170-190 km contain isometric rather than tabular neoblasts. Their absence implies the restriction of fluid-assisted grain boundary migration and static recrystallization to shallower depth and localized fluid penetration at these depths. This fluid penetration may also assist in localized strain at this depth, as the presence of water is known to decrease the effective viscosity of olivine (Mei and Kohlsted, 2000).

Sheared peridotites from Jericho show more deformation than sheared peridotites from Muskox. In Jericho peridotites, stronger pyroxenes and garnet are deformed in mosaic, fluidal and disrupted textures (Kopylova et al., 1999). By contrast, Muskox peridotites show only moderately strained porphyroclastic textures with no more than 20% olivine recrystallization. There is a positive correlation in the degree of shearing and modes of clinopyroxene between the Muskox and Jericho sample suites. Muskox deformed peridotite samples have a maximum of 20% neoblasts and ≤5% clinopyroxene, whereas the Jericho deformed peridotites (70-90% neoblasts) can have up to 10% clinopyroxene. This general correlation suggests that the infiltration of metasomatizing melts or fluids that introduced CaO and triggered clinopyroxene formation (Simon et al., 2007; Miller et al., 2014) is possibly linked to deformation. The

relationship between metasomatizing fluids and deformation of peridotitic cratonic mantle has been observed widely (Smith and Boyd, 1987; Drury and van Roermund, 1989; Harte and Hawkesworth, 1989; O'Reilly and Griffin, 2010). The presence of hydrous fluids has been shown experimentally to lower the effective viscosity of the mantle and enhance strain in both the diffusion and dislocation creep regimes (Wang, 2010; Skemer et al., 2013). These refertilization events that formed late clinopyroxene and garnet may have had a larger impact in the Jericho mantle than in the mantle below Muskox. The evidence for this is the more deformed Jericho peridotites and the presence of the 'fertile layer' of peridotite at Jericho (Kopylova and Russell, 2000), which is largely absent at Muskox. As sheared peridotites in general are thermally disturbed and displaced to higher temperatures from steady-state geotherms (Pearson et al., 2003), one may also expect a difference between the thermal disturbance at Jericho and Muskox. However, the lack of Brey and Kohler (1990) garnet-orthopyroxene pressure estimates for Muskox samples with the most sheared textures prevent us from making this comparison. Univariant P-T lines for sheared Muskox peridotites cross the cloud of thermally disturbed Jericho P-T points at lower pressure and project on the steady-state Jericho geotherm at higher pressure (Fig. 7), and both options are equally possible.

5.4 Characteristics of the Muskox pyroxenitic mantle

Two contrasting types of pyroxenites occur in the Muskox mantle, orthopyroxenites and garnet websterites. Both show unequilibrated textures (Figs. 1E, 1F) and therefore must be younger than the texturally equilibrated coarse peridotitic mantle with metamorphic textures (Goetze, 1975; Kopylova et al., 1999). The textural disequilibrium in websterites is manifested in complex curvilinear grain boundaries (Fig. 1E), common in magmatic rocks, and widespread

exsolution lamellae, whereas orthopyroxenites have sheared textures unequilibrated with respect to a wide range of grain sizes (Fig. 1F). A higher proportion of minerals in pyroxenites show chemical zoning than those in peridotites. Zoning is expressed in 1) A rimward decrease in and CaO and increase in, MgO and Na_2O in garnet 2) a rimward decrease in Al_2O_3, Cr_2O_3 and CaO in orthopyroxene and 3) a rimward increase in Al_2O_3, Cr_2O_3, CaO and decrease in MgO and Na_2O in clinopyroxene. This observation suggests that pyroxenites in the northern Slave Province formed within a short period of time before being sampled by the kimberlite. The younger textures of the Muskox pyroxenites contrast with equilibrated, granoblastic textures of pyroxenites from the central Slave, which are Proterozoic (1.78 ± 0.66 Ga; Aulbach, 2007) in age and are proposed to have crystallized from melts produced during delamination of a Proterozoic subducting slab (Foley et al., 2003). Similar equilibrated textures of pyroxenites are also found in samples from pipes on the Siberian craton (Solovjeva et al., 1987).

Mineral compositions of the two pyroxenite groups from the Muskox pipe are unusual in the global context. Only at Muskox are minerals in the pyroxenites more Cr-rich than the respective minerals in the surrounding peridotitic mantle (Fig. 4). Commonly, pyroxenitic minerals are less chromian and magnesian than peridotitic minerals, typical for the general relationship between mafic and ultramafic rocks. At Muskox, less magnesian pyroxenitic minerals are more chromian (Fig. 4), which cannot be explained by a simple distinct degree of melting compared to worldwide pyroxenites. High Cr_2O_3 and Na_2O in these minerals is compensated for with lower SiO_2, with a negative correlation seen when comparing Muskox orthopyroxenites, Muskox garnet websterites, Jericho pyroxenites and Jericho megacrysts. High Cr_2O_3 pyroxenitic minerals such as those found in the Muskox sample suite have not been reported elsewhere.

Comparison with Jericho pyroxenites (Kopylova et al., 1999) may give us additional insights on formation of the Muskox pyroxenites. The following traits are common to pyroxenites in both pipes: 1) the presence of young, magmatic textured websterites; 2) the occurrence of pyroxenites at a restricted depth approaching the lithosphere-asthenosphere boundary, where they coexist with both coarse and sheared peridotites; 3) the thermal equilibration of pyroxenites along the ambient cratonic geotherm.

The following traits distinguish Muskox pyroxenites from Jericho pyroxenites: 1) the presence of two distinct types of pyroxenite in the Muskox sample suite; 2) more chromian compositions of all minerals; 3) the absence of rock types transitional to peridotites with respect to modal mineralogy and mineral chemistry (Fig. 4); 4) the wider range of formation pressures and temperatures (Figs. 9, 10); and 5) a higher proportion of these rock types in the Muskox xenolith suite.

Muskox pyroxenites cannot be samples of the locally pyroxene-enriched peridotitic mantle, produced either by a process of mechanical crystal segregation in magma conduits in peridotite (Pearson et al., 1993) or a metasomatic process (Kopylova et al., 2009), as evident from the lack of mineral compositions transitional between peridotite and pyroxenite (Fig. 4). Therefore, pyroxenites could only be crystallized pockets of mafic melts. These melts were atypically Cr-rich. An Al- and Ca-poor variety of this Cr-rich melt crystallized into orthopyroxenites, with low garnet and clinopyroxene modes. The extremely high Cr_2O_3 content of orthopyroxenes in the orthopyroxenite can be partly explained by its high-pressure, high-temperature frozen composition which did not allow for exsolution of clinopyroxene component. The evidence for this is the occurrence of clinopyroxene as lamellae in orthopyroxene and a negative correlation between the mode of clinopyroxene and the Cr_2O_3 content in orthopyroxene.

The deep origin of the orthopyroxenites match their calculated equilibrium P-Ts (Fig. 8). These melts may have originated in response to the presence of fluids near the lithosphere-asthenosphere boundary. Timing of pyroxenite formation suggests that these fluids may have been proto-kimberlitic or shortly preceding kimberlite formation.

5.5 Concluding remarks

Xenoliths from the Muskox kimberlite emplaced simultaneously with the adjacent Jericho kimberlite give us an opportunity to examine the same mantle sampled by a different ascending magma batch and thus separate the ambient mantle characteristics from the traits imposed by the kimberlite formation and emplacement. The vagaries of kimberlite sampling led to a more complete representation of the mantle column in the Jericho xenoliths, wheras the Muskox did not sample in the depth range 150-165 km (Fig. 9) and did not entrain 4-phase porphyroclastic peridotites that make it possible to check for a possible deviation from the ambient geotherm that marks the thermal lithosphere-asthenosphere boundary. Thus, the thickness of the lithosphere beneath Muskox is unknown.

Besides sampling contrasts, the following distinctions are found when comparing more detailed features of sample suite from Muskox against those from the Jericho kimberlites: 1) a slightly higher overall level of depletion in most depth ranges of the Muskox peridotitic mantle; 2) metasomatism in the spinel facies shallow mantle at Muskox; 3) the less deformed mantle expressed in peridotite textures resulting from lower strain and a smaller proportion of these rock types in the overall sample suite; 5) weaker refertilization of the peridotitic mantle; 6) a higher proportion of pyroxenites in the Muskox sample suite and their wider depth distribution, and 6) the presence of 2 distinct varieties of pyroxenites with uniquely Cr-rich minerals.

The slightly higher depletion of the Muskox mantle may represent the regular heterogeneity of the mantle, which typically shows a range of mineral and geochemical compositions (Hoffman, 2003; Walter, 2003). All other features can be ascribed to the effect of kimberlite generating processes, i.e., to metasomatism with pre-kimberlitic fluids. Metasomatic recrystallization of peridotite reacting with fluid to produce pyroxenes, garnet and megacrysts has been reported by Rawlinson and Dawson (1979), Boyd et al. (1984), Doyle et al. (2004) and Burgess and Harte (2004). This model of multi-stage recrystallization and metasomatism of peridotite wallrocks adjacent to percolating fluid was proposed for the origin of Jericho megacrysts and pyroxenites (Kopylova et al., 2009). This could be the same widespread type of metasomatism that introduced secondary clinopyroxene, garnet and ilmenite (±phlogopite and rutile) to cratonic xenoliths (e.g. Erlank et al., 1987; Gregoire et al., 2002; Simon et al., 2007, Rehfeldt et al., 2008). Our observations on mineral zoning in pyroxenites, textural disequilibrium of pyroxenites and phlogopite in peridotites agree with the conclusion that the metasomatism shortly preceded kimberlite formation (e.g., Dawson and Smith, 1977; Hops et al., 1989; Konzett et al., 2000) and may be genetically related to pre-kimberlitic fluids (Konzett et al., 2000; Doyle et al., 2004; Moore and Belousova, 2005; Kopylova et al., 2009).

Vagaries of fluid penetration may have led to metasomatism of the shallow mantle at Muskox, as well as the common concentration of fluid near the lithosphere-asthenosphere boundary causing formation of pyroxenites and sheared peridotites. Lower levels of strain and modal and cryptic metasomatism of peridotites suggest that these fluids have infiltrated and interacted less with the Muskox mantle than that beneath Jericho, perhaps due to lower permeability of the mantle. Instead, the fluids have pooled and triggered local partial melting due to hydrous lowering of the solidus, causing formation of abundant pyroxenites. Their distinct

high- Cr character we ascribe to a slightly distinct compositions of the Ti-, Al-, Fe-, Si- and Ca-rich Muskox metasomatizing fluids. The absence of ilmenite locally present in Jericho peridotites and pyroxenites (Kopylova et al., 1999) suggests the less Ti-rich character of Muskox metasomatism. This, in turn, prevents Cr buffering by ilmenite and ensures the chromian affinity of the pyroxenite minerals at Muskox (Kopylova et al., 2009). The variability in Cr_2O_3 contents of pyroxenitic minerals beneath various kimberlites parallels the range of Cr_2O_3 contents observed in high-Cr megacrysts and thresholds between low-Cr and high-Cr megacrystal suites in individual kimberlites (Schulze, 1987). The latter may imply the metasomatic agents were variously endowed in Cr.

Figures

Fig. 1

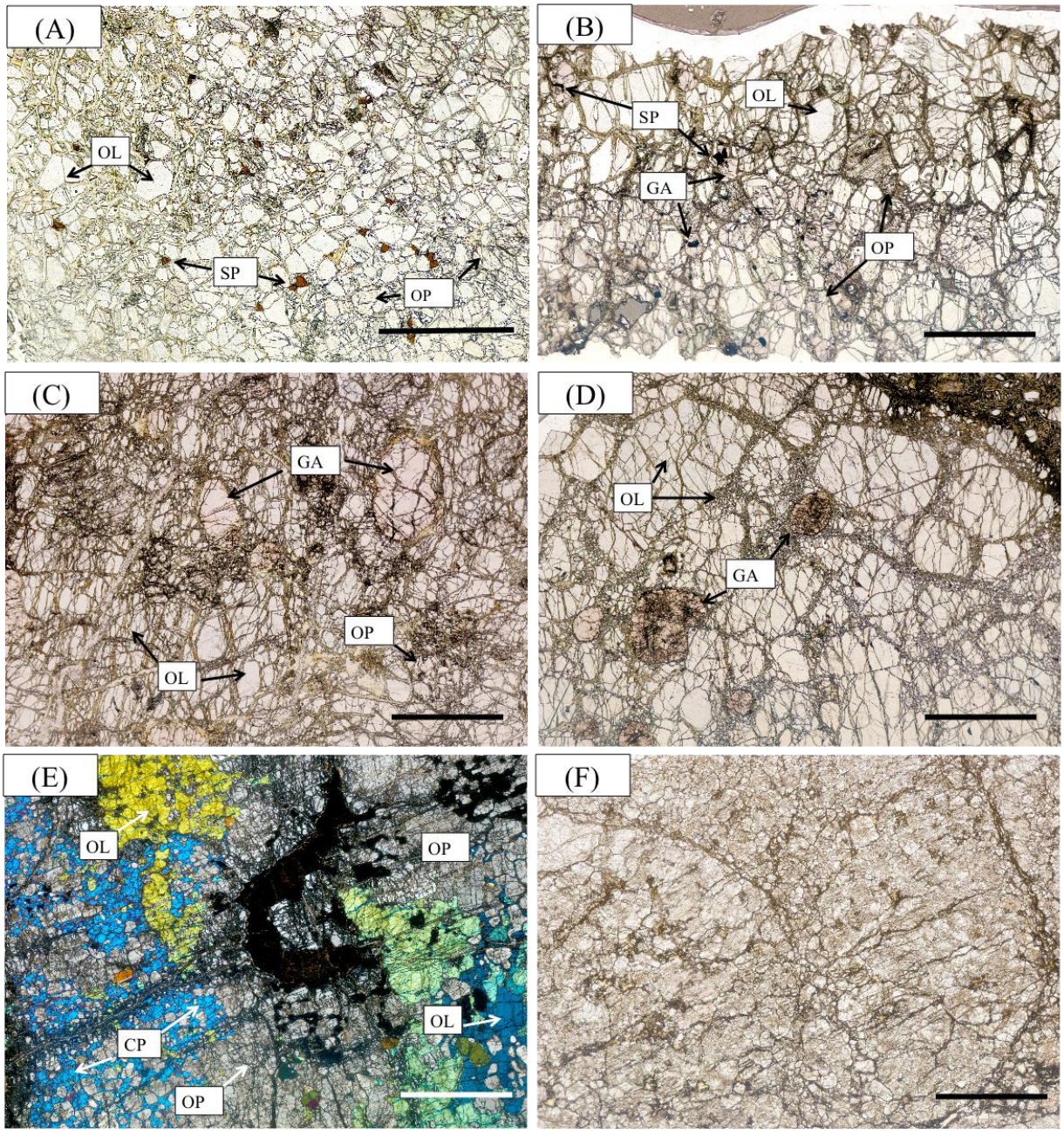

Fig. 2

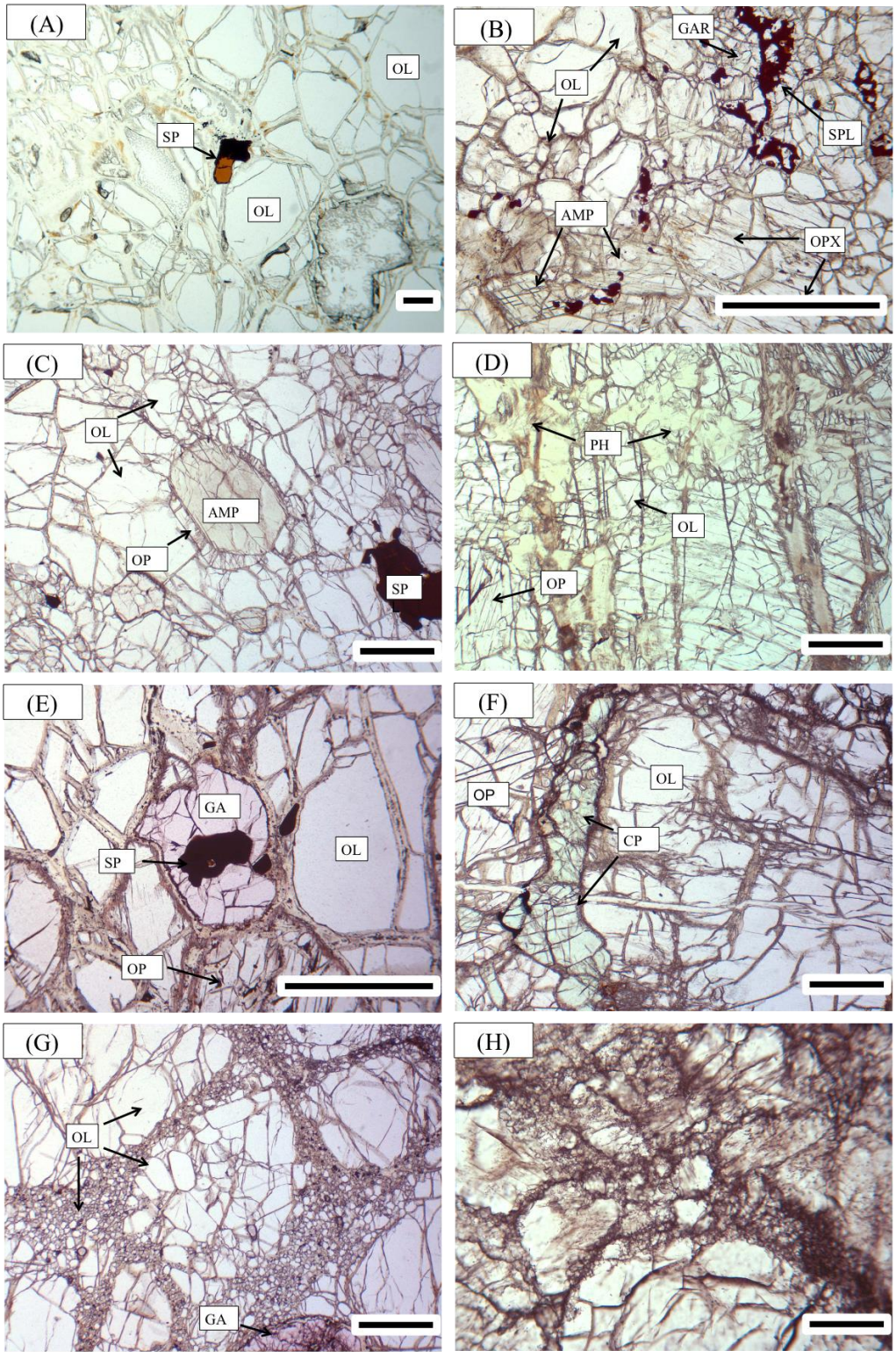
(A)
OL
SP
OL
(B)
GAR
OL
SPL
AMP
OPX
(C)
OL
AMP
OP
SP
(D)
PH
OL
OP
(E)
GA
SP
OL
OP
(F)
OL
OP
CP
(G)
OL
GA
(H)

Fig. 3

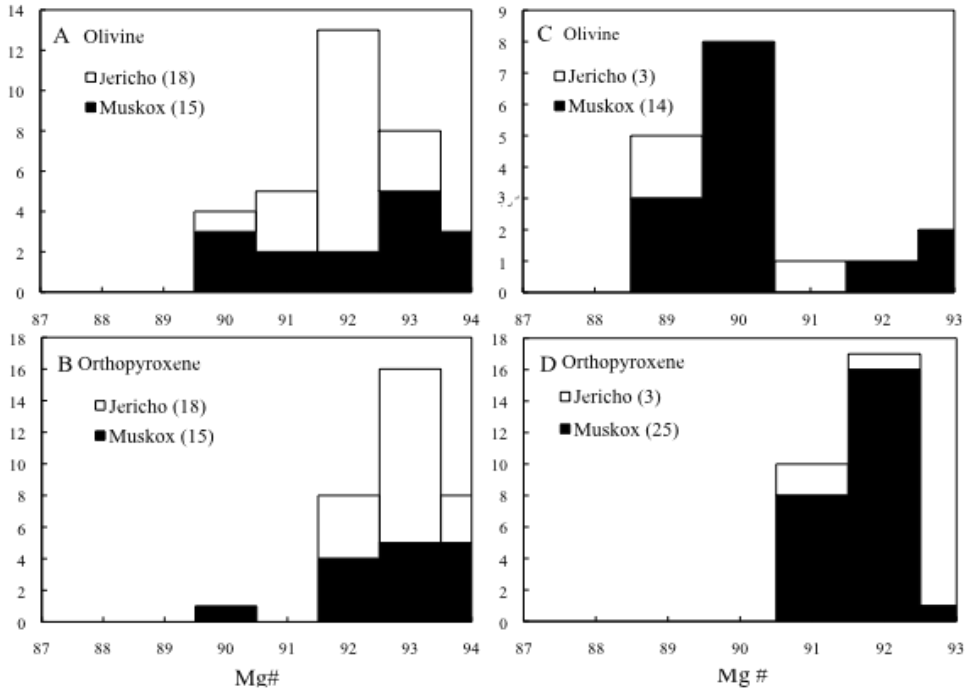
A Olivine
Jericho (18)
Muskox (15)
C Olivine
Jericho (3)
Muskox (14)
B Orthopyroxene
Jericho (18)
Muskox (15)
D Orthopyroxene
Jericho (3)
Muskox (25)
Mg#
Mg #

Fig. 4

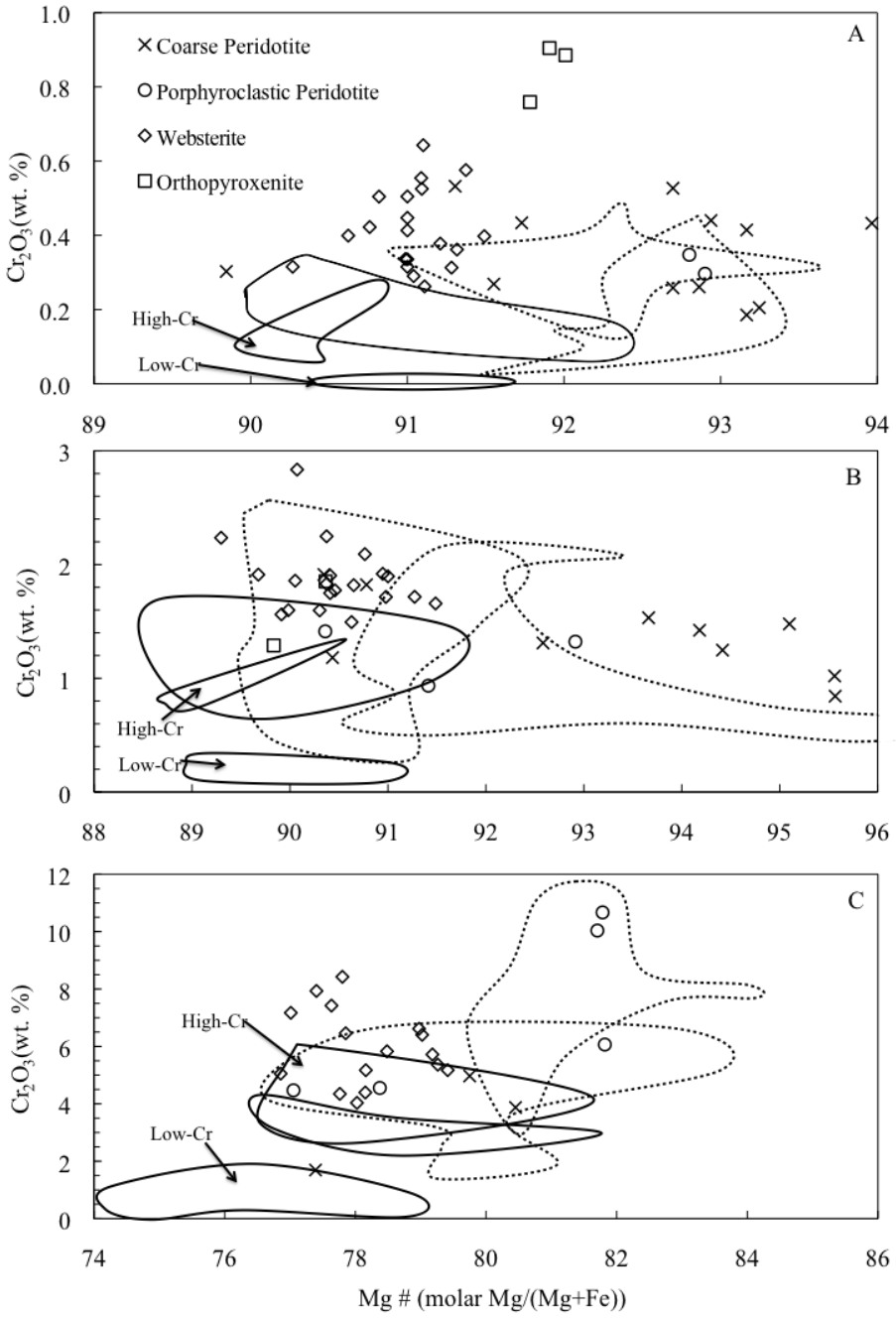
A
Coarse Peridotite
Porphyroclastic Peridotite
Websterite
Orthopyroxenite
High-Cr
Low-Cr
Cr_2O_3(wt. %)
B
C
Mg # (molar Mg/(Mg+Fe))

Fig. 5

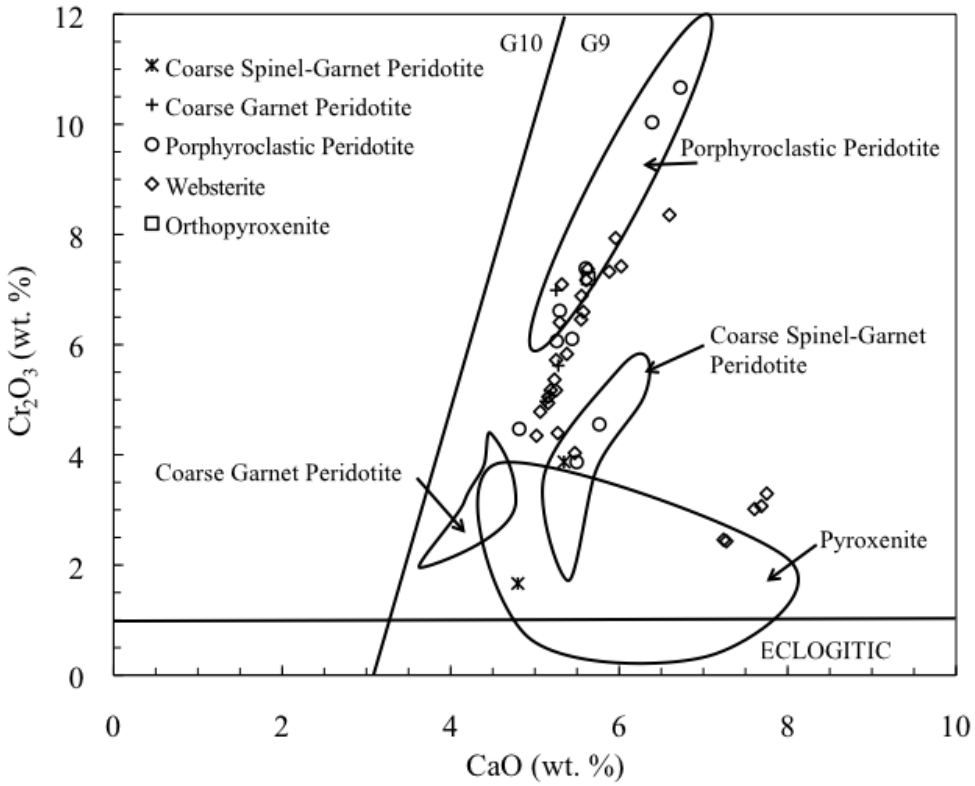
G10
G9
Coarse Spinel-Garnet Peridotite
Coarse Garnet Peridotite
Porphyroclastic Peridotite
Websterite
Orthopyroxenite
Porphyroclastic Peridotite
Coarse Spinel-Garnet Peridotite
Coarse Garnet Peridotite
Pyroxenite
ECLOGITIC
Cr_2O_3 (wt. %)
CaO (wt. %)
0
2
4
6
8
10
12

Fig. 6

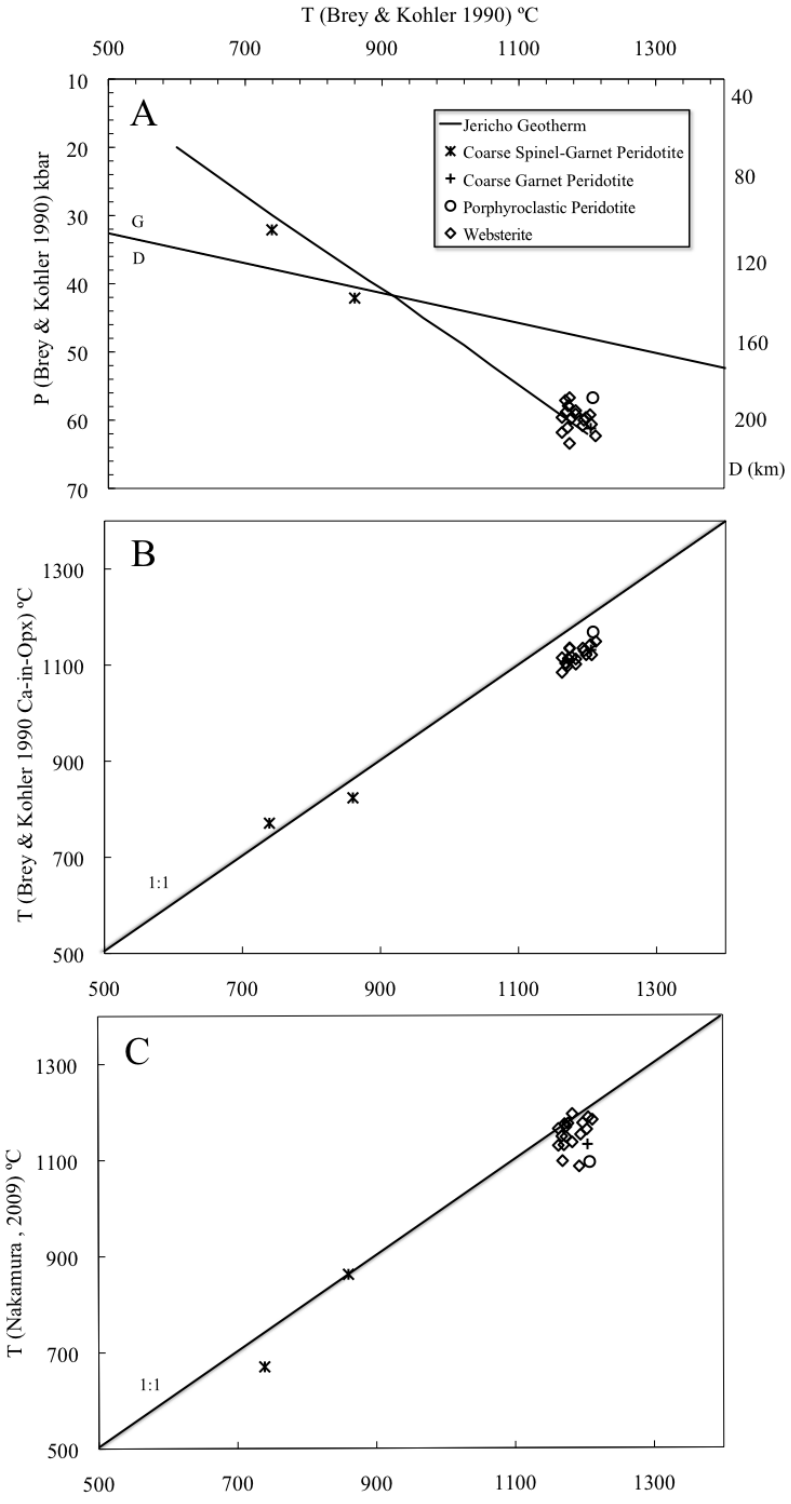
T (Brey & Kohler 1990) ºC
500
700
900
1100
1300
A
Jericho Geotherm
Coarse Spinel-Garnet Peridotite
Coarse Garnet Peridotite
Porphyroclastic Peridotite
Websterite
G
D
P (Brey & Kohler 1990) kbar
10
20
30
40
50
60
70
40
80
120
160
200
D (km)
B
T (Brey & Kohler 1990 Ca-in-Opx) ºC
1:1
C
T (Nakamura , 2009) ºC
1:1

Fig. 7

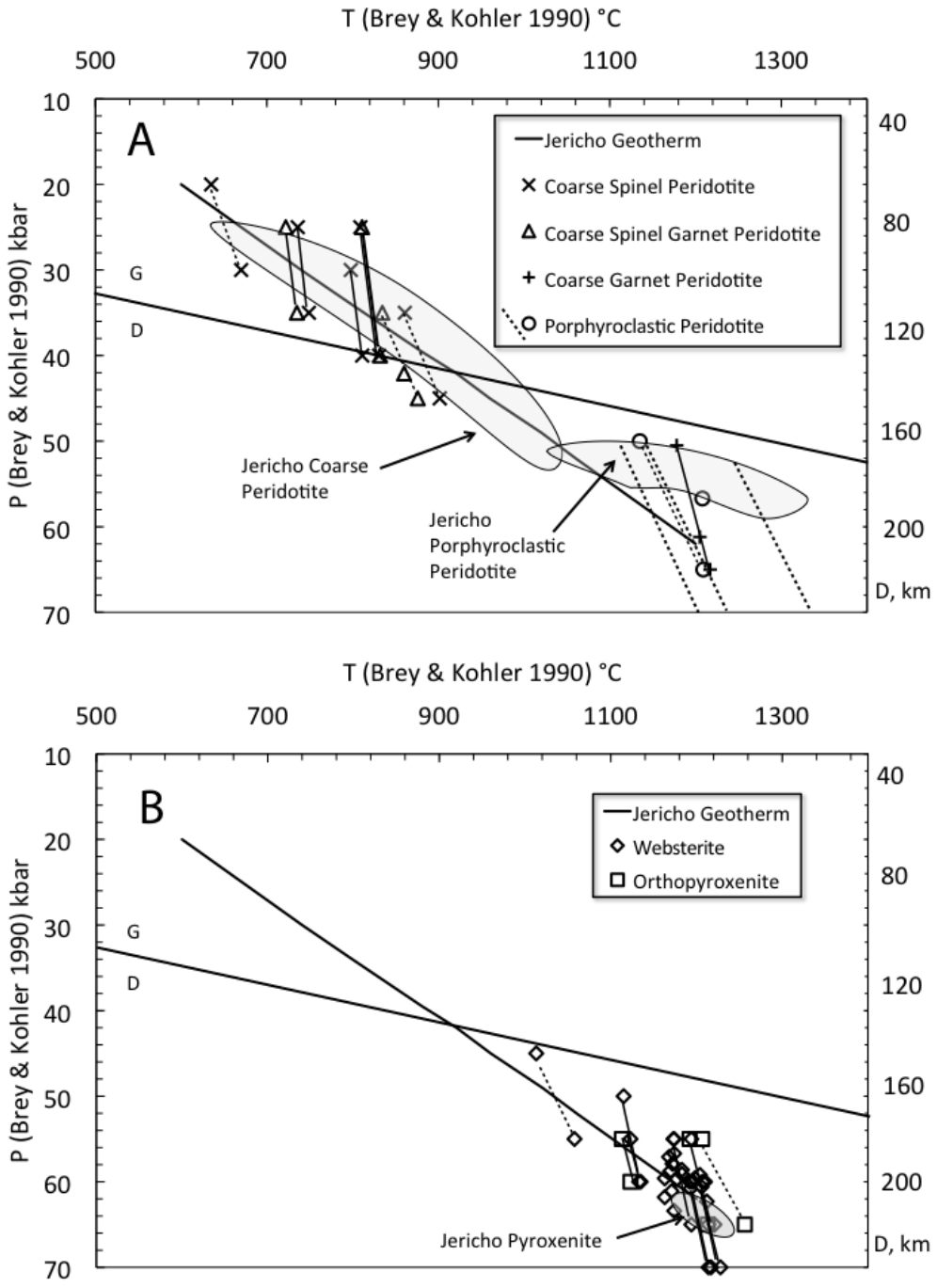
T (Brey & Kohler 1990) °C
500
700
900
1100
1300
P (Brey & Kohler 1990) kbar
10
20
30
40
50
60
70
D, km
40
80
120
160
200
A
Jericho Geotherm
Coarse Spinel Peridotite
Coarse Spinel Garnet Peridotite
Coarse Garnet Peridotite
Porphyroclastic Peridotite
G
D
Jericho Coarse Peridotite
Jericho Porphyroclastic Peridotite
B
Jericho Geotherm
Websterite
Orthopyroxenite
Jericho Pyroxenite

Fig. 8

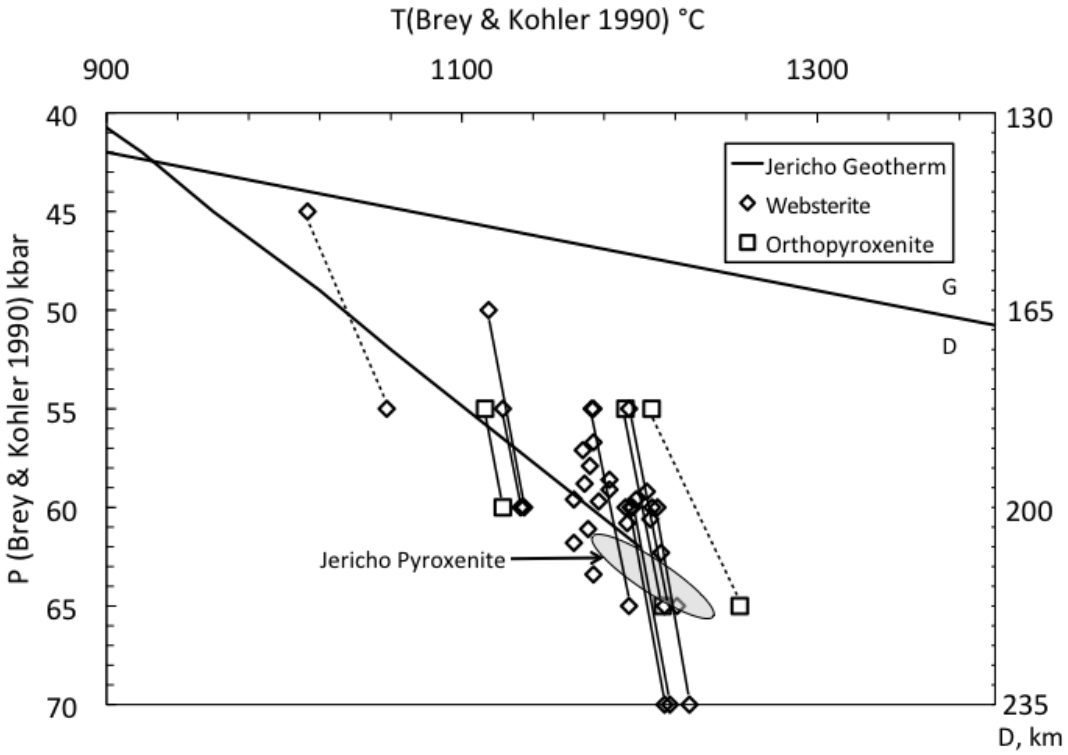
T(Brey & Kohler 1990) °C
900
1100
1300
40
45
50
55
60
65
70
P (Brey & Kohler 1990) kbar
130
165
200
235
D, km
Jericho Geotherm
Websterite
Orthopyroxenite
G
D
Jericho Pyroxenite

Fig. 9

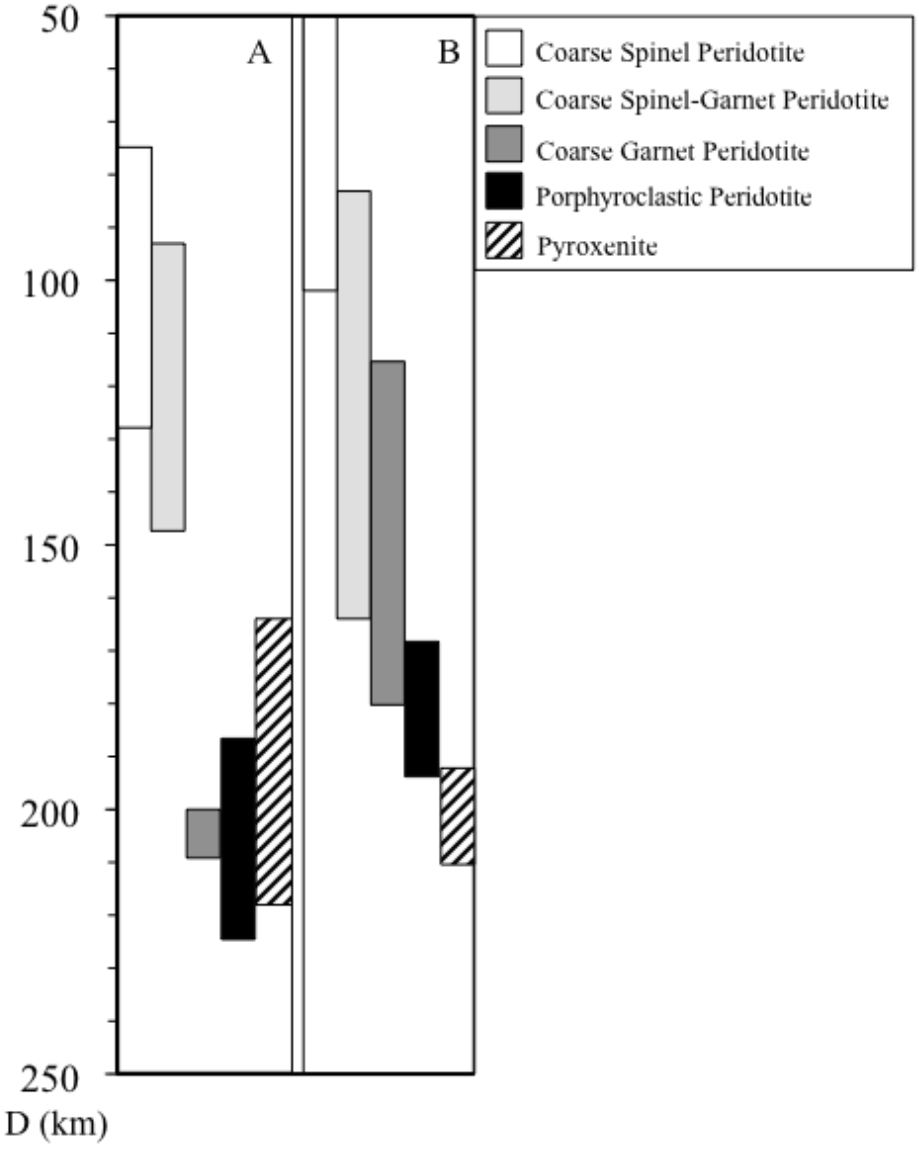
50
100
150
200
250
D (km)
A
B
Coarse Spinel Peridotite
Coarse Spinel-Garnet Peridotite
Coarse Garnet Peridotite
Porphyroclastic Peridotite
Pyroxenite

Fig. 10

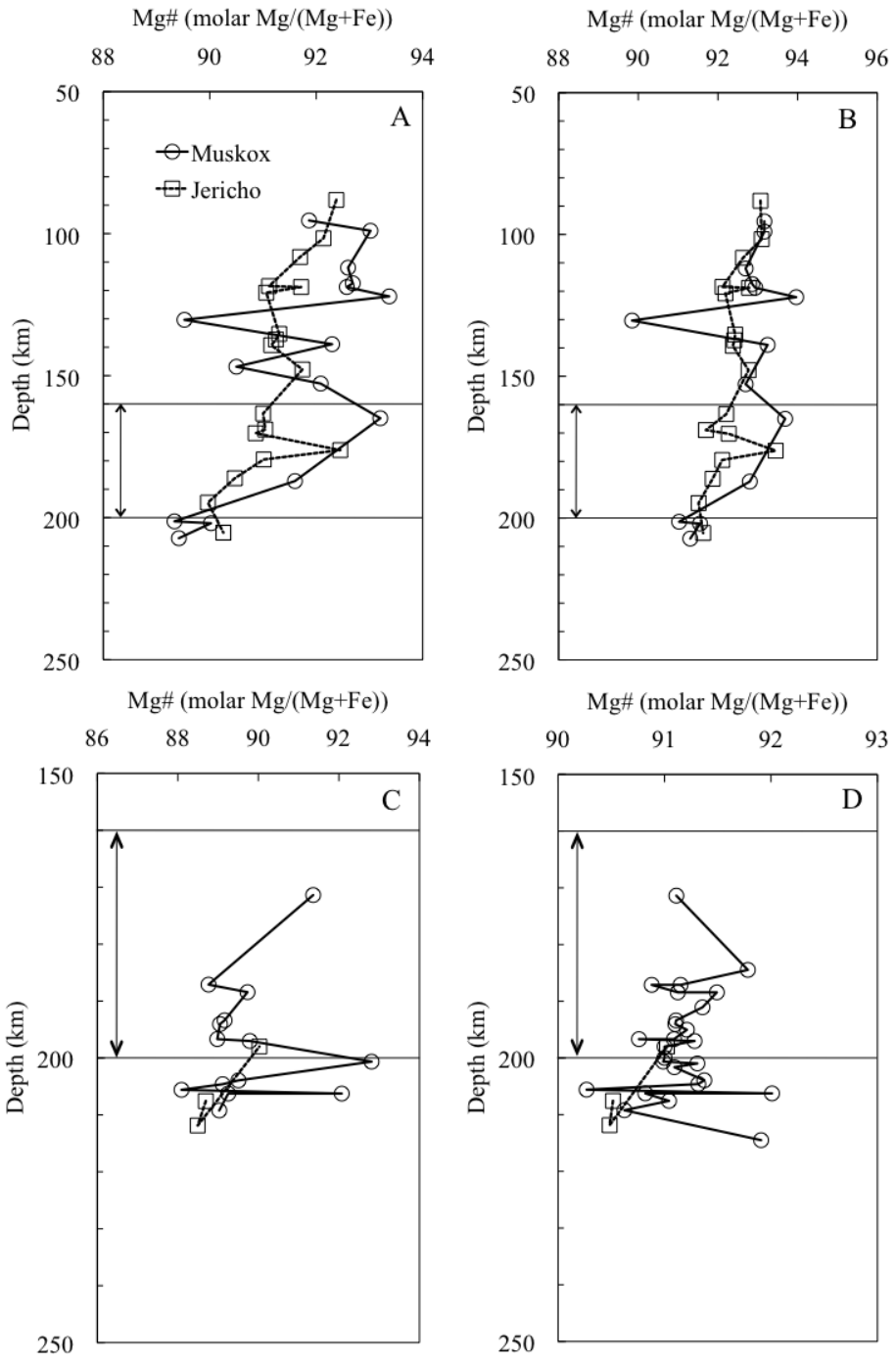
Mg# (molar Mg/(Mg+Fe))
88
90
92
94
50
100
150
200
250
Depth (km)
A
Muskox
Jericho
Mg# (molar Mg/(Mg+Fe))
88
90
92
94
96
B
Mg# (molar Mg/(Mg+Fe))
86
88
90
92
94
150
200
250
C
Mg# (molar Mg/(Mg+Fe))
90
91
92
93
D

Fig. 11

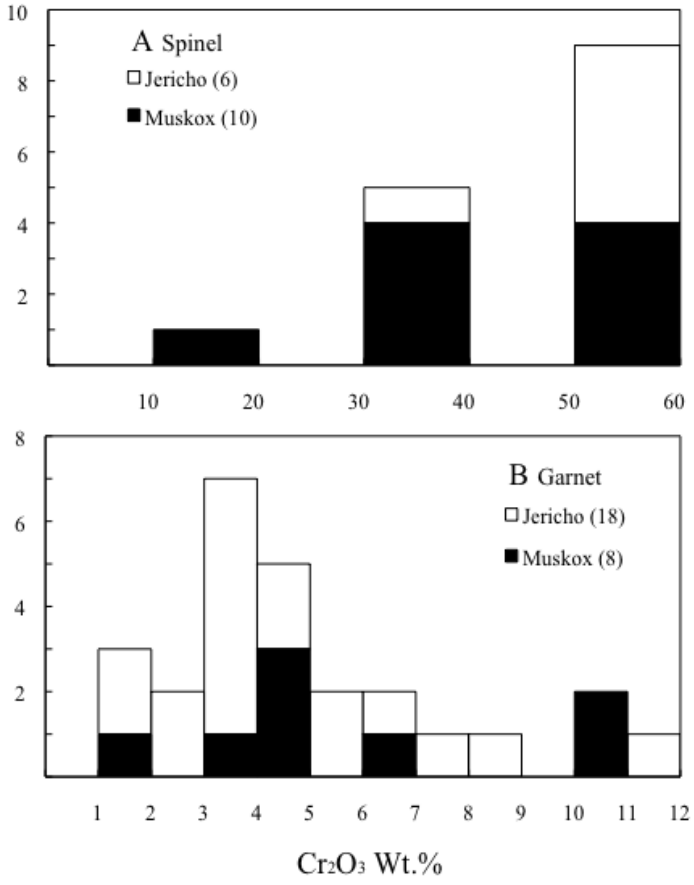
A Spinel
Jericho (6)
Muskox (10)
10
8
6
4
2
10
20
30
40
50
60
B Garnet
Jericho (18)
Muskox (8)
8
6
4
2
1
2
3
4
5
6
7
8
9
10
11
12
Cr2O3 Wt.%

Figure Captions

Fig. 1. (A) Coarse spinel peridotite composed of equant olivine and orthopyroxene grains and smaller, light brown translucent spinel. There is minimal serpentinization of all phases along grain boundaries. (B) Coarse spinel-garnet peridotite composed of equant olivine and orthopyroxene grains, light pink garnet and dark opaque spinel grains. Spinel is often hosted as an inclusion inside larger garnet grains. (C) Coarse garnet peridotite composed of large, equant and fractured olivine, orthopyroxene and garnet grains. Moderate serpentinization of all phases along grain boundaries and in fractures. (D) Porphyroclastic peridotite composed of large olivine porphyroclasts and garnet grains partially surrounded by networks of olivine neoblasts. Garnet is filled with small dark inclusions which are interpreted to be partial melting. (E) Garnet websterite composed of a large, single orthopyroxene grain hosting monogranular networks of highly anhedral clinopyroxene. A large dark patch in the center of the photograph is a cryptocrystalline aggregate of serpentine, phlogopite, spinel and carbonate possibly replacing garnet. (F) Orthopyroxenite composed of a large single orthopyroxene grain, recrystallized into subgrains and small neoblasts along boundaries of larger grains. Here and Figure 2: OL – olivine; OP – orthopyroxene; CP – clinopyroxene; GA – garnet; SP – spinel; AMP – amphibole; PH – phlogopite. All scale bars are 4 mm.

Fig. 2. (A) A coarse spinel peridotite contains translucent brown spinel grains recrystallized into a dark opaque cryptocrystalline aggregate. (B) A coarse spinel peridotite contains large subhedral amphibole grains rimmed by orthopyroxene. A large, dark brown translucent spinel grain is in the lower right hand corner. (C) A coarse spinel peridotite contains phlogopite infiltrating the sample via a network of subparallel veins, forming large anhedral grains and resorbing orthopyroxene and olivine. (D) A coarse spinel-garnet peridotite contains light green, euhedral amphibole in textural equilibrium with olivine and orthopyroxene. Anhedral garnet-rimmed spinel grows as films on primary minerals. (E) A coarse spinel-garnet peridotite contains dark opaque spinel as an inclusion inside texturally equilibrated garnet. (F) A coarse garnet peridotite contains spongy-rimmed clinopyroxene as an anhedral film on grain boundaries of olivine and orthopyroxene. (G) A porphyroclastic peridotite contains large olivine porphyroclasts and garnet grains surrounded by small, isometric olivine neoblasts. Olivine in the center of the photograph has recrystallized into larger, tabular neoblasts. (H) An orthopyroxenite contains large orthopyroxene grains recrystallized into smaller subgrains and tiny neoblasts along boundaries of grains and subgrains. All scale bars are 1 mm except (A) and (H) which are 200 μm.

Fig. 3. Histograms of Mg# (molar Mg/(Mg+Fe)) for olivine (A) and orthopyroxene (B) in Muskox and Jericho peridotites and for olivine (C) and orthopyroxene (D) in Muskox and Jericho pyroxenites. Jericho data from Kopylova et al., 1999.

Fig. 4. Compositions of Muskox minerals plotted as Cr_2O_3 wt.% vs. Mg# for (A) orthopyroxene, (B) clinopyroxene and (C) garnet. Jericho mineral compositions plotted as fields, i.e. Jericho coarse peridotite (coarse dashed line); Jericho porphyroclastic peridotite (fine dashed line); Jericho pyroxenite (solid line); Jericho low-Cr megacrysts (labeled); Jericho high-Cr megacrysts (labeled). Jericho data from Kopylova et al., 1999.

Fig. 5. Compositions of Muskox garnet plotted as Cr_2O_3 wt.% vs. CaO wt.%. Jericho garnet compositions (Kopylova et al. 1999) plotted as labeled fields. Fields for G9, G10 and eclogitic garnets from Grutter et al. (2004).

Fig. 6. (A) Pressure-temperature estimates for Muskox peridotites and pyroxenites calculated by Brey and Kohler (1990) Al-in-orthopyroxene barometer (BK P) and Brey and Kohler (1990) two-pyroxene thermometer (BK T). For this figure and figures below, solid line is the Jericho geotherm constrained by Kopylova et. al. (1999) also using BK P/BK T, solid line is the graphite diamond transition line (Kennedy and Kennedy, 1976). (B) Brey and Kohler (1990) two-pyroxene temperatures plotted against Brey and Kohler (1990) Ca-in-orthopyroxene temperatures computed for the same samples at the same BK P, solid line is a 1:1 relationship. (C) Brey and Kohler (1990) two pyroxene temperatures plotted against Nakamura (2009) temperatures computed for the same samples at the same BK P, solid line is a 1:1 relationship.

Fig. 7. Equilibrium pressure-temperature estimates for Muskox peridotites (A) and pyroxenites (B) according to Brey and Kohler (1990). Solid line is the geotherm constrained for xenoliths from the Jericho kimberlite, calculated using the combined Brey and Kohler (1990) solution (Kopylova et. al., 1999). Graphite-diamond transition line (G/D) is constrained by Kennedy and Kennedy (1976). Samples plotted as single points have both temperature and pressure calculated using combined BK 90 solution. Points joined by lines are calculated for two assumed pressures and shown to intersect the Jericho geotherm. Points joined by dashed lines use BK 90 Ca-in-orthopyroxene thermometer, points joined by solid lines use BK 90 two pyroxene thermometer. Pressure-temperature estimates for Jericho samples (Kopylova et al., 1999) plotted as fields. Dashed univariant lines in Fig. 7A not connected to symbols are for 3 porphyroclastic peridotites calculated with the Nakamura (2009).

Fig. 8. Equilibrium pressure-temperature estimates for Muskox pyroxenites according to Brey and Kohler (1990). Solid line is the geotherm constrained for xenoliths from the Jericho kimberlite, calculated using the combined BK 90 solution (Kopylova et. al., 1999). Graphite diamond equilibrium (G/D) is constrained by Kennedy and Kennedy (1976). Samples plotted as single points have both temperature and pressure calculated using combined BK 90 solution. Points joined by lines are calculated for two assumed pressures and shown to intersect the Jericho geotherm. Points joined by dashed lines use Brey and Kohler 1990 Ca-in-orthopyroxene thermometer, points joined by solid lines use BK 90 two pyroxene thermometer. Pressure-temperature estimates for Jericho pyroxenites (Kopylova et al., 1999) are plotted as a field.

Fig. 9. Depth distribution of rock types in the Muskox (A) and Jericho (B) mantle. Depths for Muskox samples are from Figs. 7, 8 and geothermal intercepts and BK thermobarometric solution in Tables 1-3. Depths for Jericho samples are from BK thermobarometric solutions (Kopylova et al., 1999).

Fig. 10. Depth profiles for Mg# (molar Mg/(Mg+Fe)) in Muskox and Jericho minerals. (A) olivine in peridotite; (B) orthopyroxene in peridotite; (C) olivine in pyroxenite; (D) orthopyroxene in pyroxenite. Depth estimates for Muskox samples are calculated as described in the text. Depth estimates and mineral compositions for Jericho samples are taken from (Kopylova et al., 1999); (Kopylova and Russell, 2000). Double arrow at 160-200 km is the localization of the fertile layer at Jericho manifest in Ca- and Al-rich bulk composition of the mantle (Kopylova and Russell, 2000). Error is within the size of the symbol, standard error of barometry is +/- 6.6 km and the propagated error in the microprobe analyses is +/- .003 Mg#.

Fig. 11. Histograms of wt.% Cr_2O_3 for spinel (A) and garnet (B) in Muskox and Jericho peridotites. Jericho data from Kopylova et al., 1999.

References

1. Artemieva, I.M. 2009. The continental lithosphere: reconciling thermal, seismic, and petrologic data. Lithos. 109 23-46.

2. Aulbach, S., Griffin, W.L., Pearson, N.J., O'Reilly, S.Y., Kivi, K. 2005. Os-Hf-Nd isotope constraints on subcontinental lithospheric mantle evolution, Slave Craton (Canada). Geochimica et Cosmochimica Acta. 69 284.

3. Aulbach, S., Griffin, W.L., Pearson, N.J., O'Reilly, S.Y., Doyle, B.J. 2007. Lithosphere Formation in the central Slave Craton (Canada): Plume Subcretion or Lithosphere Accretion? Contributions to Mineralogy and Petrology. 154 409-427.

4. Bowie, C. 1994. Slave NATMAP; digital release of preliminary Transactions, American Geophysical Union 68, 553–558. datasets on CD-ROM media. In: Kusick, R. and Goff, S. P. (compilers) Geological Investigations. Yellowknife, NWT: Geological Survey of Canada, Northern Affairs Program, NWT Geology Division. 25.

5. Boyd, F.R., Nixon, P.H. 1978. Ultramafic nodules from the Kimberley pipes, South Africa. Geochimica et Cosmochimica Acta. 42 1367-1382.

6. Boyd, F. R., P. H. Nixon, N. Z. Boctor. 1984. Rapidly crystallized garnet pyroxenite xenoliths possibly related to discrete nodules. Contributions to Mineralogy and Petrology. 86.2 119-130.

7. Boyd, F.R., Gurney, J.J. 1986. Diamonds and the African lithosphere. Science. 232 472-477.

8. Boyd, F.R. 1987. High- and low-temperature garnet peridotite xenoliths and their possible relation to the lithosphere-asthenosphere boundary beneath southern Africa. In: Mantle Xenoliths. Nixon P.H. (Ed.) Wiley, New York. 403-412.

9. Boyd, F.R., Canil, D. 1997a. Peridotite xenoliths from the Slave Craton, Northwest Territories. Abstracts, Goldschmidt Conference. 34-35.

10. Boyd, F.R., Pokhilenko, N.P., Pearson, D.G., Mertzman, S.A., Sobolev, N.V., Finger, L.W. 1997b. Composition of the Siberian cratonic mantle: evidence from Udachnaya peridotite xenoliths. Contributions to Mineral Petrology. 128 228-246.

11. Brey, G.P., Kohler, T. (1990). Geothermobarometry in four-phase lherzolites I. Experimental results from 10 to 60 kb. Journal of Petrology. 31 1313-1352.

12. Brey, G.P., Kohler, T. (1990). Geothermobarometry in four-phase lherzolites II. New thermobarometers, and practical assessment of existing thermobarometers. Journal of Petrology. 31 1353-1378.

13. Burgess, S.R., and Harte, B. 2004. Tracing lithosphere evolution through the analysis of heterogeneous G9–G10 garnets in peridotite xenoliths, II: REE chemistry. Journal of Petrology 45.3 609-633.

14. Carbno, G.B., Canil, D. 2002. Mantle structure beneath the SW Slave craton: constraints from garnet geochemistry in the Drybones Bay kimberlite. Journal of Petrology. 43 129-142.

15. Carlson, R.W., Pearson, D.G., James, D.E. 2005. Physical, chemical and geochronological characteristics of continental mantle. Reviews of Geophysics. 43 1-24.

16. Chu, X., Korenaga, J. 2012. Olivine rheology, shear stress, and grain growth in the lithospheric mantle: geological constraints from the Kaapvaal craton. Earth and Planetary Science Letters. 333–334 52-6.

17. Cookenboo, H. 1998. Emplacement history of the Jericho kimberlite pipe, northern Canada. In: Extended Abstracts of the 7th International Kimberlite Conference. 161–163.

18. Creighton, S., Stachel, T., Eichenberg, D., Luth, R.W. 2010. Oxidation State of the Lithospheric Mantle Beneath Diavik Diamond Mine, Central Slave Craton, NWT, Canada. Contributions to Mineralogy and Petrology. 159 645-657.

19. Dawson, J.B., Smith, J.V. 1977. The MARID (mica-amphibole-rutile-ilmenite-diopside) suite of xenoliths in kimberlite. Geochimica et Cosmochimica Acta. 41 301-323.

20. Davis, W.J., Jones, A.G., Bleeker, W., Grutter, H. 2003. Lithosphere development in the Slave craton: a linked crustal and mantle perspective. Lithos. 71 575-589.

21. Doyle, P. M., D. R. Bell, A. P. Le Roex. 2004. Fine-grained pyroxenites from the Gansfontein kimberlite, South Africa: Evidence for megacryst magma–mantle interaction. South African Journal of Geology 107. 1-2 285-300.

22. Drury, M.R., Van Roermund, H.L.M. 1989. Fluid assisted recrystallization in upper mantle peridotite xenoliths from kimberlites. Journal of Petrology. 30 133-152.

23. Erlank, A. J., Waters, F. G., Hawkesworth, C. J., Haggerty, S. E., Allsopp, H. L., Rickard, R. S., Menzies, M. A. 1987. Evidence for mantle metasomatism in peridotite nodules from the Kimberley pipes, South Africa. Mantle metasomatism. 221-311.

24. Finnerty, A.A., Boyd, J.J. 1987. Thermobarometry for garnet peridotites: basis for the determination of thermal and compositional structure of the upper mantle. In: Mantle Xenoliths. 381-402.

25. Foley, S.F., Buhre, S., Jacob, D.E. 2003 Evolution of the Archaean crust by delamination and shallow subduction. Nature. 421 249-252.

26. Girnis, A.V., Brey, G.P. (1999). Garnet-spinel-orthopyroxene equilibria in the FeO-MgO-Al_2O_3-SiO_2-Cr_2O_3 system: II. Thermodynamic analysis. European Journal of Mineralogy. 11 619-636.

27. Goetze, C. 1975. Sheared lherzolites: from the point of view of rock mechanics. Geology. 3 172-173.

28. Gregoire, M., Bell, D.R., Le Roex, A.P. 2002. Trace element geochemistry of Glimmerite and MARID mantle xenoliths: their classification and relationship to phlogopite-bearing peridotites and to kimberlites revisited. Contributions to Mineralogy and Petrology. 142 603-625.

29. Gregoire, M., Bell, D.R., Le Roex, A.P. 2003. Garnet lherzolites from the Kaapvaal craton, (South Africa): trace element evidence for a metasomatic history. Journal of Petrology. 44 629-657.

30. Griffin, W.L., Smith, D., Ryan, C.G., O'Reilly, S.Y., Win, T.T. 1996. Trace-element zoning in mantle minerals: metasomatism and thermal events in the upper mantle. The Canadian Mineralogist. 34 1179-1193.

31. Griffin, W.L., O'Reilly, S.Y., Ryan, C.G. 1999a. The composition and origin of subcontinental lithosphere. In: Fey, Y. (ed.) Mantle Petrology: Field Observations in High Pressure Experimentation.

32. Griffin, W.L., Doyle, B.J., Ryan, C.G., Pearson, N.J., O'Reilly, S.Y., Davies, R., Kivi, K., VanAchterberg, E., Natapov, L.M. 1999b. Layered Mantle Lithosphere in the Lac de Gras Area, Slave Craton: Composition, Structure and Origin. Journal of Petrology 40 705-727.

33. Grutter, H.S., Apter, D.B., Kong, J. 1999. Crust-mantle coupling: evidence from mantle-derived xenocrystic garnets. In: Proceedings of the 7th International Kimberlite Conference. 307-313.

34. Grutter, H., Latti, D., Menzies, A. 2006. Cr-saturation arrays in concentrate garnet compositions from kimberlite and their use in mantle barometry. Journal of Petrology. 47 801-820.

35. Gurney, J. J., and Harte, B. 1980. Chemical variations in upper mantle nodules from southern African kimberlites." Philosophical Transactions of the Royal Society of London. Series A, Mathematical and Physical Sciences. 297 273-293.

36. Gurney, J.J., Zweistra, P. 1995. The interpretation of the major element compositions of mantle minerals in diamond exploration. Journal of Geochemical Exploration. 53 239-309.

37. Harte, B. (1977). Rock nomenclature with particular relation to deformation and recrystallization textures in olivine-bearing xenoliths. Journal of Geology. 85 279-288

38. Harte, B., Hawkesworth, C.J. 1989. Mantle domains and mantle xenoliths. In Kimberlites and Related Rocks. 2 649-686.

39. Hayman, P. C., R. A. F. Cas, and Michael Johnson. 2008. Difficulties in distinguishing coherent from fragmental kimberlite: a case study of the Muskox pipe (Northern Slave Province, Nunavut, Canada). Journal of Volcanology and Geothermal Research. 174 139-151.

40. Heaman, L. M., Kjarsgaard, B., Creaser, C.A. 1997. Multiple episodes of kimberlite magmatism in the Slave Province, North America. Lithoprobe Workshop Report. 56.

41. Heaman. L.M., Pearson, D.G. 2010. Nature and evolution of the Slave province subcontinental lithosphere. Canadian Journal of Earth Sciences. 47 369-388.

42. Helmstead, H. H., Pehrsson, S. J. 2012. Geology and tectonic evolution of the Slave province- a post-Lithoprobe perspective. In: Tectonic Styles in Canada: The Lithoprobe Perspective. 379-466.

43. Hoffman, P.F. 1989. Precambrian geology and tectonic history of North America. In: The Geology of North America-An Overview. Bally, A.W., Palmer, A.R. (Eds.) GSA Boulder, VA. 447-512.

44. Hofmann, A. W. 2003. Sampling mantle heterogeneity through oceanic basalts: isotopes and trace elements. Treatise on geochemistry. 2 61-101.

45. Hops, J.J., Gurney, J.J., Harte, B., Winterburn, P. 1989. Megacrysts and high temperature nodules from the Jagersfontein kimberlite pipe. Geological Society of Australia. Special Publication. 14 759-770.

46. Irvine, G.J., Kopylova, M.G., Carlson, R.W., Pearson, D.G., Shirey, S.B., Kjarsgaard, B.A. 1999. Age of lithospheric mantle beneath and around the slave craton: a Re-Os isotope study of peridotite xenoliths from the Jericho and Somerset Island kimberlites. Abstract. Goldschmidt Conference 1999.

47. Jones, R.A., Smith, J.V., Dawson, J.B. 1982. Mantle metasomatism in 14 veined peridotites from Bulfontein mine, South Africa. Journal of Geology. 90 435-453.

48. Jung, H., Karato, S.I. 2001. Effects of water on dynamically recrystallized grain-size of olivine. Journal of Structural Geology. 9 1337-1344.

49. Karato, S., Wu, P. 1993. Rheology of the upper mantle: a synthesis. Science. 260 771-778.

50. Kennedy, C.S., Kennedy, G.C. (1976). The equilibrium boundary between graphite and diamond. Journal of Geophysical Research. 14 2467-2470.

51. Kennedy, L.A., Russell, J.K., Kopylova, M.G. 2001. Mantle shear zones revisited: the connection between the cratons and mantle dynamics. Geology. 2002. 30 419-422.

52. Konzett. J., Armstrong, R.A., Sweeney, R.J., Compston, W. 2000. Modal metasomatism in the Kaapvaal craton lithosphere: constraints on timing and genesis from U-Pb zircon dating of metasomatized peridotite and MARID-type xenoliths. Contributions to mineral petrology. 139 794-719.

53. Koornneef, J.M., Davies, G.R., Dopp, S.P., Vukmanovic, Z., Nikogosian, I.K., Mason, P.R.D. 2009. Nature and timing of multiple metasomatic events in the sub-cratonic lithosphere beneath Labait, Tanzania. Lithos. 112S 896-912.

54. Kopylova, M.G., Russell, J.K., Cookenboo, H. 1998. Mapping the lithosphere beneath the North Central Slave Craton. In: Proceedings of the 7th International Kimberlite Conference. 468-479.

55. Kopylova, M.G., Russell, J.K., Cookenboo, H. 1999. Petrology of peridotite and pyroxenite xenoliths from the Jericho Kimberlite: Implications for the thermal state of the mantle beneath the Slave craton, northern Canada. Journal of Petrology. 40 79-104.

56. Kopylova, M.G., Russell, J.K. 2000. Chemical stratification of cratonic lithosphere: constraints from the northern Slave craton, Canada. Earth and Planetary Science Letters. 181 71-87

.

57. Kopylova, M. G., Caro, G. 2004. Mantle xenoliths from the southeastern slave craton: evidence for chemical zonation in a thick, cold lithosphere. Journal of Petrology. 5 1045-1067

58. Kopylova, M.G., Hayman P. 2008. Petrology and textural classification of the Jericho kimberlite, northern Slave Province, Nunavut, Canada. Canadian Journal of Earth Sciences. 45 701-723.

59. Kopylova, M.G., Nowell, G.M., Pearson, D.G., Markovic, G. 2009. Crystallization of megacrysts from protokimberlitic fluids: geochemical evidence from high-Cr megacrysts in the Jericho kimberlite. Lithos. 112S 284-295.

60. Lock, N.P., Dawson, J.B. 2013. Contrasting garnet lherzolite xenolith suites from the Letseng kimberlite pipes: inferences for the northern Lesotho geotherm. Proceedings of the 10th International Kimberlite Conference. 1 29-44.

61. MacGregor, I.D. 1974. The system MgO-Al_2O_3-SiO_2: solubility of Al_2O_3 in enstatite for spinel and garnet peridotite compositions. American Mineralogist. 59 110-119.

62. MacKenzie, J.M., Canil, D. 1999. Composition and thermal evolution of cratonic mantle beneath the central Archean Slave Province, NWT, Canada. Contributions to Mineral Petrology. 134 313-324.

63. McCammon, C., Kopylova, M.G. (2004). A redox profile of the Slave mantle and oxygen fugacity control in the cratonic mantle. Contributions to Mineral Petrology. 148 55-68.

64. Mei. S., Kohlstedt, D.L. 2000. Influence of water on plastic deformation of olivine aggregates 2. Dislocation creep regime. Journal of Geophysical Research. 105 21,471-21,481.

65. Menzies, A., Westerlund, K., Grutter, H., Gurney, J., Carlson, J., Fung, A., Nowicki, T. 2004. Peridotitic mantle xenoliths from kimberlites on the Ekati diamond mine property, N.W.T., Canada: major element compositions and implications for the lithosphere beneath the central Slave craton. Lithos. 77 395-412.

66. Miller, C.E., Kopylova, M., Smith, E.M. 2014. Mineral inclusions in fibrous diamonds: constraints on cratonic mantle refertilization and diamond formation. Mineralogy and Petrology. 108 317-331.

67. Moore, A., Belousova E. 2005. Crystallization of Cr-poor and Cr-rich megacryst suites from the host kimberlite magma: implications for mantle structure and the generation of kimberlite magmas. Contributions to Mineralogy and Petrology. 149 462-481.

68. Nakamura, D. 2009. A new formulation of garnet-clinopyroxene geothermometer based on accumulation and statistical analysis of a large experimental data set. Journal of Metamorphic Geology. 27 495-508.

69. Nickel, K.G., Green, D.H. 1985. Empirical geothermobarometry for garnet peridotites and implications for the nature of the lithosphere, kimberlites and diamonds. Earth and Planetary Science Letters. 73 158-170.

70. Nixon, P.H., Boyd, F.R. 1973. Petrogenesis of the granular and sheared ultrabasic nodule suite in kimberlite. In: Nixon, P.H. (ed.) Lesotho Kimberlites. Cape and Transvaal, Cape Town. 48-56.

71. O'Neill, H., Wood, B.J., 1979. An experimental study of Fe-Mg partitioning between garnet and olivine and its calibration as a geothermometer. Contributions to Mineralogy and Petrology. 70 59-70.

72. O'Neill. H.S.C., 1981. The transition between spinel lherzolite and garnet lherzolite, and its use as a geobarometer. Contributions to Mineralogy and Petrology. 77 185-194.

73. O'Neill, H., Wall, V.J. 1987. The olivine-orthopyroxene –spinel oxygen geobarometer, the nickel precipitation curve, and the oxygen fugacity of the Earth's upper mantle. Journal of Petrology. 28 1169-1191.

74. O'Reilly, S.Y., Griffin, W.L. 2010. The continental lithosphere-asthenosphere boundary: can we sample it? 2010. Lithos. 120 1-13.

75. O'Reilly, S.Y., Griffin, W.L., Ryan, C.G. 1991. Residence of trace elements in metasomatized spinel lherzolite xenoliths: a proton-microprobe study. Contributions to Mineralogy and Petrology. 109 98-113

76. Pearson, D.G., Davies, G.R., Nixon, P.H. 1993. Geochemical constraints on the petrogenesis of diamond facies pyroxenites from the Beni Bousera peridotite massif, North Morocco. Journal of Petrology. 34 125-172.

77. Pearson, N.J., Griffin, W.L., Doyle, B.J., O'Reilly, S.Y., Van Achterbergh, E., Kivi, K. 1999. Xenoliths from Kimberlite Pipes of the Lac de Gras area, Slave Craton, Canada. Proceedings of the 7th international Kimberlite conference. 2 644-658.

78. Pearson, D.G., Canil, D., Shirey, S.B. 2003. Mantle samples included in volcanic rocks: xenoliths and diamonds. In: Holland, H.D. and Turekian, K.K. (eds.) Treatise on Geochemistry. Elsevier, Amsterdam. 171-275.

79. Pearson, D.G., Wittig, N. 2008. Formation of Archean continental lithosphere and its diamonds: the root of the problem. Journal of the Geological Society. 165 895-914.

80. Pell J.A. 1997. Kimberlites in the Slave craton, Northwest Territories, Canada Geoscience Canada. 24 77–91.

81. Rawlinson, P.J., Dawson, J. B. J. 1979. A Quench Pyroxene-Ilmenite Xenolith from Kimberlite: Implications for Pyroxene-Ilmenite Intergrowths. The Mantle Sample: Inclusions in Kimberlites and Other Volcanics 292-299.

82. Rehfeldt, T., Foley, S.F., Jacob, D.E., Carlson, R.W., Lowry, D. 2008. Contrasting types of metasomatism in dunite, wehrlite and websterite xenoliths from Kimberley, South Africa. Geochimica et Cosmochimica Acta 72 5722-5756.

83. Sen, C., Denn, T. 1994. Experimental modal metasomatism of a spinel lherzolite and the production of amphibole-bearing peridotite. Contributions to Mineral Petrology. 119 422-432

84. Skemer, P. Warren, J.M. Hirth, G. 2013. The influence of water and LPO on the initiation and evolution of mantle shear zones. Earth and Planetary Science Letters. 375 222-233.

85. Simon, N.S.C., Carlson, R.W., Pearson, D.G., Davies, G.R. 2007. The Origin and evolution of the Kaapvaal cratonic mantle lithosphere. Journal of Petrology. 48 589-625.

86. Smith, D., and F. R. Boyd. 1987. Compositional heterogeneities in a high-temperature lherzolite nodule and implications for mantle processes. In: Mantle Xenoliths. 551 561.

87. Smith, D. (1999). Temperatures and pressures of mineral equilibrium in peridotite xenoliths: review, discussion and implications. The Geochemical Society Special Publication. 6 171-187.

88. Sobolev, N.V., Lavrent'ev, Y.G., Pokhilenko, N.P., Usova, N.P. 1973. Chrome-rich garnets from the kimberlites of Yakutia and their parageneses. Contributions to Mineralogy and Petrology. 40. 39-52.

89. Solovjeva, L.V., Vladimirov, B.M., Zavjalova, L.L. 1987. Evolution of the upper mantle: evidence from the deep seated xenoliths in the Siberian kimberlites. In: Deep-seated xenoliths and the lithosphere structure. Nauka. Moscow. 96-108. (in Russian).

90. van Breemen, O., Thompson, P. H., Hunt, P. A,, and Culshaw, N. 1987. U - Pb zircon and monazite geochronology from the northern Thelon Tectonic Zone, District of Mackenzie. In: Radiogenic age and isotopic studies: report 1. Geological Survey of Canada. 87-2 81 -93.

91. Wallace, M.E., Green, D.H. 1991. The effect of bulk rock composition on the stability of amphibole in the upper mantle: implications for solidus positions and mantle metasomatism. Mineralogy and Petrology., 44 1-19.

92. Walker, R.J., Carlson, R.W., Shirey, S.B., Boyd, F.R. 1989. Os, Sr, Nd and Pb isotope systematics of southern African peridotite xenoliths: implications for the chemical evolution of subcontinental mantle. Geochimica et Cosmochimica Acta. 53 1583-1595.

93. Wang, Q. 2010. A review of water contents and ductile deformation mechanisms of olivine: implications for the lithosphere-asthenosphere boundary of continents. Lithos. 120 30-41.

94. Walter, M. J. 2003. Melt extraction and compositional variability in mantle lithosphere. *Treatise on geochemistry* 2: 363-394.

95. Waters, F.G., Erlank, A.J., Daniels, L.R.M. 1989. Contact relationship between MARID rock and metasomatized peridotite in a kimberlite xenolith. Geochemical Journal 23 11-17.

96. Winterburn, P.A., Harte, B., Gurney, J.J. 1990. Peridotite xenoliths from the Jagersfontein kimberlite pipe: I. Primary and primary-metasomatic mineralogy. Geochimica et Cosmochimica Acta. 54 39-34

Appendix A: Muskox Xenolith Sample List

Sample ID	Rock Type	Macrospecimen Description	Size (cm^3)	Thin Section?
DDH2 91.5	Porphyroclastic Peridotite	Mosaic garnet peridotite. 10% round garnet, 90% neoblasts. Pyroxenes stand out.	5x7x3	Yes
MOX0 157.45*	Websterite	Clinopyroxene+olivine+garnet+phlogopite rock. 20% phlogopite	3x3	
MOX0 158.8*	Websterite	Garnet pyroxenite. Purple garnet, Cr-diopside. 50% altered to chlorite.	3x2	
MOX0 162.8 A	Websterite	Fine-grained. Possibly sheared.	3x3x0.5	Yes
MOX0 162.8 B	Websterite	Garnet-olivine websterite. Fine-grained with 30% melt pockets.	1x1x1	
MOX0 179.3	Websterite	Fine-grained garnet pyroxenite.	4x3x0.5	Yes
MOX0 197.0	Websterite	Garnet-olivine websterite. Large orthopyroxenes, 10% phlogopite.	4x3x0.5	
MOX0 198.37	Websterite	Garnet websterite with 10% phlogopite.	4x2x1	Yes
MOX0 216.83	Websterite	Large grained pyroxenite with minor garnet and olivine. Clinopyroxene exsolution lamellae in orthopyroxene along xenolith margin.	10x6x2	
MOX0 233.5	Websterite	Fine-grained pyroxenite with olivine? 50% altered to serpentine+phlogopite in melt patches.	4x3x3	
MOX1 45.5	Coarse Garnet Peridotite	Garnet lherzolite. Orthopyroxene is difficult to see. Rare clinopyroxene.	5x5x3	Yes
MOX1 48.6	Orthopyroxenite	Orthopyroxenite. Clinopyroxene is rare. 1 cm margin of xenolith is 100% serpentinized. Xenolith is melted with 10% melt pockets.	8x3x1	
MOX1 59	Websterite	Garnet (?) pyroxenite containing 10% melt pockets. Central portion of xenolith is a large olivine grain. Marginal portion is pyroxene intergrowth possibly containing garnet.	5x4x3	Yes
MOX1 107.5	Coarse Spinel Peridotite	Coarse spinel-harzburgite with no clinopyroxene.	7x5x3	Yes
MOX3 33	Coarse Spinel-Garnet Peridotite	Fresh, coarse spinel-garnet lherzolite.	4x3x2	Yes
MOX3 42.1	Websterite	Fresh, coarse olivine websterite with 20% melt pockets.	5x4x3	Yes

Sample ID	Rock Type	Macrospecimen Description	Size (cm^3)	Thin Section?
MOX3 69.2	Coarse Spinel Peridotite	Coarse or deformed spinel-lherzolite with 2% clinopyroxene and 20% othopyroxene.	8x3x4	Yes
MOX3 74.4	Websterite	Olivine websterite with magmatic texture and 10% melt pockets.	2x1x4	
MOX3 78.8A	Websterite	Pyroxenite. Clinopyroxene is rare, spinel is rare.	5x4x4	
MOX3 78.8B	Websterite	Pyroxenite, contains 30% melt pockets.	1x3x1	
MOX7 30	Websterite	Olivine websterite, 50% black melt pockets. Medium grained with equal modes of orthopyroxene and clinopyroxene and 10% olivine.	6x6x6	
MOX7 54	Websterite	Coarse-grained websterite with no olivine, garnet or spinel.	3x2x1	
MOX7 62.3	Coarse Spinel-Garnet Peridotite	Fine-grained harzburgite. Clinopyroxene is rare. Sample is possibly deformed.		Yes
MOX7 97.6	Coarse Spinel Peridotite	Spinel-harzburgite with 0.5 cm serpentinized margin.	4x4x5	
MOX11 122.2	Websterite	Coarse-grained pyroxenite with 90% orthopyroxene and inclusions of garnet and clinopyroxene, possibly recrystzallized lamellae. 10% melt pockets.	6x6x4	Yes
MOX11 162.1	Porphyroclastic Peridotite	Garnet harzburgite with G10 garnets and rare clinopyroxene.	4x4x2	Yes
MOX11 200.5	Websterite	Coarse grained olivine websterite with 30% melt pockets and possibly rare garnets.	3x3x2	
MOX11 287.6	Websterite	Olivine-garnet pyroxenite containing 10% black serpentine, 30% garnet, 50% orthopyroxene, 10% olivine and 5% clinopyroxene.	4x3x3	
MOX24 31.1A*	Coarse Spinel Peridotite	Fine-grained spinel lherzolite.	2x5	Yes
MOX24 31.1B	Orthopyroxenite	Fresh, medium grained orthopyroxenite. 5% clinopyroxene.	5x1x0.5	
MOX24 42.6	Websterite	Garnet pyroxenite with abundant melt pockets and phlogopite-carbonate veinlets.	8x3x3	Yes
MOX24 43.35	Websterite	Garnet pyroxenite 30% fine-grained melt pockets.	8x4x3	Yes
MOX24 65.1	Coarse Spinel Peridotite	Spinel harzburgite with rare clinopyroxene.	1x1x1	

Sample ID	Rock Type	Macrospecimen Description	Size (cm^3)	Thin Section?
MOX24 84.8	Coarse Spinel Peridotite	Fine-grained spinel lherzolite.	3x4x2	
MOX24 105.2	Websterite	Large grained pyroxenite with 10% exsolved clinopyroxene. Xenolith margin is serpentinized with melt pockets.	5x2x1	
MOX24 124.0A	Porphyroclastic Peridotite	Garnet harzburgite with rare clinopyroxene.	8x6x4	Yes
MOX24 124.0B*	Coarse Spinel Peridotite	Fine-grained spinel-lherzolite.	2x1	
MOX24 206.7	Websterite	Large grained garnet (?)-olivine(?) websterite with 10% melt pockets, 40% clinopyroxene, 40% orthopyroxene, 5% olivine (?), 5% fine-grained brown garnet possibly serpentine+phlogopite.	8x3x3	Yes
MOX24 240	Websterite	Partially molten olivine websterite, mostly orthopyroxene with large clinopyroxenes at xenolith margin. 50% serpentine, phlogopite and melt pockets.	3x3x6	
MOX24 255.4	Websterite	Garnet-olvine pyroxenite. 80% recrystallized clinopyroxene, 10% fine-grained melt pockets, 5% orthopyroxene, 5% fine-grained garnet.		
MOX25 120.6A	Websterite	Olivine websterite, 30% fine-grained melt pockets.	8x3x5	
MOX25 120.6B	Orthopyroxenite	Medium-grained orthopyroxenite with unusual lath texture. No clinopyroxene, garnet or spinel.	5x3x1	Yes
MOX25 124.8	Porphyroclastic Peridotite	Coarse or porphyroclastic garnet harzburgite or dunite. Contains rare clinopyroxene.	8x5x3	Yes
MOX25 161.5B	Coarse Spinel Peridotite	Coarse lherzolite, 10% serpentinized, contains no spinel or garnet.	6x4x4	Yes
MOX25 161.5C	Websterite	Olivine pyroxenite containing 50% melt pockets.	4x4x1	Yes
MOX25 246.1*	Websterite	Garnet websterite, possibly contains olivine.	1x2	Yes
MOX28 269.6	Orthopyroxenite	Coarse-grained, 30% orthopyroxene and 1% clinopyroxene, 1% olivine. Contains no spinel or garnet.	10x5x4	Yes
MOX28 320.1	Porphyroclastic Peridotite	2 xenoliths of the same rock. Coarse grained garnet-lherzolite with 30% olivine and 50% clinopyroxene, garnet ansd spinel.	8x6x4	Yes

Sample ID	Rock Type	Macrospecimen Description	Size (cm^3)	Thin Section?
MOX31 224.5	Coarse Garnet Peridotite	Medium-grained lherzolite, 30% serpentinized. No spinel or garnet.	4x4x2	Yes
MOX31 230.7	Websterite	Olivine-garnet pyroxenite with large garnet grains and 50% melt pockets.	5x3x3	
MOX31 242.5	Websterite	Altered websterite with <70% of pyroxenes serpentinized. Veins of white carbonate, sulfides may be present.	3x3x2	
MOX31 242.6	Websterite	Coarse-grained pyroxenite with 20-30% clinopyroxene and possibly spinel.	5x1x1	
MOX31 281.2	Websterite	Coarse-grained magmatic textured websterite with 30% melt pockets.		

Appendix B: Petrographic Descriptions

Sample ID: DDH2 91.5

Sample Type: Porphyroclastic Peridotite

This is a 100% altered mosaic-porphyroclastic garnet peridotite. Almost all phases are altered to either serpentine or talc. Some larger anhedral grains are replaced by talc but retain what looks like the shape of curvilinear clinopyroxene. Other talc replacements have more rectangular shapes and may have been olivine porphyroclasts. Some of these grains have possible olivine selvage islands inside them, others have selvages that look more like pyroxenes, based on cleavage. Based upon relic texture this may be a porphyroclastic or mosaic-porphyroclastic wehrlite, lherzolite or dunite. Most of the thin section is small equigranular grains of what were possibly olivine neoblasts, now replaced by serpentine, talc or a cryptocrystalline mixture of serpentine and talc. Garnet is present with a broad grain size distribution. All grains have a thick rim of serpentine, with some patches of spinel-phlogopite kelyphite. Talc and serpentine replaces almost all pyroxenes, some of these replacements have selvages of precursor mineral inside. Based upon the shape of these replacements and the color of precursor selvages, More rectangular shaped replacements have selvages of a precursor mineral with low interference colors that are possibly orthopyroxene, these are more often serpentine replacements. More curvilinear shaped replacements generally have selvages with high interference colors indicating clinopyroxene as a precursor mineral, these are more often talc replacements.

Modal Mineralogy:

Primary Phases:

Garnet: 10%

Pyroxene: 1%

Secondary Phases:

Serpentine after Olivine: 50%

Talc after Olivine: 20%

Talc after Clinopyroxene: 10%

Serpentine after Orthopyroxene: 5%

Magnetite: 5%

Talc after Orthopyroxene: 3%

Spinel: <1%

Phlogopite: <1%

Garnet: 10% of thin section. Some grains are large but there is a broad grain size distribution overall, from 1.5mm to 5mm. They are subhedral and rounded, with a circular or ovular shape. There is some fracturing and some partial melt in these grains, but garnets are fresh in comparison to other phases in the sample. All grains have thick (up to 400 μm) rims of what is possibly fine grained serpentine and phlogopite with a radiating habit. Some areas of these rims are typical spinel/phlogopite kelyphite.

Pyroxene: These are only found as selvages in the cores of talc and serpentine replacements. Some of these replacements have curvilinear grain boundaries, others are more rectangular with rounded off corners. Sizes of replacements and thus original precursor pyroxenes are around 6mm for the irregularly shapes grains, and 1.5-2mm for the more rectangular grains. Interference colors of the selvages of precursor mineral suggest that the smaller rectangular grains were orthopyroxene and the larger curvilinear grains were clinopyroxene.

Spinel: These are rare but found in kelyphite portions of rims around garnets. Most of the rims are altered to cryptocrystalline mineral mixtures but some coarse grained spinel remains along

with large phlogopites. Grains are 10-80 µm in size, are black opaques with a euhedral cubic habit.

Phlogopite: These are rare but found in kelyphite portions of rims around garnets. Grains are coarse, up to 280 µm. Those grains that remain look quite fresh.

Magnetite: These are ubiquitous. There are clusters of small grains in grains boundaries around altered neoblasts. While very small they are found throughout, and amount to about 5% of the sample.

Serpentine after Olivine: This amounts to a large proportion of the thin section. This exists as replacement of olivine neoblasts, and possibly rare porphyroclasts. All olivine is altered 100% to this serpentine with accessory magnetite. It is yellow in plane polarized light, grey-back in crossed polars and found as cryptocrystalline masses, sometimes coarse enough to display an acicular habit. Relict shapes of the precursor minerals show the original olivine neoblasts to be rounded and equigranular between 100-250 µm. Most grains are surrounded by tiny magnetites.

Serpentine after Orthopyroxene: There are rare examples of this. These grains are 100% serpentinized but size and shape suggest orthopyroxene as a precursor. These are found near or included in larger clinopyroxenes replaced to talc. Grains are subhedral rectangular and between 600 µm and 1.5 mm. All are replaced by fibrous masses of acicular serpentine. Yellow in PPL, grey-black in XPL.

Talc + Serpentine after Pyroxene: Small amount of this. These are of variable size and shape. There appear to be 2 populations. A large anhedral set and a smaller subhedral set. Both are 80-90% altered to a cryptocrystalline serpentine + talc with only small selvages of precursor mineral. Large curvilinear grains are up to 6mm in size, and contain probably clinopyroxene

selvages. Smaller subhedral grains are 2mm across and contain probably orthopyroxene selvages.

Sample ID: MOX0 162.8A

Sample Type: Websterite

This is an altered, deformed garnet orthopyroxenite. It is made up mostly of large strained orthopyroxene grains, followed by a large amount of garnet. Orthopyroxenes show undulatory extinction, development of subgrains and some minor recrystallization to neoblasts. Orthopyroxenes are highly fractured and contain partial melt and alteration to serpentine, carbonate and talc along fractures. Many orthopyroxene grains show exsolution lamellae of clinopyroxene. Garnets fit into a population of subhedral grains and a population of irregularly shaped grains. Both populations are rimmed by phlogopite + spinel kelyphite. Spinel is present as anhedral blebs with curvilinear grain boundaries found in one portion of the thin section. The sample is infiltrated by veins containing secondary phlogopite, serpentine, spinel and talc. These phases are found in veins, along grain boundaries and in fractures inside primary grains.

Modal Mineralogy:

Primary Phases:

Orthopyroxene: 60%

Garnet: 20%

Clinopyroxene: 10%

Spinel: 5%

Secondary Phases:

Phlogopite: 5%

Talc: 5%

Serpentine: 5%

Spinel: 1%

Orthopyroxene: Most of the sample is strained orthopyroxene grains. They have a broad grain size distribution and a broad range of shapes, possibly due to development of subgrains and neoblasts. Grains are between 200 µm and 4mm. They have a wide range of shapes but are generally subhedral to anhedral with straight grain boundaries. They are highly fractured with replacement to serpentine, phlogopite, spinel and talc. They have abundant clinopyroxene exsolution lamellae ranging from thin white rods to larger circular blebs up to 300 µm in size. Grains near the xenolith border with kimberlite can be up to 60% replaced by the serpentine + talc aggregate.

Garnet: Garnet makes up a significant proportion of this sample (20 %). It has a wide range of shapes and sizes, from euhedral to anhedral and from 200 µm to 4mm. Euhedral grains are quite fresh with minimal fracturing and replacement and a thin kelyhpite rim. More irregularly shaped grains can be completely disaggregated and near 100% replaced to phlogopite + spinel kelyphite with only small garnet selvages remaining. Intermediate forms range between these two morphological end members. There are also rare inclusions of orthopyroxene in some garnets.

Clinopyroxene: Clinopyroxene exists as small 100 µm to 2 mm anhedral grains and exsolution phases inside larger orthopyroxene. It is altered to serpentine and contains abundant small dark inclusion, interpreted to be partial melt. Grains are irregularly shaped with curvilinear grain boundaries.

Spinel: Primary spinel is present here. Grains are highly anhedral blebs with curvilinear grain boundaries. Most spinel is concentrated in one section in the center of the thin section, where most garnet is also found. Grains are 0.5-1mm in size. They range from dark black opaque to brown and translucent around the edges. Some orthopyroxene may be included in spinels, these inclusions have brown reaction rims.

Phlogopite: Phlogopite is well represented in this sample. It is found along with spinel in veins that appear to be infiltrating the xenolith from the kimberlite, though kimberlite is not visible in the thin section. It is also found replacing all primary phases along fractures, especially in kelyphite in and around garnet. It is also found in veins and patches of cryptocrystalline aggregates along with serpentine, spinel and talc. Coarse phlogopites in garnet kelyphite can be up to 2mm in length and are subhedral elongate.

Spinel: Secondary spinel is found along with phlogopite in veins and in kelyphytic replacement of garnet. Grains are 20-80 μm and are euhedral cubic black opaques.

Talc: Talc is found in high abundance in this sample. It is found as coarse subhedral grains throughout the thin section and in cryptocrystalline replacement along fractures in orthopyroxene and garnet. It is variably mixed with serpentine and more rarely spinel + phlogopite. Larger grains are up to 300 μm in size and form irregularly shaped grains or grain aggregates. Cryptocrystalline masses mix with serpentine and replace primary orthopyroxene and less often garnet along fractures.

Serpentine: This sample is highly altered and contains a high proportion of serpentine. This forms mixtures with both cryptocrystalline and coarser grained talc in veins and patches and as replacement of orthopyroxene and garnet.

Sample ID: MOX0 179.3

Sample Type: Websterite

This thin section is allotriomorphic with generally irregular grain boundaries for all phases. It is composed of orthopyroxene and clinopyroxene with minor garnet and possibly olivine. These primary phases appear to have crystallized simultaneously or by subsolidus exsolution as evidenced by magmatic intergrowth of grains. Secondary minerals include serpentine replacing of orthopyroxene, clinopyroxene and garnet, phlogopite, spinel, carbonate and magnetite. This

thin section also includes large patches of what appears to be mostly cryptocrystalline serpentine, phlogopite and magnetite (SPM zones)

Modal Mineralogy:

Primary Phases:

Orthopyroxene: 50%

Clinopyroxene: 30%

Garnet: 5%

Olivine: Possibly 1%

Secondary Phases:

Serpentine: 5%

Phlogopite: 1%

Spinel: <1%

Carbonate: <1%

Magnetite: <1%

SPM Zones: 5%

Orthopyroxene: Orthopyroxene is large (4-8mm) anhedral grains with irregular grain boundaries. They are highly fractured and altered with pervasive serpentinization especially near xenolith border with kimberlite fluid, where they are more than 50% serpentinized. They are loaded with exsolution lamellae of clinopyroxene in various stages of development from nascent white streaks to large rounded inclusions. Some orthopyroxene also exists as smaller rounded inclusions in garnets and clinopyroxenes. Orthopyroxenes have veins and inclusions of cryptocrystalline serpentine, phlogopite, magnetite and spinel.

Clinopyroxene: Clinopyroxenes are generally smaller than orthopyroxenes, with the exception of a single large (5mm) grain near the center of the thin section. Clinopyroxene is anhedral with highly irregular grain boundaries. There are larger grains (3mm) between orthopyroxenes and smaller rounded grains (80 μm) as inclusions inside orthopyroxene and garnet. They are pleochroic green in plane polarized light with typical high interference colors in crossed polars. Clinopyroxenes also have veins and inclusions of cryptocrystalline serpentine, phlogopite, magnetite and spinel.

Garnet: Garnet is moderately large (2-8mm) and are generally anhedral. They are altered and fractured with partial melts and veins and inclusions of cryptocrystalline serpentine and phlogopite and small grains of phlogopite. Most are bounded by discontinuous kelyphitic rims of coarse phlogopite and small euhedral spinels. These spinels however, are in lower abundance compared to kelyphite rims around garnets in porphyroclastic garnet dunites.

Olivine: Olivine is rare here, only a couple of small rounded grains that are questionable and may be pyroxene. They would be less than 1% of thin section.

Serpentine: Serpentinization is pervasive especially of orthopyroxenes near xenolith borders. It is cryptocrystalline and exists in fractures in orthopyroxene and as small pods both inside and between orthopyroxene grains. It is associated with phlogopite carbonate and magnetite and/or spinel. Along xenolith borders, clinopyroxene appears to be much less altered by serpentine, with relatively fresh clinopyroxene sitting next to almost completely serpentinized orthopyroxene. It is also found as a major constituent of the SPM zones.

Phlogopite: Phlogopites are found in kelyphitic rims around garnets and in serpentine-phlogopite zones in orthopyroxene, clinopyroxene and garnet where they are often larger visible grains set in an otherwise cryptocrystalline mass. They are also a major constituent of SPM zones. They

range in size from cryptocrystalline to larger grains up to 200 µm that are sometimes euhedral with rational faces. Grains show typical good cleavage in one direction, brown pleochroic in plane PPL with high interference colors. They show minimal birds-eye extinction.

Carbonate: Carbonates are found in serpentine-phlogopite zones where they are macrocrystalline grains (100-200 µm) in the centers of cryptocrystalline patches of serpentine, phlogopite and spinel. They are white in PPL and grey with anomalous high interference colors in XPL.

Spinel: Spinels are small (50 µm) angular, dark black euhedral grains. They are found with phlogopite in kelyphitic rims around garnets, and in cryptocrystalline SPM zones.

Magnetite: Magnetite is small (10 µm) rounded, dark black grains found pervasively in and around SPM zones. Some of these may be confused with spinel or another opaque.

Black Replacement: This is found in patches and veins around and inside of orthopyroxene, clinopyroxene and garnet. One particularly large patch surrounds a large clinopyroxene near the center of the thin section. These zones are cryptocrystalline and composed of a mixture of what appears to be serpentine, phlogopite, magnetite, carbonate, opaque kelyphite and possibly spinel.

Sample ID: MOX0 198.37

Sample Type: Websterite

This xenolith is a magmatic websterite. The xenolith is mostly orthopyroxene, there is a large single continuous grain in the center of the thin section. All orthopyroxene grains are large and are anhedral to subhedral with mostly straight grain boundaries, though some grains are more irregular with curved grain boundaries. There are many 120° triple junctions between orthopyroxene grains. Clinopyroxene and garnet are both anhedral with wormlike shapes and curved grain boundaries. Both of these phases include small rounded orthopyroxenes. The rest of the xenolith is made up of veins and blebs of microcrystalline S-P-M mixtures, which are usually found near garnets. There are also a couple of large pure carbonate veins that cross-cut the thin section and may be traced to the kimberlite.

Modal Mineralogy:

Primary Phases:

Orthopyroxene: 70%

Clinopyroxene: 10%

Garnet: 10%

Secondary Phases:

Black Replacement: 5%

Serpentine: 1%

Phlogopite: 1%

Spinel: 1%

Magnetite: 1%

Carbonate: 1%

Orthopyroxene: Orthopyroxene makes up the majority of this thin section. Grains are generally large, the center of this thin section is a single large grain that looks to be ~6mm across. Most grains are subhedral with generally straight grain boundaries showing minimal resorption. There are often 120° triple junctions between these grains. There is some early development of subgrains in orthopyroxene, especially in the large central grain. Some grains are more irregularly shaped, especially those near magmatic looking clinopyroxene and garnet grains. Other grains are small rounded inclusions inside clinopyroxene and garnet grains. There is pervasive clinopyroxene exsolution lamellae, especially in the cores of grains.

Clinopyroxene: There is a small amount of clinopyroxene in this xenolith. They are anhedral and look very much different than orthopyroxenes. They show very irregular and curved grain boundaries and have a broad grain size distribution from 100 μm to 4 mm. They have many inclusions of small rounded orthopyroxenes.

Garnet: Garnet shapes are very similar to those of clinopyroxene in this xenolith. They are anhedral grains with irregular and curved grain boundaries. They also have a broad grain size distribution with sizes ranging from 200 μm to 4 mm. These grains are altered with partial melting and cryptocrystalline inclusions of S-P-M mixtures.

Black Replacement: These are found in veins and irregularly shaped blebs throughout the thin section. They are cryptocrystalline to microcrystalline mixtures of serpentine, phlogopite, magnetite and possibly spinel, at least where these zones intersect a garnet. There is also a lesser contribution from carbonate. These patches are often concentrically zoned with areas of differing mineral contributions. The larger of these patches are often found near garnets.

Phlogopite: Phlogopite is found in S-P-M zones and in kelyphite rims and inclusions in garnet. They are generally cryptocrystalline to microcrystalline, though phlogopite grains in this xenolith seem to be coarser than those found in others. Larger grains are around 500 μm in size.

Spinel: Spinel grains are found in kelyphite rims and inclusions in garnets and possibly within S-P-M zones. Larger grains are 50 μm in size. All grains are cubic euhedral and angular. They are dark black and opaque.

Magnetite: Magnetite grains are tiny (5 μm) rounded dusty looking black opaque grains. They are found in clusters in S-P-M zones, often making up the cores of these zones.

Serpentine: Serpentine is found as a major contributor to S-P-M zones as cryptocrystalline masses. It is rare outside of these occurrences.

Carbonate: Carbonate is found as large grains (2mm) in large veins of pure carbonate. These veins are often traceable back to the kimberlite bordering the xenolith. It is also found as a lesser constituent in S-P-M zones in certain areas, as small discreet grains or groups of grains. It may also be present but unresolvable in cryptocrystalline masses of S-P-M zones.

Sample ID: MOX1 45.5

Sample Type: Coarse Garnet Peridotite

This is a coarse harzburgite, made up largely of olivine with some orthopyroxene, some garnet and minor clinopyroxene. The small amount of clinopyroxene that is found exists as irregularly shaped inclusions in orthopyroxene, suggesting that they are perhaps exsolution lamellae from orthopyroxene. Olivine grains show faint deformation textures with the beginnings of undulatory extinction seen in light and dark parallel lines of extinction, and some minor development of olivine neoblasts perhaps concentrated near carbonate veins and perhaps also associated with serpentine zones. Olivine grains are large and subhedral with mostly straight grain boundaries. The small amount of orthopyroxenes look similar in shape to olivine with regular subhedral shapes. Garnets are quite large and subhedral with some resorption. They have kelyphite rims with large phlogopite and spinel grains. There is moderately heavy alteration of olivine and orthopyroxene going to serpentine, especially near xenolith borders and near large carbonate veins that cross cut the xenolith. This xenolith is on the border of coarse and porphyroclastic, as there is development of some olivine neoblasts but they have not yet fully enveloped olivine porphyroclasts. Full envelopment of olivine porphyroclasts by neoblasts is Harte's (1977) definition of porphyroclastic texture.

Modal Mineralogy:

Primary Phases:

Olivine Porphyroclasts: 65%

Olivine Neoblasts: 5%

Orthopyroxene: 10%

Clinopyroxene: 5%

Garnet: 10%

Secondary Phases:

Black Replacement: 1%

Phlogopite: <1%

Spinel: <1%

Serpentine: 1%

Carbonate: 5%

Olivine: Olivine grains have a wide grain size distribution but can be large. They range between 1mm-10mm. They are anhedral but generally regularly shaped with mostly straight grain boundaries. They show faint undulatory extinction with parallel lines of extinction suggesting an early phase of deformation. There is some development of neoblasts and subgrain growth. Neoblasts are few, less than 5% of total olivine, and most seem to be concentrated in certain areas, near large veins of carbonate and serpentine. Olivine porphyroclasts are not surrounded by neoblasts as they would be in a porphyroclastic peridotite.

Orthopyroxene: There is a small amount of orthopyroxene here. These grains have a broad grain size distribution up to 2mm. Some grains are subhedral, rounded and regularly shaped while others are anhedral, more irregularly shaped and seem to fill grain interstices between larger olivine grains. Some orthopyroxenes contain irregularly shaped inclusions of clinopyroxene with small rounded orthopyroxenes included in those. Most grains are highly fractured and serpentinized.

Clinopyroxene: Clinopyroxene is rare in this xenolith. It exists only as irregular grains inside orthopyroxenes. These grains themselves contain smaller rounded inclusions of orthopyroxene,

and this texture suggests that the clinopyroxenes exsolved from solid solution with orthopyroxene. They are small and have curvilinear grain boundaries, and all grains have low interference colors of a greenish-yellowish white.

Garnet: Garnets are quite large with sizes between 1mm-4mm. They are generally subhedral and rounded with moderate resorption. They have coarse grained kelyphite rims of phlogopite and spinel. They show varying degrees of partial melting and serpentinization but are generally quite fresh.

Serpentine: Serpentine is present in present in replacement of all phases, especially orthopyroxene where it is in networks of thin veins. Also present in thick veins and small patches throughout the thin section. Orthopyroxene replacement is most advanced near the xenolith border with kimberlite. Garnet seems most robust against serpentinization. It is associated with phlogopite and magnetite and some carbonate in most instances. There is an unusual light blue/grey color to some examples.

Black Replacement: These are less abundant than in websterites and only present in grain interstices and veins rather than distinct blebs found in magmatic rocks. They are cryptocrystalline mixtures of serpentine, magnetite, phlogopite, carbonate and spinel where near garnets.

Phlogopite: Phlogopite is present in kelyphite rims around garnet and in S-P-M zones. In kelyphite it is associated with spinel and can be large (up to 500 μm). These are subhedral to anhedral but show the occasional rational face and good mica cleavage. In S-P-M zones they are cryptocrystalline but can be spotted by brownish color of these zones. These zones also host the occasional large grain, some up to 500 μm.

Spinel: Spinel is present in kelyphite rims around garnets and perhaps also in S-P-M zones. In kelyphite they are small (50 micron) subhedral angular cubic crystals and are dark black opaques. They are found inside of larger phlogopites. These may be found in S-P-M zones, but generally when near a garnet so this may be kelyphite intermixing with S-P-M.

Carbonate: Carbonate is present in several large veins that are 400 μm thick and made up of large grains that are 3mm in length.

Sample ID: MOX1 59.0

Sample Type: Websterite

This xenolith is a magmatic textured intergrowth of orthopyroxene and clinopyroxene with minor garnet. There is also a large singular olivine grain in the center of the xenolith, also represented in the described thin section. Texture is magmatic with fluid looking grains. Most of the thin section is made up of large anhedral orthopyroxene grains with irregularly shaped, worm like intergrowths of clinopyroxene. Clinopyroxenes are large, continuous, anhedral grains with curved and irregular grain boundaries and many inclusions of small rounded orthopyroxenes. There are many veins and irregularly shaped blebs of dark colored mixtures of serpentine, phlogopite, magnetite and possibly spinel and carbonate (S-P-M zones). These patches are often found next to garnet. Garnet is present but in low abundance. There is one large subhedral grain, but most are anhedral, appear broken up and altered, and are surrounded by S-P-M zones. A large single olivine is found in this thin section, it is undeformed and relatively fresh aside from some serpentine veining. There are small inclusions of clinopyroxene, garnet and orthopyroxene in this olivine. Where this large olivine borders the websterite, there is a reaction zone where it borders clinopyroxene, but a clean border against orthopyroxene. There is also a nice continuous and uniform 2mm thick serpentine rim along the xenolith border with kimberlite.

Modal Mineralogy:

Primary Phases:

Orthopyroxene: 50%

Clinopyroxene: 20%

Olivine: 15%

Garnet: 5%

Secondary Phases:

Serpentine-Phlogopite-Magnetite Zones: 5%

Serpentine: 5%

Spinel: <1%

Phlogopite: <1%

Carbonate: <1%

Magnetite: <1%

Orthopyroxene: The orthopyroxene present in this thin section is possibly a single huge grain. It continues beyond the edges of the thin section but is at least 2 cm in longest dimension. It is moderately altered with fractures and veins of partial melt, serpentine or both. It does not show any undulatory extinction but may show early development of subgrains. It is filled with wormlike intergrowths of clinopyroxene and S-P-M zones. These intergrowths themselves show inclusions of small rounded orthopyroxenes. These orthopyroxene inclusions look to be in the same extinction position as the large grain. Orthopyroxene is serpentinized, 50% or more in areas near S-P-M veins or near xenolith border with kimberlite. There is also pervasive development of exsolution lamellae in various stages of development.

Clinopyroxene: Clinopyroxenes are anhedral and magmatic looking with irregular and curved grain boundaries. There is a broad grain size distribution, with grains anywhere from 500 μm to 10mm across. They are intergrowths inside of a large orthopyroxene that dominates the thin section. They show typical pleochroic green color in plane polarized light and moderately high interference colors with polars crossed. They are cut across by thin veins of partial melt or serpentinization, though they appear more resistant to serpentinization than orthopyroxene. They

contain inclusions of small rounded orthopyroxene and garnet and some infiltration of S-P-M veins.

Olivine: The upper right corner of this thin section is a large single olivine grain, though the rest of the xenolith appears absent of olivine. This olivine is fractured and serpentinized with large serpentine veins (250 μm wide). No deformation textures are observed. It includes small subrounded inclusions of clinopyroxene and garnet from the websterite.

Garnet: Garnet is in low abundance in this xenolith. There is one large subhedral grain and several smaller altered anhedral grain. They are all pink in plane polarized light. All grains but especially the larger one have kelyphite rims and inclusions of phlogopite and spinel. The large grain has a coarse grained kelyphite rim with resolvable spinel and phlogopite, all other grains have finer grained or cryptocrystalline rims that cannot be accurately identified. Many garnets are surrounded by S-P-M zones with resorption and embayments of this material into the garnet. These garnets are always rimmed by a dark opaque cryptocrystalline rim, with finer grained and less obvious kelyphite with no coarse spinels or phlogopites.

Serpentine: Serpentine exists in fractures and veins variably altering all phases, and in a reaction zone at the xenolith-kimberlite border. It is also found as a component in S-P-M zones throughout the thin section. It is always cryptocrystalline, clear-yellow in plane polarized light and dark grey to black with cross polars. It is associated with magnetite and phlogopite in all instances and carbonate and spinel in some others.

Phlogopite: Phlogopite is found in kelyphite rims and inclusions in and around garnet. These are often relatively coarse grains (250 μm), some of which are euhedral with some rational faces. They are brown pleochroic in plane polarized light with high order interference colors with

crossed polars. Larger grains show characteristic mica cleavage. Phlogopite is most likely also present in cryptocrystalline S-P-M zones, but there are no large resolvable grains to confirm this.

Magnetite: Magnetite is found concentrated in S-P-M zones and veins. They are small (10 μm) rounded opaque black grains that form dense clusters in these zones. Often these clusters form the cores of concentrically zoned S-P-M zones.

Spinel: Spinel is found in kelyphite rims and inclusions in garnet. They are small (40-50 μm) angular cubic euhedral grains found in and around larger phlogopite grains in kelyphite. They are rounded dark black opaque grains. Some magnetite in S-P-M zones may be confused with spinel as these zones are cryptocrystalline and have to resolve.

Carbonate: Carbonate is in low abundance in this xenolith. It is found in one large enclave, where kimberlite fluid has penetrated the xenolith. This enclave contains a patch of large carbonate grains, as well as S-P-M and a resorbed garnet. It is also found occasionally in S-P-M zones. They are pearly white grains in plane polarized light with typical anomalous interference colors with crossed polars.

Black Replacement: This is found as veins and enclaves throughout the thin section. They are generally cryptocrystalline and zoned with cores of clustered magnetite and serpentine and phlogopite bounding this. These zones also occasionally contain larger carbonate grains. S-P-M zones are irregularly shaped with curved grain boundaries. They often surround garnet grains with embayments into the grain. Some include the final selvages of serpentinized orthopyroxenes and some show relict circular shapes that appear to be completely serpentinized orthopyroxene grains.

Sample ID: MOX1 107.5

Sample Type: Coarse Spinel Peridotite

This sample is a relatively fresh spinel bearing harzburgite. The sample is primarily made up of olivine and orthopyroxene with dark translucent primary spinel grains. Grains are coarse and generally equant, with olivine in a slightly larger size range than orthopyroxene.

Modal Mineralogy:

Primary Phases:

Olivine: 45%

Orthopyroxene: 40%

Spinel: 5%

Secondary Phases:

Serpentine: 5%

Magnetite: 1%

Olivine: Olivine grains are large (400 μm-7 mm), and fresh with minimal fracturing and serpentinization along fractures. There is some undulatory extinction in olivine, more so in larger grains. There is some intergranular serpentine and magnetite between olivine grains. Occasional olivine grains host small rounded orthopyroxene inclusions.

Orthopyroxene: Orthopyroxene grains are coarse, equant, and in the size range 300 μm-4 mm. Rounded olivine inclusions are commonly found inside orthopyroxene. Grains show little to no undulatory extinction, and contain minor amounts of serpentine alteration and small dark inclusions, interpreted to be partial melt . This melting and alteration is concentrated along grain rims or fracture planes.

Spinel: Spinel grains are beautiful, dark brown and translucent. Grains are irregularly shaped with straight grain boundaries and are in the size range 100 μm with fewer grains up to 3.5 mm. Grains are 'splotchy' looking, with small inclusions of either partial melt, alteration or both.

Serpentine: This sample contains a relatively low amount of serpentine. It is found in fractures inside olivine and orthopyroxene, and occasionally as larger patches at junctions of fracture networks, along with small magnetite grains.

Magnetite: Magnetite grains are small (10 μm), black and rounded, and are found along with serpentine in fractures in olivine.

Sample ID: MOX3 33.0

Sample Type: Coarse Spinel-Garnet Peridotite

This sample is a coarse spinel-garnet Harzburgite. There is an even contribution from olivine and orthopyroxene with lesser clinopyroxene, garnet and spinel. There is minimal (10%) serpentinization of the sample, with some alteration to carbonate present also. Most grains are subhedral-anhedral with slightly curved grain boundaries. The sample is roughly equigranular, with larger olivine and orthopyroxene and smaller garnet, spinel and clinopyroxene. Secondary minerals exist in fine grained aggregates along grain boundaries. Deformation textures are absent except for some faint undulatory extinction in orthopyroxenes.

Modal Mineralogy:

Primary Phases:

Orthopyroxene: 40%

Olivine: 30%

Garnet: 5%

Clinopyroxene: 5%

Spinel: 2%

Secondary Phases:

Phlogopite: 5%

Spinel: 1%

Serpentine: 10%

Carbonate: 5%

Magnetite: 1%

Orthopyroxene: Orthopyroxene is abundant in this sample, making up nearly half of the thin section. Grains are subhedral-anhedral with grain boundaries straight to slightly curved. Grains are between 800 μm and 3.5 mm in size. Grains display fracturing and clinopyroxene exsolution lamellae. Lamellae are usually bright white streaks, one grain shows exsolution lamellae in a bright red color. Some show faint undulatory extinction, and some have inclusions of small square opaque grains, possibly spinel.

Olivine: Olivine is abundant in this sample. It makes up about one third of the thin section. Grains are in a similar size range to orthopyroxene, about 800 μm-3 mm, and are subhedral with straight to slightly curved grain boundaries. Grains are minimally fractured and replaced along these fractures with serpentine and minor magnetite. This replacement also exists along grain boundaries and between grains. Some grains have inclusions of rounded dark opaque spinel. Some grains show faint undulatory extinction with faintly visible development of subgrains.

Garnet: Garnet grains are 0.5-2.0 mm in size, are light pink in PPL and subhedral-anhedral with straight to slightly curved grain boundaries. Grains are minimally fractured and have thin rims of fine-grained spinel+phlogopite kelyphite. Many garnets have large (<0.5 mm) central inclusions of rounded dark opaque spinel grains.

Clinopyroxene: Clinopyroxene grains are 2-4 mm in size and subhedral-anhedral with slightly curved grain boundaries. They are faintly green in PPL, show moderate fracturing and contain small dark inclusions, interpreted to be partial melt. These inclusions are concentrated along grain boundaries and fracture planes. Some clinopyroxene grains contain small rounded inclusions of dark opaque spinel.

Spinel: Spinel grains are 100 μm-1 mm and dark black opaque. Smaller grains are euhedral-subhedral with straight grain boundaries and angular corners, larger grains are subhedral with

rounded grain boundaries. Some are located at triple junctions of larger phases, most are located as inclusions in olivine, clinopyroxene and especially garnet.

Secondary Phases: This sample is minimally altered by serpentine, phlogopite, carbonate, magnetite and spinel. Serpentine occurs as a cryptocrystalline replacement of olivine in fractures and along grain boundaries, along with small ~10 μm black magnetite grains. Phlogopite and spinel form microcrystalline (~10-50 μm) kelyphitic rims around garnets. All of these phases plus minor carbonate form a cryptocrystalline aggregate that replaces all phases along grains boundaries and occasionally form larger interstitial pockets. This replacement is pervasive through some sections of the sample near the xenolith border with kimberlite.

Sample ID: MOX3 42.1

Sample Type: Websterite

This sample is a magmatic textured garnet bearing olivine websterite. This thin section is allotriomorphic with irregular grain boundaries for all phases. It is composed primarily of orthopyroxene, clinopyroxene and olivine with minor garnet. These primary phases appear to have crystallized simultaneously or by subsolidus exsolution as evidenced by irregular magmatic grain boundaries. Secondary phases include serpentine alteration of all orthopyroxene, clinopyroxene and olivine as well as carbonate, magnetite, spinel and phlogopite. This thin section also hosts large patches of cryptocrystalline black replacement.

Modal Mineralogy:

Primary Phases:

Orthopyroxene: 50%

Clinopyroxene: 20-40%

Olivine: 0-20%

Garnet: 1%

Secondary Phases:

Serpentine: 5%

Carbonate: 1%

Magnetite: <1%

Spinel: <1%

Phlogopite: <1%

Black Replacement: 5%

Orthopyroxene: Orthopyroxene is large, with grain boundaries between orthopyroxenes hard to define. There may be some grains that are extremely large (1cm) and enclose many other grains of clinopyroxene. They are anhedral except for rounded rectangular grains enclosed by larger clinopyroxenes. They are fractured and pervasively altered by serpentine, especially near xenolith borders with kimberlite and near fluid veins infiltrating from the kimberlite. They also exist as exsolution lamellae preferentially oriented inside clinopyroxene.

Clinopyroxene: Clinopyroxenes are mostly large (8mm) and anhedral with irregular grain boundaries. There are some instances of smaller (500 μm), subhedral rounded grains. They are fractured and altered with cryptocrystalline veins and inclusions of serpentine, phlogopite, magnetite and possibly spinel. They also host exsolution lamellae of orthopyroxene.

Olivine: There may be olivine in this thin section, but it may also be clinopyroxene. The habit of this phase looks very much like clinopyroxene, but it lacks the pleochroic green color in PPL typical of clinopyroxene. These exist as a few extremely large (1cm) magmatic looking continuous grains that enclose many smaller orthopyroxene and clinopyroxene grains. They are fractured and altered with inclusions of cryptocrystalline serpentine.

Garnet: Garnet is in low abundance in this thin section. They are subhedral with a broad grain size distribution from 100-800 μm. They are included in large olivines or clinopyroxenes. They are fractured and contain serpentine and/or partial melt. Those included in clinopyroxene have typical kelyphite rim of phlogopite and spinel, those included in olivine do not display such a clear rim.

Serpentine: Serpentine fills veins and fractures replacing orthopyroxene, clinopyroxene and olivine. It is more pervasive near xenolith borders and near large veins that infiltrate deep into the xenolith from the kimberlite. It also occurs in large (4-8mm) SPMSC zones that appear to be

fed by veins extending into the kimberlite. It is cryptocrystalline, clear to yellow in PPL and dark grey to black in XPL.

Carbonate: Carbonate occurs in veins throughout the xenolith extending from the kimberlite. These can be either pure carbonate veins or in zoned veins including serpentine and phlogopite as well. In these veins it grows as long fibrous needles oriented normal to the vein wall. It is also makes up discontinuous coarse grained rims around SPMSC zones. It is clear in PPL and grey in XPL with anomalous high interference colors.

Magnetite: Magnetite occurs with spinel in and around SPMSC zones and veins. They are small (5 μm) rounded dark black opaque grains.

Spinel: Spinel occurs with magnetite in and around SPMSC zones and with phlogopite in kelyphitic rims around garnet. In either case, they are small (20 μm) angular, square opaque grains.

Phlogopite: Phlogopite occurs in SPMSC zones, as cryptocrystalline masses mixed in with the other constituents. It also occurs as coarser grains along with spinel in kelyphitic rims around garnets. They are brown pleochroic in PPL with high interference colors in XPL. They show a single good cleavage but minimal birds-eye extinction.

Black Replacement: These are cryptocrystalline veins and patches of what appears to be serpentine, phlogopite, magnetite, spinel and carbonate. In some instances they are too dark and cryptocrystalline to accurately describe. Some patches appear to be fed by veins extending from the xenolith center into the kimberlite. These veins are zoned with discrete bands of carbonate, serpentine, phlogopite and magnetite. One large patch near the center of the thin section is circled by a discontinuous rim of coarse grained carbonate.

Sample ID: MOX3 69.2

Sample Type: Coarse Spinel Peridotite

This sample is a coarse amphibole bearing spinel harzburgite. It is made up primarily of olivine and orthopyroxene with yellow-green amphibole and primary spinel. Grains are mostly coarse, fresh and equant. Olivine and orthopyroxene show some undulatory extinction. Olivine is slightly more equant, with orthopyroxene slightly more irregularly shaped and fitting into olivine interstices. Amphibole grains often have thick rims of orthopyroxene. Spinel grains are found in a wide size range, are irregularly shaped with curvilinear grains boundaries and are variably translucent. Some rare clinopyroxene grains may also be present.

Modal Mineralogy:

Primary Phases:

Olivine: 40%

Orthopyroxene: 30%

Amphibole: 20%

Spinel: 10%

Clinopyroxene: 1%

Secondary Phases:

Serpentine: 1%

Magnetite: 1%

Olivine: Olivine is mostly large (2-4 mm) and equant. Grains are fresh with little fracturing except near the edge of the xenolith. Grains show minor serpentine alteration, and some undulatory extinction especially in larger grains.

Orthopyroxene: Orthopyroxene grains are 100 μm-2 mm, are slightly irregularly shaped and fit into interstices of olivine and amphibole grains and show some undulatory extinction.

Amphibole: Amphibole grains are large (2-4 mm) and regularly shaped with straight grain boundaries. Grains are yellow-green, show occasional amphibole cleavage, and have prominent rims of orthopyroxene.

Spinel: Spinel grains are found in a wide size range (150 μm-2.5 mm). Small grains have straight grain boundaries with angular corners, larger grains are anhedral with curvilinear grain boundaries. Grains show variable color from opaque black to light brown translucent. Larger grains have fractures, some have 5-30 μm rims of serpentine+phlogopite.

Serpentine: Small amounts in fractures in olivine.

Magnetite: Small (~10 μm) black, rounded grains. Grains are found along with serpentine alteration of olivine and in proximity to amphibole.

Sample ID: MOX7 62.3

Sample Type: Coarse Spinel-Garnet Peridotite

This sample is mostly relatively fine grained with a domain of larger grains. Fine grained areas show a lattice-preferred orientation of elongate grains. The sample contains olivine, orthopyroxene and amphibole with subhedral spinel and minor anhedral garnet-rimmed spinel. The sample is fresh with minor serpentinization of olivine in fractures and along grain boundaries. Amphibole and garnet-rimmed spinel is absent in coarse grained domain.

Modal Mineralogy:

Primary Phases:

Olivine: 50%

Orthopyroxene: 35%

Amphibole: 5%

Spinel: 5%

Garnet: 2%

Secondary Phases:

Serpentine: 2%

Olivine: Olivine has a wide grain size distribution, they are <5 mm in a larger grained domain and 100-700 μm in a smaller finer grained domain. Large grains are subhedral with straight-subrounded grain boundaries. Small grains are euhedral-subhedral with straight grain boundaries. Most grains are fresh with minor fracturing and serpentinization. Olivine forms a fabric with smaller grains concentrated in bands and some lattice-preferred orientation of elongate grains and a ‘wave’ of extinction of olivine through fine grained domain. Some undulatory extinction of larger grains.

Orthopyroxene: Grains are anhedral to subhedral with straight to slightly curved brain boundaries and are in a similar size range to olivine, larger grains up to 4 mm and smaller grains down to ~200 µm. Grains are quite fresh with some fracturing and serpentinization.

Amphibole: Grains are euhedral-subhedral and are oriented as both basal sections and long needles. Grains are pale green in PPL and show strong cleavage in basal sections. Grains are 400-800 µm basal sections by <3mm long needles. Many have inclusions of olivine and orthopyroxene but are free of fracturing and alteration.

Spinel: The sample contains 2 distinct generations of spinel. The coarse grained domain of the thin section contain larger subhedral spinel grains. These grains are 80-280 µm in size and have straight grain boundaries with rounded corners. They are dark opaque with rare and slight translucence. They are found in grain boundaries of, and occasionally as inclusions in, larger olivine grains. A second generation of grains are messy, anhedral, poikilitic grains inside in centers of anhedral garnets. They are dark with some translucence, up to 2 mm and may be located in bands parallel to olivine foliation.

Garnet: Garnet are messy, anhedral and poikilitic and contain spinel. Grains are <2 mm and are found in interstices and triple junctions of larger olivine, orthopyroxene and amphibole. Grains are often extensively fractured, serpentinized and contain small dark inclusions, interpreted to be partial melt.

Serpentine: There is minimal serpentinization of this sample, it is found in intergranular areas and in fractures replacing all phases, especially garnet.

Sample ID: MOX11 122.2

Sample Type: Websterite

This is a magmatic garnet-spinel orthopyroxenite. Most of the xenolith is large grained orthopyroxene, most of this thin section is a single large continuous orthopyroxene grain that is at least 4 cm across. This grain is fractured and minimally serpentinized and contains veins and patches of cryptocrystalline serpentine-phlogopite-magnetite mixtures (S-P-M zones). It also shows evidence of early development of subgrains, along with including smaller discreet orthopyroxene grains that may or may not be fully developed subgrains of the larger host. These grains are 2-3mm across and are subhedral with mostly straight grain boundaries. There are pervasive occurrences of clinopyroxene exsolution lamellae in various stages of development. Other phases in this xenolith are magmatic looking wormlike inclusions in this larger orthopyroxene. These include garnet, clinopyroxene, olivine and possibly primary spinel. All of these phases are irregularly shaped with curved grain boundaries. There is a single large subhedral garnet grain but all other garnet is found as these irregularly shaped wormlike grains. There are veins and patches of cryptocrystalline serpentine-magnetite-phlogopite mixtures (S-P-M zones), these also include lesser contributions from carbonate and possibly secondary spinel. Patches of this material are irregularly shaped much like the garnet and clinopyroxene, and some patches that are very dark and opaque may be primary spinel.

Modal Mineralogy:

Primary Phases:

Orthopyroxene: 70%

Clinopyroxene: 5%

Garnet: 5%

Spinel: 3%

Olivine: 2%

Secondary Phases:

Black Replacement: 5%

Serpentine: 5%

Spinel: <1%

Phlogopite: <1%

Magnetite: <1%

Carbonate : <1%

Orthopyroxene: Most of this xenolith is very large grained orthopyroxene. This thin section is mostly a single large continuous orthopyroxene that is at least 4 cm across. This large orthopyroxene hosts small magmatic looking inclusions of clinopyroxene, garnet and olivine. There are some smaller orthopyroxenes within this large grain also, which mat or may not be fully developed subgrains, as there is evidence of early development of subgrains from this larger host. These smaller orthopyroxenes are subhedral with straight grain boundaries. Orthopyroxene is relatively fresh except near S-P-M veins or near the xenolith border with the kimberlite. There is pervasive but heterogeneous clinopyroxene exsolution lamellae throughout this large orthopyroxene and in the cores of subgrains. These lamellae are in various stages of development.

Clinopyroxene: Clinopyroxene is rare here and exists as irregularly shaped magmatic looking intergrowths in the larger orthopyroxene. Larger grains themselves contain small rounded inclusions of orthopyroxene. There is a broad grain size distribution, from 200 μm up to ~2 mm. Much of the clinopyroxene appears to occur near S-P-M veins or near spinel or both.

Garnet: Garnet is rare in this xenolith. There is a single larger subhedral grain, it is 4 mm in size and is altered with veins and inclusions of partial melt, phlogopite, spinel, serpentine, clinopyroxene and carbonate. All other garnet occurs as wormlike shapes with irregular and curved grain boundaries and are generally found near S-P-M veins along with spinel and S-P-M patches.

Spinel: Primary spinel may be present in this thin section but also may be confused with S-P-M zones. They are dark black opaque blebs that are shaped similarly to garnet and S-P-M zones. Spinels are distinguished from S-P-M zones by their dark black color as opposed to the lighter brown translucence of the latter. They are rounded irregularly shaped grains with curved grain boundaries and are around 800 μm in size. They are often found near garnet, clinopyroxene and black replacement veins.

Olivine: Olivine is extremely rare here and has a habit that I have not seen before. It looks very similar in shape to garnets and clinopyroxenes, as irregular wormlike shapes with curved grain boundaries. I would think it is clinopyroxene but it is distinguished based on bright white versus green color in plane polarized light.

Black Replacement: This is found in veins and irregularly shaped patches of a cryptocrystalline mixture of serpentine, phlogopite and magnetite along with microcrystalline carbonate and possibly secondary spinel. This is often found near garnet and/or primary spinel. These patches are often zoned with a core of either carbonate of clusters of tiny magnetites, with serpentine and phlogopite surrounding this.

Spinel: Secondary spinel is found along with phlogopite in S-P-M zones and in inclusions in garnet. They are small (20 μm) angular cubic euhedral grains and are dark black opaque.

Phlogopite: This is found in S-P-M zones and veins and in inclusions in garnet. These phlogopites have an extremely brown color compared to those in other xenoliths in the suite.

Magnetite: These are found in black replacement zones as large clusters of tiny grains. Grains are tiny (10 μm) rounded and opaque.

Serpentine: Serpentine is found in cryptocrystalline masses in black replacement zones and veins and variably serpentinizes orthopyroxene near these veins and near the xenolith border.

Carbonate: Carbonate is found in black replacement zones and veins often as larger resolvable grains in the center of cryptocrystalline mixtures of serpentine and phlogopite. Individual grains can be quite large (300-400 μm).

Sample ID: MOX11 162.1

Sample Type: Porphyroclastic Peridotite

This sample is a porphyroclastic garnet harzburgite. It is on the edge of porphyroclastic and coarse texture as olivine neoblasts just barely envelope olivine porphyroclasts. Undulatory extinction and subgrains are seen in larger porphyroclasts. There is a small amount of orthopyroxene found as regularly shaped subhedral grains. These are all fairly similar in size and smaller than the average olivine. Garnet is present and are quite large subhedral grains that are variably resorbed and rimmed with kelyphite depending on proximity to serpentine veins. There are olivine neoblasts in veins and small interstitial patches. Serpentinization of these is variable from minimal to nearly 100% in some areas. There is a xenolith-kimberlite border along which there is a 3-5mm thick band of serpentinized olivine neoblasts and porphyroclasts. A reasonably fresh garnet sits in this zone. Olivines at this border have carbonate replacement but otherwise there is not much carbonate in this xenolith. Serpentine infiltrates the xenolith from the kimberlite border along grain boundaries.

Modal Mineralogy:

Primary Phases:

Olivine Porphyroclasts: 60%

Garnet: 5%

Orthopyroxene: 5%

Olivine Neoblasts: 5%

Secondary Phases:

Serpentine: 15%

Phlogopite: 1%

Spinel: 1%

Carbonate: 1%

Magnetite: 1%

Black Replacement: 5%

Olivine Porphyroclasts: These make up the majority of the xenolith. Some are very large but there is a broad grain size distribution from 4-20mm in length. Some smaller grains are subhedral but larger are anhedral. Most show strong undulatory extinction with development of subgrains and neoblasts along grain boundaries. All are heavily fractured with serpentine veins and some grains or parts of larger grains are 100% serpentinized near xenolith border at serpentinization front. As this front moves into the xenolith there is a zone of olivine selvages surrounded by serpentine veins. These selvages are rimmed by carbonate. These rims are 80 μm thick and uniform.

Olivine Neoblasts: There is a broad grain size distribution of these from 30-150 μm. They are rounded and subhedral and are concentrated at grain boundaries and in some small interstitial zones. They are not in high abundance, and just barely surround olivine porphyroclasts putting this xenolith right on the border of Harte's (1977) porphyroclastic classification. Serpentine works its way along grain boundaries from xenolith border and variably serpentinizes zones of neoblasts from 20-100% alteration.

Orthopyroxene: These are 2-4mm grains and are generally found between larger olivines. There is the rare inclusion inside olivine porphyroclasts, these are smaller at around 1mm. They are heavily serpentinized compared to other phases, some grains near or in serpentine veins are almost 100% altered. Most but not all grains show some undulatory extinction.

Garnet: These are moderately abundant here. They are rounded and subhedral with variable resorption. They are quite large (2-4mm). Most show kelyphite rims of phlogopite and spinel, the thickness and grain size of these rims depends on proximity to kimberlite and serpentine veins. One garnet this is inside a zone of fully serpentinized olivine at xenolith border is highly resorbed with a 200 micron thick kelyphite rim of coarse phlogopite and spinel while a garnet inside xenolith is shielded by an olivine and shows no visible rim at all. All garnets lack large amounts of partial melts and fracturing.

Serpentine: This xenolith is heavily serpentinized. Along xenolith border there is a 4mm thick zone of completely altered olivine porphyroclasts and neoblasts. As well as this there is pervasive intergranular veins infiltrating the xenolith altering the interior in the xenolith. All olivine porphyroclasts are heavily fractured and have 80-100 micron thick veins of serpentine. It is also found in interstitial patches of what look to be olivine neoblasts now fine grained to cryptocrystalline aggregates of serpentine, phlogopite and magnetite. Some phlogopites in these zones also appear to be serpentinized themselves.

Phlogopite: These are found in kelyphite rims around garnets and is S-P-M zones. Can be variable in size in kelyphite depending on proximity to serpentine veins. Largest grains are up to 800 μm. These are associated with spinel. In S-P-M zones they are also variable in size from cryptocrystalline to 400 μm. Some larger grains in S-P-M seem to be serpentinized which has not been observed before.

Spinel: These are found with phlogopite in kelyphite as small 10-80 μm angular grains.

Magnetite: These are abundant and are found with serpentine in replacement of olivine. They are tiny rounded opaques (5-10 μm).

Carbonate: This is found at the xenolith border replacing olivine selvages at the xenolith serpentinization front. Olivine selvages are rimmed by 80 micron thick rims of grains that are 20-100 μm in size.

Sample ID: MOX24 31.1A

Sample Type: Coarse Spinel Peridotite

This is a fine grained coarse spinel harzburgite. It is composed mostly of roughly equal amounts of olivine and orthopyroxene with primary spinel and secondary serpentine and carbonate. It is quite fresh except for areas of more extensive alteration near visible border with kimberlite. Olivine and orthopyroxene grains are equigranular , generally polygonal with slightly rounded grain boundaries. Harte (1977) would call this equigranular granuloblastic. Kimberlite contains much carbonate, and a single pure carbonate vein penetrates the xenolith. It is 1mm wide, coarse grained and penetrates about 5mm into the xenolith. Low amounts of magnetite reflect low serpentinization.

Modal Mineralogy:

Primary Phases:

Olivine: 40%

Orthopyroxene: 40%

Spinel: 5%

Secondary Phases:

Serpentine: 10%

Carbonate: 1%

Magnetite: 1%

Olivine: Olivines are small with a tight grain size distribution between 0.5-2.5mm. The are generally fresh. Some fracturing and serpentinization along these fractures is apparent, but low alteration compared to other xenoliths in the suite. Some undulatory extinction, low angle tilt boundaries and minor subgrain development. Olivines are present as polygonal grains with

rounded corners to rounded grains. An occasional large olivine is seen to enclose orthopyroxenes.

Orthopyroxene: Orthopyroxene is small with a tight grain size distribution in a similar range to olivine ~0.5-2.5mm. These grains are slightly more fractured and altered than olivine, with more serpentinization along fractured and cleavages. Grains are polygonal with rounded corners to rounded grains to more irregularly shaped grains. Some of these irregularly shaped grains enclose or partially enclose olivines.

Spinel: Spinel is small with a tight grain size distribution between 200-600 μm. They are irregularly shaped with rounded and curvilinear grain boundaries and fit into interstices between larger olivines and orthopyroxenes. Some grains are highly irregularly shaped with a trigonal habit and fit into triple junctions of larger grains. Grains are translucent light brown with few defects. Roughly half the spinel population are 20-80% replaced by a black, cryptocrystalline material. There are some patches that are made entirely of this material, and it looks to be possibly serpentine + magnetite. These may be fully altered spinels but that cannot be confirmed under the microscope. One spinel looks to have a garnet at its center, though this cannot be confirmed, it is very small and slightly rose colored. The locations of black cryptocrystalline patches are consistent with those of spinels, these may be areas of more extensive alteration of spinel in areas of more extensive serpentinization near xenolith borders and infiltrating veins.

Serpentine: This xenolith is quite fresh so there is a low amount of serpentine. It is found in areas of alteration of primary minerals at grain boundaries and in fractures and cleavage surfaces. It is more extensive near xenolith border and near infiltrating veins. It forms an intergranular network throughout the thin section. It is found as cryptocrystalline fibrous aggregates, it is yellow in PPL

and grey-black in XPL. There is less magnetite associated with this serpentine than is found in most other samples in the suite.

Carbonate: Carbonate is a major constituent of the kimberlite magma surrounding the xenolith, as seen in thin section. There is a prominent monomineralic vein infiltrating the xenolith from the kimberlite. It is 1mm wide and penetrated 5mm into the thin section. It is an aggregate of coarse, fibrous grains. Despite abundant carbonate segregations in the kimberlite groundmass and the single large vein in the xenolith, there is no other carbonate in the xenolith.

Magnetite: There is not much magnetite in the xenolith despite the interstitial serpentine. It is present along with serpentine but in smaller proportions than usually seen in other samples. It may be more abundant in areas of serpentinization in the vicinity of spinel. It may also be a constituent in fine grained black replacement of spinel.

Sample ID: MOX24 42.6

Sample Type: Websterite

This is a magmatic textured garnet olivine websterite. It contains a high proportion of olivine, which are large and subrounded. They are subhedral, but not magmatic looking. There is clinopyroxene in lower abundance which does appear magmatic with irregular wormlike curved grain boundaries. These have small rounded inclusions of orthopyroxene and garnet. Orthopyroxenes are subhedral with irregular and curved grain boundaries but are not magmatic looking like clinopyroxene. Very broad grain size distribution of these orthopyroxenes. Garnet is quite abundant here, there are a couple that are euhedral, others are irregular and fragmented and show some resorption. They are found close to either primary spinel or irregularly shaped cryptocrystalline phlogopite-magnetite-spinel (S-P-M) zones or both. There could be primary spinel here, these are dark opaque irregularly shaped blebs. They are shaped very similarly to S-P-M zones but distinguished based on dark opaque color. These are associated with S-P-M zones and with garnet. The xenolith is extensively fractured, veined and serpentinized, especially near borders. There is no evidence of deformation.

Modal Mineralogy:

Primary phases:

Olivine: 40%

Orthopyroxene: 20%

Clinopyroxene: 10%

Garnet: 10%

Spinel: 5%

Secondary phases:

Black Replacement: 5%

Serpentine: 5%

Phlogopite: 1%

Magnetite: 1%

Carbonate: <1%

Spinel: 1%

Olivine: Much of the xenolith is olivine. They are large grains (3-5mm). They are subhedral with generally straight grain boundaries. They are fractured with veins of serpentine. They have inclusions of small rounded orthopyroxenes.

Orthopyroxene: These are abundant here. They have a broad grain size distribution from 160 micron inclusions in clinopyroxene and olivine to ~8mm grains. These is also much diversity in grain shapes, from large subhedral grains with straight grain boundaries to irregular magmatic looking intergrowths with clinopyroxene. They are variably serpentinized and fractured, those near the xenolith border are more than 50% serpentinized. They show exsolution lamellae especially in the cores of larger grains, these lamellae are in various stages of development.

Clinopyroxene: Clinopyroxene is in low abundance here and some may be hard to tell from olivine. They are distinguished based on faint green color in plane polarized light. They occur as magmatic looking intergrowths with irregular and curved grain boundaries. They are fractured and show more serpentinization than olivine, but not as much as orthopyroxene.

Garnet: Garnet is abundant here. One grain is large (3mm) and subhedral, most others are fragmented and resorbed. They are filled with fractures and veins of partial melt or serpentine or both. They have inclusions of phlogopite, olivine and possibly primary and secondary spinel. All

grains have coarse grained kelyphite rims of phlogopite and spinel and many are surrounded by or near S-P-M zones and or primary spinel blebs.

Spinel: I think there is primary spinel here. They are wormlike irregularly shaped blebs with curved grain boundaries. They are around 400-1200 μm in size and are deep black and opaque. They are shaped and sized just like S-P-M zones but are much darker black and transmit no light. They are always found next to garnet or S-P-M zones or both.

Serpentine: There is extensive serpentinization of all phases here except primary spinel. It is present in veins cutting through all grains. Some of these are traceable to the kimberlite. Orthopyroxenes near the xenolith border are almost 100% serpentinized. It is also found in S-P-M zones in cryptocrystalline mixtures with phlogopite and magnetite.

Phlogopite: Phlogopite is found in kelyphite rims and inclusions in garnet as coarser sometimes euhedral grains showing a single good cleavage. It is also found in cryptocrystalline mixtures with serpentine and magnetite in S-P-M zones.

Magnetite: Magnetite is found in most places where serpentine is found. It is present as tiny (5 micron) grains, they are subrounded dusty looking dark black and opaque.

Carbonate: Carbonate is found in S-P-M zones as cryptocrystalline or microcrystalline patches. It is quite abundant compared with other xenoliths from the collection. The S-P-M patches are often zoned with a patch of carbonate in the center with serpentine surrounding this and finally phlogopite around that.

Black Replacement: This is present in veins and irregularly shaped patches of dark cryptocrystalline mixtures. It is made up of mostly serpentine, phlogopite and magnetite with lesser spinel and carbonate. They are often zoned with patches of one mineral inside another, often with either magnetite or carbonate in the centers. Patches are found near garnet and/or

primary spinel and often envelope partially or completely serpentinized orthopyroxenes. These patches also include dendritic looking opaque grains. These are the same color as spinel and magnetite but have a very interesting radiating needle-like habit. These needles are generally about 100 μm in length.

Sample ID: MOX24 43.35

Sample Type: Websterite

This is a highly altered garnet websterite. It contains abundant garnet, carbonate veins and cryptocrystalline serpentine-phlogopite-magnetite zones. Clinopyroxene, orthopyroxene and garnet are all irregularly shaped with curvilinear grain boundaries. All of these phases are intergrown with one another. There are abundant inclusions of orthopyroxene in garnet and clinopyroxene. There is a kimberlite-xenolith border in this thin section, with orthopyroxene at this border nearly 100% serpentinized, though clinopyroxene in the same region appears to be less altered. All garnets in this thin section are heavily fractured and contain partial melting and have very coarse grained kelyphite rims containing much spinel. Some faint undulatory extinction seen in orthopyroxene and possibly clinopyroxene. There may also be evidence of garnet deformation with appearance of subgrains. Like other thin sections, there is the appearance of an unusual blue/grey serpentine.

Modal Mineralogy:

Primary Phases:

Orthopyroxene: 30%

Clinopyroxene: 20%

Garnet: 20%

Secondary Phases:

Carbonate: 5%

Phlogopite: <1%

Spinel: <1%

Serpentine: 15%

Serpentine-Phlogopite-Magnetite (S-P-M) Zones: 10%

Magnetite: <1%

Orthopyroxene: Orthopyroxene is the most abundant phase in this xenolith. They are irregularly shaped, and have a broad grain size distribution between 0.5mm to 2.0cm. Larger grains show faint undulatory extinction, smaller grains do not. All grains are fractured and have veins and patches of partial melt and cryptocrystalline S-P-M. There is extensive (near 100%) serpentinization of orthopyroxenes near xenolith border with kimberlite. Some but not all grains have clinopyroxene exsolution lamellae in grain cores, with these lamellae ranging from thin white streaks to small rounded clinopyroxene inclusions.

Clinopyroxene: These are large, up to 8mm in longest dimension. They are highly irregularly shaped, even more so than orthopyroxene, with curvilinear grain boundaries. They contain many small rounded orthopyroxene inclusions. They are highly fractured with veins of partial melt, carbonate and cryptocrystalline S-P-M aggregate. Some clinopyroxenes look like they may be fully replaced by this S-P-M aggregate.

Garnet: There is abundant garnet in this xenolith. There are some smaller subhedral grains but most are large (5mm-10mm) and more irregularly shaped with some curvilinear grain boundaries. They contain abundant veins and patches of partial melt and carbonate and have rims and inclusions of kelyphite. Kelyphite rims contain large phlogopite grains and large and abundant spinel grains. Garnets are often found close to S-P-M patches and may suggest that S-P-M has been replacing garnet.

Carbonate: Carbonate is found in large veins cross cutting the xenolith. One vein is very large (400 μm thick) and spans the entire thin section. It cannot be traced outside of the xenolith. It contains needlelike grains oriented perpendicular to vein walls. Carbonate is also found in

inclusions in garnet as microcrystalline clusters up to 0.5mm in size. It is also found with phlogopite and serpentine in grain interstices where it is found as clusters of larger (50 micron) grains. These grains are sometimes angular and square shaped. Carbonate veins seem to cut through all phases regardless of their state of alteration which suggests that emplacement of these veins is a late if not final stage process.

Phlogopite: Phlogopite in this xenolith is both abundant and found in large grains. They are found in kelyphite rims and inclusions in and around garnets, and in S-P-M zones and veins. In kelyphite they are very large grains in comparison to those found in other xenoliths in the suite, up to 300 μm. In S-P-M zones they are sometimes microcrystalline to cryptocrystalline aggregates but larger grains are found here also. Thee grains show birds-eye extinction and have some rational faces.

Spinel: Spinel is found in kelyphite rims and inclusions in and around garnet and in S-P-M zones both near and away from garnets. In both cases, much like the phlogopite in this xenolith, grains are larger (up to 100 μm) and more abundant than have been observed in the suite so far. Spinel is a more abundant component of S-P-M, even when not in contact with garnet, than is usually found.

Serpentine: There is abundant serpentine here as this xenolith is heavily altered, especially near veins and near the xenolith border with kimberlite. Orthopyroxene is extensively replaced while clinopyroxene appears fresher. Serpentine is also a major constituent of cryptocrystalline S-P-M zones. This xenolith contains unusual looking replacement of orthopyroxene, it appears to be serpentine but has a blue-grey color in crossed polarized light.

Black Replacement: This microcrystalline to cryptocrystalline aggregate is found in veins and irregularly shaped blebs throughout the xenolith. There are two textural types of this material. There are cryptocrystalline blebs which cannot be accurately resolved, but based on colors and textures probably contains some mixture of phlogopite magnetite and serpentine. There are also more coarse grained fillings of grain interstices that contain larger phlogopite and spinel and carbonate as well as serpentine and magnetite. These may be differentially crystallized examples of the same material or may be reflect different processes. Cryptocrystalline patches are zoned with dark cores probably made up of magnetite clusters and lighter brown rims, probably serpentine and phlogopite.

Magnetite: Magnetite is found in cryptocrystalline S-P-M zones as clusters of tiny grains. These grains are 10-20 μm in size and are dark black rounded opaques.

Sample ID: MOX24 124.0A

Sample Type: Porphyroclastic Peridotite

This sample is a porphyroclastic garnet harzburgite. Olivines are moderately deformed, showing undulatory extinction and the development of subgrains, and there is development of olivine neoblasts along grains boundaries. Olivine porphyroclasts make up a large proportion of the thin section (70%). Olivines are fractured with fractures infilled with serpentine, lesser magnetite and minor carbonate. Olivine neoblasts are 50% serpentinized, this serpentine again associates with magnetite. Orthopyroxene occurs as euhedral laths, as anhedral filling of grain interstices and as subhedral inclusions in olivine. This range in habit of orthopyroxene may reflect multiple generations of growth, considering that orthopyroxene is found as an inclusion in olivines and also as an apparently secondary phase filling interstices among these olivines. A small amount of garnet is present as non disrupted but variably resorbed grains with rims of clinopyroxene and spinel. This spinel is likely secondary however and does not suggest that this rock straddles the garnet-spinel transition.

Modal Mineralogy:

Primary Phases:

Olivine: 70%

Orthopyroxene: 10%

Garnet: 5%

Olivine neoblasts: 10%

Clinopyroxene: 1%

Secondary Phases:

Serpentine: 3%

Spinel: 1%

Carbonate: <1%

Magnetite: <1%

Olivine Porphyroclasts: These make up 70% of the thin section. Large grains (.5-1 cm) are anhedral with irregular grain boundaries and are extensively fractured. All show high degrees of undulatory extinction. Fractures are infilled with zoned veins of serpentine, minor carbonate and magnetite found mostly in interior areas of these veins. Several instances of large subhedral orthopyroxenes as inclusions in olivine. Two garnet inclusions found in olivine. Olivines are moderately deformed as evidenced by the development of neoblasts at grains boundaries, the development of subgrains and undulatory extinction.

Orthopyroxene: 10% of thin section. Orthopyroxene grains are smaller than olivines (.5-2.5 mm) and range in habit from euhedral rectangular laths, subhedral subrounded inclusions in olivine to anhedral grains filling space between larger olivines. Most are fractured with black fracture lines, some of the fractures in orthopyroxenes included in olivine are continuous through both the orthopyroxene and the host olivine. Some show rims of serpentine and neoblasts of neighboring olivines, though those included in olivine have less pronounced rims. Two instances of small rounded olivines included in orthopyroxene. Orthopyroxene shows varying degrees of undulatory extinction. In general, euhedral laths show least undulatory extinction, the anhedral grains between olivine interstices have moderate undulatory extinction and the orthopyroxenes that include olivines have pronounced undulatory extinction.

Garnet: Low abundance of garnet, there are ten of them in this thin section. They show a tight grain size distribution with a range of .5-1.0 mm. All show generally subhedral, subrounded grain habits. Most are found at multiple grain junctions of larger olivines, these are fractured

with pervasive inclusions of a fine brown dusty looking material. These grains are resorbed with ragged grain margins and have thin rims of a medium grained colorful clinopyroxene inset with small abundant euhedral angular spinels. One garnet is ¾ enclosed by a large olivine. The clinopyroxene+spinel rim is only seen on the remaining face exposed to the rock, while the three faces enclosed by olivine have a thin rim of serpentine, much like is seen infilling olivine fractures. One garnet is fully enclosed by an olivine grain, this garnet has no fracturing or brown dusty inclusions, lacks a clinopyroxene+spinel rim and instead has a thick halo of fresh olivine neoblasts.

Clinopyroxene: A very small amount of clinopyroxene (~1%) is found in this thin section. One very small grain is present, it is .2 mm in length, shows typical high interference colors and one very good cleavage plane. It is subhedral and angular with two rational faces. This grain sits next to another larger grain that may also be clinopyroxene. This one is 1 mm in length, is anhedral with rounded grain margins and is fractured and serpentinized. There is also some development of exsolution lamellae. It shows no cleavage, an has low grayish yellow interference colors and so cannot be confirmed as clinopyroxene but does appear green in a plane polarized light large format photograph of the slide. All remaining clinopyroxene exists as rims around garnets. These grains appear quite fresh with little fracturing or alteration. They are up to 1mm in length, show typical high interference colors and one very good cleavage. These clinopyroxenes are always found with abundant inclusions of euhedral spinel.

Spinel: A small amount (~1%) of spinel is present in this thin section. These are small (<.15 mm) fresh, dark black opaque grains. They are euhedral, angular boxy grains found only in clinopyroxene rims of garnets.

Olivine Neoblasts: These are quite abundant, making up perhaps 10% of the thin section. They are small with a tight grain size distribution, ranging from 10-50 μm. They are rounded subhedral grains, existing along all grain boundaries and in a few small zones (2 x 2 mm). Neoblasts are about 50% serpentinized, and are associated with small dusty looking magnetite, similar to what is found in olivine fracture zones. The degree of serpentinization varies from zone to zone, with zones of more serpentinization having more abundant magnetite.

Serpentine: Serpentine makes up about 3% of the thin section, not including altered olivine neoblasts. Remaining serpentine exists as alteration along boundaries of all phases, and as infilling in fractures in olivine and some orthopyroxenes. Serpentine in fine grained/cryptocrystalline, clear to yellow in plane polarized light and grey to black in crossed polarized light.

Carbonate: Very minor amounts of carbonate found in this thin section (<1%). It is found only in some of the larger fractures in the largest olivine grain. It is fine grained/cryptocrystalline, shows typical third order interference colors and is associated with serpentine and magnetite in olivine fractures.

Magnetite: Magnetite is also very minor (<1%). It occurs along with serpentine in both olivine porphyroclast fracture zones and in areas of olivine neoblast alteration. Grains are fine grained/cryptocrystalline, are very small (2-10 μm) rounded dusty black colored.

Sample ID: MOX24 206.7

Sample Type: Websterite

This is a large grained websterite. It is composed of large, blocky subhedral orthopyroxene grains with anhedral, irregularly shaped clinopyroxene and garnet grains with exsolution textures. The sample also contains a black aggregate in anhedral pockets, with similar textural characteristics to garnet and clinopyroxene and may have replaced these phases.

Modal Mineralogy:

Primary Phases:

Orthopyroxene: 70%

Clinopyroxene: 10%

Garnet: 10%

Secondary Phases:

Black Replacement: 5%

Serpentine: 1%

Carbonate: 1%

Secondary Spinel: 1%

Phlogopite: 1%

Orthopyroxene: Most of this sample is large (<9 mm), blocky subhedral orthopyroxene grains. All other phases appear to have exsolved out of these grains. Grains are subhedral with straight grain boundaries except where disturbed by intergrowth with other phases. Grains are variably fractured and contain small dark inclusion, interpreted to be partial melt. The amount of partial melt may be negatively correlated with grain size. Grains have abundant exsolution lamellae of clinopyroxene from thin bright rods to larger rounded blebs. Grains with more exsolution also

have more partial melt. Some undulatory extinction and lots of subgrain formation. Subgrains contain less partial melt and less exsolution lamellae.

Clinopyroxene: Clinopyroxene grains are large (<9 mm) anhedral and skeletal and are found inside host orthopyroxenes and poikilitically enclosing smaller rounded orthopyroxenes. Some grains are more regularly shaped with straight grain boundaries and subgrain development. These grains also show more fracturing and small dark inclusions, interpreted to be partial melt.

Garnet: Garnet looks textually similar to clinopyroxene, e.g. as an irregular exsolved phase inside larger orthopyroxene. Sometimes grains are found in complex intergrowths with clinopyroxene. Grains are fractured and contain small dark inclusions, interpreted to be partial melt. Small amounts of phlogopite+spinel kelyphite is found included in and mantling some garnet grains, more of this alteration is found in grains near xenolith border with kimberlite.

Black Replacement: Black replacement patches are rare in this sample. They are anhedral blebs of cryptocrystalline aggregates of phlogopite+spinel+carbonate+magnetite+serpentine. Some are slightly coarser grained and more dominantly phlogopite+carbonate with visible individual grains, these patches have a thin serpentine halo. A rare textural variety of common black replacement patches.

Sample ID: MOX25 120.6B

Sample Type: Orthopyroxenite

This is a porphyroclastic orthopyroxenite. It is almost 100% orthopyroxene aside from some interstitial phlogopite, serpentine and carbonate. Grains have a large range of sizes and shapes and are surrounded by tiny neoblasts. Grains are fractured and moderately serpentinized and show strong undulatory extinction. Grain interstices are filled with cryptocrystalline serpentine and serpentinized neoblasts and phlogopite and possibly carbonate and/or talc. There are few and

widely dispersed olivines and spinels between orthopyroxene grains. Porphyroclast interstices contain some fresh neoblasts and some areas of near complete alteration of neoblasts. These areas are replaced by cryptocrystalline masses of serpentine with phlogopite.

Modal Mineralogy:

Primary Phases:

Orthopyroxene Porphyroclasts: 90%

Orthopyroxene Neoblasts: 5%

Olivine: <1%

Secondary Phases:

Serpentine: 5%

Phlogopite: <1%

Spinel: <1%

Orthopyroxene Porphyroclasts: These make up 90% of the sample. They are anhedral but have generally straight grain boundaries. They have a wide range of grain sizes from 200 μm up to 4mm. Smaller grains may be subgrains. All grains show strong undulatory extinction and development of subgrains, and most are surrounded by tiny neoblasts. Grains are fractured and contain serpentine and partial melt along fractures.

Orthopyroxene Neoblasts: These are found surrounding orthopyroxene porphyroclasts. They are small rounded grains 10-20 μm in size and around as small collections. Many of these collections are partially or completely altered to fine grained aggregates of serpentine and phlogopite. Relict structure of neoblasts can sometimes be seen in altered masses.

Olivine: Olivine is rare but present in the interstices of larger orthopyroxene porphyroclasts. The are <200 μm, and anhedral with straight grain boundaries and angular corners.

Serpentine: Serpentine is found in the interstices of larger orthopyroxene porphyroclasts mainly as replacement of orthopyroxene neoblasts. It is found as fine grained films along grain boundaries and small patches 1-2mm in size.

Phlogopite: This is found in areas of orthopyroxene neoblast alteration along with serpentine. Often cryptocrystalline, with some larger grains up to 200 µm. Subhedral with some rational faces.

Spinel: This is found in areas of serpentine replacement of orthopyroxene neoblasts along with phlogopite. In low abundance but scattered homogenously throughout sample. Grains are 10-80 µm. Dark black opaques, cubic euhedral and angular.

Sample ID: MOX25 124.8

Sample Type: Porphyroclastic Peridotite

This sample is a porphyroclastic garnet dunite. It is highly deformed with extensive development of deformation textures. Olivines porphyroclasts are deformed, showing undulatory extinction, development of subdomains and advanced development of neoblasts. They also show alteration with fracturing and serpentinization along these fractures. These deformed olivine porphyroclasts make up a large proportion of the thin section (70%). Olivine neoblasts are the next most abundant phase (20%). These exist along grain boundaries and in some larger zones. Neoblasts are about 50% serpentinized. Garnet makes up 5% of the thin section, these garnets show the beginnings of deformation with partial melting of the interiors, minimal resorption of grain boundaries with recrystallized kelyphite rims and some development of subdomains. Serpentine makes up another 5% of the thin section, located in fractures of olivine and in alteration of olivine neoblasts. Accessory phases include secondary spinel and phlogopite in kelyphite rims of garnet, and magnetite associated with the serpentinization of olivine.

Modal Mineralogy:

Primary Phases:

Olivine Porphyroclasts: 70%

Olivine Neoblasts: 20%

Garnet: 5%

Clinopyroxene: 1%

Secondary Phases:

Serpentine: 5%

Spinel: <1%

Phlogopite: <1%

Magnetite: <1%

Olivine Porphyroclasts: Olivine porphyroclasts are generally large (<8mm) with a broad grain size distribution and some grains as small as 2mm. All are extensively deformed with advanced undulatory extinction and development of subgrains. Subgrains are non deformed with plain extinction and are subhedral and rectangular or ovular. They are moderately fractured with serpentine and associated magnetite filling of these fractures. They are generally anhedral to subhedral, with some highly irregular grain boundaries due to the formation of subgrains and neoblasts.

Olivine Neoblasts: This thin section show extensive development of neoblasts (20% of section). They are small (10-50 μm) and subhedral and rounded. They are found along all grains boundaries and in some larger zones that can be up to 4mm across. They are about 50% serpentinized, with this serpentinization associated with small magnetite grains found in neoblast zones.

Garnet: Garnets are large with a broad grain size distribution (1-4mm). They are rounded subhedral grains and are pinkish in plane polarized light. They are moderately deformed with partial melting of grain interiors and some development of subgrains. They are minimally resorbed with ragged grain boundaries and coarse grained kelyphite rims of phlogopite and spinel. One single garnet appears more extensively resorbed and partially melted, this grain does not show typical kelyphite rim.

Serpentine: Serpentine is cryptocrystalline fine grained and yellowish in plane polarized light. It is found in zoned veins in fractures of olivine porphyroclasts and in alteration of olivine

neoblasts. In both cases it is found alongside magnetite. Serpentinization of both olivine porphyroclasts and neoblasts is more advanced near xenolith boundary with kimberlite.

Spinel: Spinels are small (20-50 μm) euhedral angular squares. They are dark black and opaque and occur only along with phlogopite in coarse grained kelyphite rims around garnets.

Phlogopite: These occur in coarse grained kelyphite rims around garnets. They are moderately large (up to 0.5mm) with some euhedral faces. They are pleochroic from clear-green to yellow-brown. They show excellent cleavage in one direction, but do not display typical birdseye extinction.

Magnetite: Magnetites are small and have a wide grain size distribution with a range of 1-40 μm. They are rounded opaque grains and occur along with serpentine in alteration of olivine porphyroclasts and neoblasts.

Clinopyroxene: This section contains a tiny amount of clinopyroxene (<<1%). This occurs in a single grain as an inclusion in a garnet along with possibly what may be either partial melt, spinel or magnetite. It is a small grain (~10 μm) and is pale green in plane polarized light.

Sample ID: MOX25 161.5B

Sample Type: Coarse Spinel Peridotite

This sample is a coarse spinel harzburgite. It is composed of olivine and orthopyroxene with abundant secondary phlogopite infiltrating the xenolith via set of parallel veins and replacing primary phases. Phlogopite is associated with a domain of finer grained olivine and orthopyroxene, a coarser grained domain lacks phlogopite.

Modal Mineralogy:

Primary Phases:

Olivine: 35%

Orthopyroxene: 40%

Phlogopite: 20%

Spinel: 1%

Secondary Phases:

Serpentine: 2%

Olivine: Olivine has a wide grain size distribution due to a coarse grained domain and a fine grained domain. Coarse grained olivine is up to 4.5 mm, fine grained olivine is 700-800 μm. Grains are subhedral with straight to slightly curved grain boundaries. Large grains show subdomains defined by blocky extinction and moderate fracturing and serpentinization. Some olivine grains have highly irregular grain boundaries due to complex intergrowths with replacing phlogopite.

Orthopyroxene: Grains are 200 μm -~6 mm and have mostly straight grain boundaries. Some smaller grains may be subgrains formed by deformation and phlogopite replacement. Larger grains have curvilinear grain boundaries except where made irregular by recrystallization and

resorption by phlogopite. Some grains have abundant rod-like exsolution lamellae of clinopyroxene. Many grains are replaced by phlogopite and serpentine aggregates at grains boundaries and in fractures.

Phlogopite: This sample contains abundant anhedral-subhedral phlogopite, up to 1.5 mm, that has infiltrated the xenolith via a set of parallel veins. Phlogopite resorbs and replaces primary phases in a domain that looks to have been recrystallized to finer grains. Grains appear bent and deformed and show undulatory extinction and subgrain formation. Grains are not pleochroic. Some grains have highly complex shapes due to intergrowth and replacement of primary phases. Often times undulatory extinction is uniform through intergrowths of phlogopite and primary phases, suggesting that deformation post-dates phlogopite replacement. Phlogopite is also present in cryptocrystalline aggregates in parallel vein set and are bent and sheared in these fractures.

Spinel: There is rare spinel in this sample, in one small group of grains. These grains are ~500 μm translucent brown with curvilinear grain boundaries and are found in the coarser grained domain that lacks abundant phlogopite. There is also a second generation of spinel, found as smaller (40 μm), euhedral blocky grains with angular grain boundaries. They are found in the finer grained domain along with abundant phlogopite, and resemble secondary spinel found along with phlogopite in kelyphitic replacement of garnet.

Serpentine: Serpentine is found in this sample as a blue-grey cryptocrystalline aggregate intergrown with phlogopite in fractures through orthopyroxene, or as pure cryptocrystalline serpentine in fractures through olivine.

Sample ID: MOX25 161.5C

Sample Type: Websterite

This is an altered and recrystallized olivine websterite. There are a few domains of coarser grains but most of the thin section is fine grained, and probably recrystallized with extensive dark patches and interstitial filling of a black replacement aggregate. Distinction of pyroxenes is sometimes difficult. There is a lattice-preferred orientation of recrystallized grains.

Modal Mineralogy:

Primary Phases:

Olivine: 40%

Orthopyroxene: 10%

Clinopyroxene: 25%

Secondary Phases:

Black Replacement: 20%

Serpentine: 2%

Carbonate: 1%

Phlogopite: 1%

Olivine: Olivine has a wide grain size distribution, possibly due to recrystallization. Larger grains are up to 4.3 mm and have irregular grain boundaries due to recrystallization and subgrain formation. Grains are fractured and serpentinized and contain inclusions of smaller olivines and pyroxenes. Smaller possibly recrystallized grains are uniform in size at 100-200 μm. Grains are often elongate and show a lattice-preferred orientation that defines a wavy foliation through the thin section.

Orthopyroxene: Orthopyroxene grains have a wide size range distribution but are smaller than olivine. Grains are anhedral and are 200-800 µm in size. There is little to no exsolution lamellae in orthopyroxene. Smaller grains are in the size range of recrystallized olivine, but do not show a similar LPO.

Clinopyroxene: Clinopyroxene is similar to olivine in that there are larger grains and smaller possibly recrystallized grains. Smaller grains are 100-150 µm, larger grains are up to 4 mm. Large grains are fractured and have irregular grain boundaries due to recrystallization. Grains contain small dark inclusions, interpreted to be partial melt, that are concentrated in bands and along fractures along with small bright spots that may be orthopyroxene exsolution. Small grains are not elongate and do not show LPO.

Black Replacement: There is a high modal proportion of black replacement in this sample. They are zoned cryptocrystalline mixtures of probably serpentine, magnetite, phlogopite, carbonate and possibly secondary spinel. Replacement patches have selvages of host minerals that are 20-80% serpentinized.

Secondary Minerals: Secondary alteration minerals include serpentine, carbonate, phlogopite and possibly secondary spinel and variably alter the xenolith along veins and fractures throughout the thin section. These alteration minerals are also the same constituents found in pervasive black replacement patches.

Sample ID: MOX25 246.1

Sample Type: Websterite

This sample is a garnet bearing websterite. Grains are anhedral with curvilinear grain boundaries and apparent exsolution textures. The sample contains abundant clinopyroxene along with orthopyroxene and garnet. The sample contains abundant orthopyroxene exsolution lamellae in clinopyroxene, and is extensively altered and replaced by serpentine, phlogopite and secondary spinel.

Modal Mineralogy:

Primary Phases:

Clinopyroxene: 70%

Orthopyroxene: 20%

Garnet: 5%

Secondary Phases:

Serpentine: 1%

Phlogopite: 1%

Spinel: 1%

Clinopyroxene: Grains are large (<4 mm), anhedral and extensively altered by the host kimberlite, especially near xenolith border with kimberlite. Grain boundaries are irregular and curvilinear due to intergrowth with orthopyroxene, and contain small rounded orthopyroxene inclusions.

Orthopyroxene: Grains have a wide size range distribution (~500 µm-2 mm). Orthopyroxene grains are highly altered by serpentine, and contain numerous small dark inclusions, interpreted to be partial melt. There are abundant bright rods of clinopyroxene exsolution in larger grains.

There is possibly a positive correlation between degree of partial melting and abundance of exsolution.

Garnet: Garnet occurs as larger discrete grains (<3 mm) with straight grain boundaries, and as irregular anhedral grains appearing as an exsolved phase in orthopyroxene. Grains are fractured and serpentinized, with abundant small dark inclusions interpreted to be partial melt. Larger discrete grains have thin rims of spinel+phlogopite kelyphite.

Secondary Minerals: Secondary alteration minerals include phlogopite, serpentine and secondary spinel. All are found in patches and veins of alteration of primary phases, especially along borders with host kimberlite. Phlogopite (<200 μm) and spinel (<50 μm) occur together in kelyphitic rims around garnet. Serpentine occurs as cryptocrystalline aggregates replacing primary phases along fractures and grain boundaries.

Sample ID: MOX28 269.6

Sample Type: Orthopyroxenite

This sample is 90% orthopyroxene in mostly coarse grains. It is intensely deformed with undulatory extinction, subgrain formation and some neoblast formation along porphyroclast boundaries. Orthopyroxene is partially molten and fractured but shows little exsolution lamellae.

Modal Mineralogy:

Primary Phases:

Olivine: 1%

Orthopyroxene: 90%

Clinopyroxene: 1%

Secondary Phases:

Phlogopite: 1%

Orthopyroxene: Mostly large grains (~10 mm). Grains are broken down into subgrains ~800 µm which are broken down into ~200 µm subgrains. Extensive undulatory extinction throughout. Grains are subhedral with straight grain boundaries and are fractured and contain abundant dark inclusions, interpreted to be partial melt.

Olivine: Scarce, fractured partially molten subhedral grains. ~800 µm in size.

Clinopyroxene: Just a few small subhedral grains ~800 µm in size. Found between orthopyroxene porphyroclasts, but never as inclusions.

Phlogopite: Cryptocrystalline to 400 µm grain-size aggregates found between orthopyroxene porphyroclasts.

Sample ID: MOX28 320.1

Sample Type: Porphyroclastic Peridotite

This is a coarse grained porphyroclastic garnet dunite. Most of the sample consists of large strained olivine grains with lesser clinopyroxene and garnet. Olivine grains are large and subhedral to anhedral and display undulatory extinction, development of subgrains and some development of neoblasts. Porphyroclasts are not fully surrounded by neoblasts indicating low levels of deformation. Grains are fractured and variably altered to serpentine and cryptocrystalline mixtures of serpentine + phlogopite + magnetite. Garnets are subhedral to anhedral with fracturing and partial melting and are rimmed by phlogopite + magnetite kelyphite. Clinopyroxene is present, orthopyroxene may also by present in small amounts. The sample contains veins and patches of replacement of primary phases to a cryptocrystalline aggregate of serpentine + phlogopite + magnetite.

Modal Mineralogy:

Primary Phases:

Olivine Porphyroclasts: 65%

Clinopyroxene: 5%

Garnet: 5%

Olivine Neoblasts: 5%

Secondary Phases:

Black Replacement: 10%

Serpentine: 5%

Magnetite: 1%

Phlogopite: 1%

Carbonate: 1%

Olivine Porphyroclasts: These make up most of the sample. Grains have a broad grain size distribution ranging from 3-15mm and are subhedral-anhedral. All grains are strained and display development of undulatory extinction and deformation lamellae. There is development of subgrains within these porphyroclasts, and some recrystallization to neoblasts. These do not fully envelope porphyroclasts. Porphyroclasts are highly fractured and replaced by serpentine and cryptocrystalline aggregates of serpentine + phlogopite + magnetite.

Olivine Neoblasts: These are small and rounded and found in interstices between and partly surrounding olivine neoblasts. They are 40-100 μm in size. Some are partially serpentinized, and some interstitial areas of serpentine + phlogopite + magnetite may be completely altered olivine neoblasts.

Garnet: This is moderately abundant in this sample, and grains throughout are uniform in size and shape. They are subhedral and 1-3mm in size. All are moderately fractured with some partial melting. Most have rims and inclusions of coarse phlogopite + spinel kelyphite. One grain included in an olivine porphyroclast lacks kelyphite rim.

Pyroxene: There is a small amount of pyroxene in this sample. Most is probably clinopyroxene based on hand sample characteristics and green color of thin section in PPL. It is hard to differentiate from orthopyroxene due to fracturing and alteration. Grains are 2-4mm in size and are irregularly shaped with curvilinear grain boundaries. Grains are fractured, variably altered to serpentine, and contain olivine inclusions.

Spinel: Spinel is in low abundance in this sample. It is found along with phlogopite in kelyphite rims around garnets. Small (10 micron) grains are dark black opaques with a euhedral cubic habit.

Phlogopite: These are found in kelyphite rims around garnets and possibly in cryptocrystalline aggregates along with serpentine and magnetite, based on high interference color of some phase in these zones. In kelyphite grains are 200-500 μm, elongate euhedral.

Serpentine: This is found in cryptocrystalline aggregates between grains and within fractures of larger grains, sometimes along with phlogopite and magnetite and some carbonate. Some of these aggregates show a bluish grey color in XPL.

Magnetite: These are found in cryptocrystalline aggregates along with phlogopite and serpentine. They are small (5-10 micron) rounded opaque grains.

Black Replacement: This is found in small rounded patches between grains and in fractures in olivine porphyroclasts. It is fine grained to cryptocrystalline and dark brown in PPL. Patches are 0.5-2mm in size. Some areas may contain minor carbonate and/or talc.

Carbonate: This is rare but found occasionally in small patches in grain interstices and in some fractures in olivine. It may also be a minor component in cryptocrystalline serpentine + phlogopite + magnetite aggregates.

Sample ID: MOX31 224.5

Sample Type: Coarse Garnet Peridotite

This sample is a large grained coarse garnet harzburgite. It is made up of large subhedral grains of olivine and orthopyroxene with smaller anhedral clinopyroxene grains in interstices of larger subhedral grains. Anhedral, oikocrystic garnet grains are also found in interstices of larger grains. These grains enclose numerous rounded olivine grains. There is also a moderate amount of serpentinization and carbonate replacement of primary phases.

Modal Mineralogy:

Primary Phases:

Orthopyroxene: 45%

Olivine: 40%

Clinopyroxene: 5%

Garnet: 2%

Secondary Phases:

Black Replacement: 2%

Serpentine: 2%

Carbonate: 1%

Magnetite: 2%

Olivine: Olivine are large subhedral grains (800 μm – 4.5 mm) with curvilinear grain boundaries. No undulatory extinction. Some fracturing and serpentinization but fresher than orthopyroxene. Another generation of olivine are smaller anhedral grains between larger olivine and orthopyroxene. These grains enclose smaller rounded olivine and may be associated with garnet

as they have similar textural character. Olivine is also found as smaller (~200 μm) rounded inclusions in garnet.

Orthopyroxene: Orthopyroxene are large (800 μm - <7 mm) anhedral-subhedral, blocky grains with often complex grain boundaries intergrown with interstitial phases. Abundant clinopyroxene exsolution lamellae in bright rods and small anhedral inclusions. Grains are fractured and full of small black inclusions interpreted to be partial melt. Smaller grains are blocky and less altered and fractured.

Clinopyroxene: Clinopyroxene grains are 100 μm to 1 mm and are found as anhedral interstitial blebs between larger olivine and orthopyroxene grains and as anhedral inclusions in orthopyroxene. They are long blobby grains with curvilinear grain boundaries and contain small rounded inclusions of orthopyroxene and olivine. Grains are fractured and contain small dark inclusions, interpreted to be partial melt.

Garnet: Garnets are small anhedral grains found between larger olivine and orthopyroxene grains. They are anhedral and skeletal with inclusions of probably olivine and orthopyroxene. They are fractured and contain small dark inclusions, interpreted to be partial melt.

Black Replacement: Rare patches of aggregated magnetite+phlogopite+serpentine+carbonate. Patches are zoned with magnetite cores and phlogopite rims and serpentine in between. Patches are longish blobs between larger olivine and orthopyroxene grains, in a similar textural character to clinopyroxene and garnet.

Serpentine: Found as cryptocrystalline aggregates replacing primary phases via fractures and infiltrating the xenolith from the host kimberlite.

Carbonate: There is minimal carbonate replacement of xenolith along borders with kimberlite.

Magnetite: Magnetite is found as small ~10 μm dusty inclusions in serpentine replacement of olivine.

Appendix C: Major Element Chemistry of Muskox Xenoliths

Table C1 Major element chemistry of minerals from

Muskox coarse spinel peridotite MOX1 107.5

Phase:	OL	OPX*	SPL
Description:			
# Analyses Averaged:	2	3	
SiO_2	41.78	58.04	<MDL
TiO_2		0.01	<MDL
Al_2O_3	<MDL	0.91	16.41
Cr_2O_3	<MDL	0.43	54.37
FeO	6.58	4.23	16.72
MnO	0.1	0.11	0.07
MgO	52.03	36.96	11.68
CaO	<MDL	0.29	<MDL
Na_2O		<MDL	
NiO	0.35	0.09	<MDL
ZnO			<MDL
K20			
F			
Cl			
Total:	100.85	101.01	99.25
Si	1.001	1.965	<MDL
Ti		0	<MDL
Al	<MDL	0.036	0.618
Cr	<MDL	0.012	1.374
Fe(T)	0.132	0.12	0.447
Mn	0.002	0.003	0.002
Mg	1.858	1.865	0.556
Ca	0	0.011	<MDL
Na		<MDL	
Ni	0.007	0.002	<MDL
Zn			<MDL
K			
Fe			
Cl			
Total:	2.999	4.013	2.997

Muskox coarse spinel peridotite MOX3 69.25

Phase:	OL	CPX*	AMPH
Description:	C=R	C=R	C=R
# Analyses Averaged:	6	6	5
SiO_2	41.65	54.48	43.37
TiO_2		0.22	0.85
Al_2O_3	<MDL	3.99	12.6
Cr_2O_3	<MDL	1.53	1.62
FeO	7.23	1.84	2.81
MnO	0.1	0.08	0.05
MgO	51.43	15.28	18.66
CaO	<MDL	20.95	10.72
Na_2O		2.11	3.34
NiO	0.33	<MDL	0.08
ZnO			
K20			1.03
F			0.8
Cl			0.13
Total:	100.72	100.42	96.06
Si	1.001	1.957	6.324
Ti		0.006	0.093
Al	<MDL	0.169	2.165
Cr	<MDL	0.044	0.187
Fe(T)	0.145	0.055	0.342
Mn	0.002	0.002	0.006
Mg	1.843	0.818	4.055
Ca	<MDL	0.806	1.675
Na		0.147	0.943
Ni	0.006	<MDL	0.009
Zn			
K			0.191
Fe			0.37
Cl			0.032
Total:	2.999	4.005	16.394

Muskox coarse spinel peridotite MOX7 97.68

Phase:	OL	OPX*	SPL
Description:			
# Analyses Averaged:	5	4	3
SiO_2	40.23	55.31	<MDL
TiO_2		0.07	0.05
Al_2O_3	<MDL	3.01	53.34
Cr_2O_3	<MDL	0.3	13.76
FeO	10.24	6.88	13.32
MnO	0.13	0.15	0.09
MgO	49.1	34.15	18.08
CaO	<MDL	0.26	<MDL
Na_2O		<MDL	
NiO	0.42	0.1	0.27
ZnO			0.25
K20			
F			
Cl			
Total:	100.12	100.12	98.94
Si	0.989	1.913	<MDL
Ti		0.002	0.001
Al	<MDL	0.123	1.685
Cr	<MDL	0.008	0.292
Fe(T)	0.211	0.199	0.299
Mn	0.003	0.005	0.002
Mg	1.799	1.761	0.722
Ca	<MDL	0.01	<MDL
Na		<MDL	
Ni	0.008	0.004	0.006
Zn			0.005
K			
Fe			
Cl			
Total:	3.01	4.02	3.007

Muskox coarse spinel peridotite MOX24 31.1A

Phase:	OL	OPX*	CPX*	CPX	SPL	SPL
Description:	C=R	C=R	Grain 1	Grain 2	Grain 1	Grain 2
# Analyses Averaged:	6	4			4	4
SiO_2	41.3	56.79	54.72	54.03	0.35	<MDL
TiO_2		<MDL	<MDL	<MDL	<MDL	<MDL
Al_2O_3	<MDL	1.91	3.56	4.76	33.07	33.46
Cr_2O_3	<MDL	0.41	1.48	1.81	36.56	36.09
FeO	6.89	4.69	1.43	1.24	14.58	14.61
MnO	0.1	0.12	<MDL	<MDL	0.11	0.11
MgO	51.55	35.84	15.54	14.65	15.13	15.19
CaO	0.03	0.28	20.96	19.82	<MDL	<MDL
Na_2O		<MDL	2.23	2.94		
NiO	0.4	<MDL	<MDL	<MDL	<MDL	0.11
ZnO					0.35	0.37
K20						
F						
Cl						
Total:	100.25	100.04	99.93	99.23	99.88	99.81
Si	0.997	1.944	1.971	1.957	0.01	<MDL
Ti		<MDL	<MDL	<MDL	<MDL	<MDL
Al	<MDL	0.077	0.151	0.203	1.137	1.149
Cr	<MDL	0.011	0.042	0.052	0.843	0.831
Fe(T)	0.139	0.134	0.043	0.038	0.356	0.356
Mn	0.002	0.003	<MDL	<MDL	0.003	0.002
Mg	1.855	1.829	0.834	0.791	0.658	0.66
Ca	0.001	0.01	0.809	0.769	<MDL	<MDL
Na		<MDL	0.156	0.206		
Ni	0.008	<MDL	<MDL	<MDL	<MDL	0.003
Zn					0.007	0.008
K						
Fe						
Cl						
Total:	3.002	4.009	4.01	4.018	3.006	3.007

Muskox coarse spinel peridotite MOX24 65.16B

Phase:	OL	OPX*	CPX*	SPL
Description:				
# Analyses Averaged:	4	2	3	4
SiO_2	41.36	56.9	54.25	<MDL
TiO_2		<MDL	<MDL	<MDL
Al_2O_3	<MDL	2.03	2.01	30.6
Cr_2O_3	<MDL	0.53	0.84	38.86
FeO	7.28	5	1.43	16.08
MnO	0.1	0.13	0.08	0.14
MgO	51.12	35.61	17.32	14.22
CaO	<MDL	0.55	23.22	<MDL
Na_2O		<MDL	0.72	
NiO	0.39	0.11	<MDL	0.11
ZnO				0.25
K20				
F				
Cl				
Total:	100.25	100.81	99.85	100.02
Si	1	1.939	1.964	<MDL
Ti		<MDL	0	<MDL
Al	<MDL	0.082	0.086	1.067
Cr	<MDL	0.014	0.024	0.909
Fe(T)	0.147	0.143	0.043	0.398
Mn	0.002	0.004	0.002	0.004
Mg	1.842	1.809	0.935	0.627
Ca	<MDL	0.02	0.901	<MDL
Na		<MDL	0.051	
Ni	0.008	0.003	0.001	0.003
Zn				0.006
K				
Fe				
Cl				
Total:	3	4.011	4.006	3.007

Muskox coarse spinel peridotite MOX24 84.8

Phase:	OL	OPX	OPX*	OPX	SPL	SPL	AMPH
Description:		Grain 1	Grain 2	Grain 3	Grain 1	Grain 2	
# Analyses Averaged:	5		3	2	3	2	5
SiO_2	40.99	55.95	56.71	57.56	<MDL	<MDL	44.34
TiO_2		<MDL	<MDL	<MDL	<MDL	<MDL	0.04
Al_2O_3	<MDL	3.25	2.23	1.41	38.37	33.06	13.47
Cr_2O_3	<MDL	0.78	0.43	0.24	29.35	34.77	1.23
FeO	8.58	5.89	5.7	5.72	15.91	17	2.71
MnO	0.12	0.12	0.13	0.15	0.11	0.13	0.05
MgO	50.52	34.7	35.27	35.62	16.08	14.67	19.12
CaO	<MDL	0.09	0.12	0.1	<MDL	<MDL	12.1
Na_2O		<MDL	<MDL	<MDL			3.26
NiO	0.4	0.12	0.08	0.08	0.13	0.09	0.11
ZnO					0.38	0.3	
K20							
F							
Cl							
Total:	100.61	100.91	100.61	100.89	100.33	100.01	96.45
Si	0.994	1.912	1.939	1.961	<MDL	<MDL	6.387
Ti		<MDL	<MDL	<MDL	<MDL	<MDL	0.005
Al	<MDL	0.131	0.09	0.057	1.288	1.144	2.287
Cr	<MDL	0.021	0.012	0.006	0.661	0.807	0.14
Fe(T)	0.174	0.169	0.163	0.163	0.379	0.418	0.327
Mn	0.003	0.004	0.004	0.004	0.003	0.003	0.006
Mg	1.826	1.768	1.797	1.809	0.683	0.642	4.106
Ca	<MDL	0.003	0.004	0.004	<MDL	<MDL	1.868
Na		<MDL	<MDL	<MDL			0.91
Ni	0.008	0.003	0.002	0.002	0.003	0.002	0.013
Zn					0.008	0.006	
K							
Fe							
Cl							
Total:	3.005	4.011	4.009	4.007	3.023	3.023	16

Muskox coarse spinel peridotite MOX24 124.0B

Phase:	OL	OPX	CPX	SPL
Description:				
# Analyses Averaged:	4	2	2	
SiO_2	40.63	58.07	53.51	<MDL
TiO_2		<MDL	0.24	0.05
Al_2O_3	<MDL	0.87	1.74	14.48
Cr_2O_3	<MDL	0.26	1.18	55.11
FeO	7.85	5.1	3.31	19.2
MnO	0.1	0.16	0.1	0.15
MgO	51.23	36.29	17.55	11.36
CaO	0.03	0.15	19.31	<MDL
Na_2O		<MDL	1.66	
NiO	0.43	<MDL	<MDL	0.15
ZnO				<MDL
K20				
F				
Cl				
Total:	100.24	100.9	98.62	100.7
Si	0.987	1.972	1.968	0.003
Ti		<MDL	0.007	0.001
Al	<MDL	0.035	0.075	0.548
Cr	<MDL	0.007	0.034	1.4
Fe(T)	0.16	0.145	0.102	0.516
Mn	0.002	0.005	0.003	0.004
Mg	1.855	1.837	0.962	0.544
Ca	0.001	0.005	0.761	0
Na		<MDL	0.119	
Ni	0.008	<MDL	<MDL	0.004
Zn				0.003
K				
Fe				
Cl				
Total:	3.012	4.005	4.03	3.022

Muskox coarse spinel peridotite MOX25 161.5B

Phase:	OL	OPX	OPX*	CPX*
Description:		Grain 1	Grain 2	
# Analyses Averaged:	3			4
SiO_2	41.51	57.13	56.79	54.35
TiO_2		<MDL	<MDL	<MDL
Al_2O_3	<MDL	2.19	1.58	2.8
Cr_2O_3	<MDL	0.37	0.44	1.02
FeO	7.32	4.84	4.75	1.39
MnO	0.1	0.12	0.11	0.08
MgO	51.2	35.73	35.16	16.73
CaO	<MDL	<MDL	1.23	22.76
Na_2O		<MDL	<MDL	0.98
NiO	0.43	0.09	0.12	0.09
ZnO				
K20				
F				
Cl				
Total:	100.53	100.47	100.18	100.14
Si	1.001	1.944	1.949	1.96
Ti		<MDL	<MDL	<MDL
Al	<MDL	0.088	0.064	0.119
Cr	<MDL	0.01	0.012	0.029
Fe(T)	0.148	0.138	0.136	0.042
Mn	0.002	0.004	0.003	0.002
Mg	1.84	1.812	1.799	0.899
Ca	<MDL	<MDL	0.045	0.879
Na		<MDL	<MDL	0.069
Ni	0.008	0.002	0.003	0.003
Zn				
K				
Fe				
Cl				
Total:	2.999	3.998	4.012	4

Table C9 Major element chemistry of minerals from

Muskox coarse spinel-garnet peridotite MOX3 33.0

Phase:	OL*	OPX	OPX*	CPX*	GAR*	SPL
Description:	C=R	C	R	C=R		
# Analyses Averaged:	4		2	3	5	2
SiO_2	41.35	56.6	58.07	54.88	41.42	<MDL
TiO_2		<MDL	<MDL	0.05		0.27
Al_2O_3	<MDL	0.7	0.48	1.63	21.37	9.88
Cr_2O_3	<MDL	1.27	0.21	1.42	3.87	55.63
FeO	7.62	4.91	4.75	1.84	8.27	23.11
MnO	0.11	0.1	0.14	0.09	0.53	0.14
MgO	51.21	36.27	36.79	16.71	19.1	10.71
CaO	0.03	0.18	0.18	21.85	5.35	<MDL
Na_2O		<MDL	<MDL	1.43		
NiO	0.43	<MDL	0.09	<MDL	<MDL	0.12
ZnO						<MDL
K20						
F						
Cl						
Total:	100.72	100.04	100.58	99.8	99.91	99.8
Si	0.997	1.946	1.976	1.988	2.98	<MDL
Ti		<MDL	<MDL	0.001		0.007
Al	<MDL	0.028	0.019	0.07	1.812	0.39
Cr	<MDL	0.035	0.006	0.041	0.22	1.474
Fe(T)	0.154	0.141	0.135	0.056	0.498	0.648
Mn	0.002	0.003	0.003	0.003	0.032	0.004
Mg	1.841	1.859	1.865	0.902	2.048	0.535
Ca	0	0.007	0.007	0.848	0.412	<MDL
Na		<MDL	<MDL	0.1	0.002	0
Ni	0.008	<MDL	0.003	<MDL	<MDL	0.003
Zn						<MDL
K						
Fe						
Cl						
Total:	3.002	4.019	4.012	4.005	8.004	3.058

Muskox coarse spinel-garnet peridotite MOX7 62.38

Phase:	OL	OL	OPX	OPX*	CPX*	CPX	GAR	SPL	AMPH
Description:	Grain 1	Grain 2 C=R	C	R	Grain 1	Grain 2		C=R	C=R
# Analyses Averaged:	5	3		2	4	2	2	7	6
SiO_2	41.41	41.18	55.69	58.08	55.29	52.91	41.23	<MDL	45.92
TiO_2			<MDL	<MDL	<MDL	0.07		0.09	0.05
Al_2O_3	<MDL	<MDL	2.67	0.57	1.43	3.81	23.07	12.01	10.58
Cr_2O_3	<MDL	<MDL	0.54	0.19	1.01	1.25	1.66	53.3	1.71
FeO	7.98	8.13	4.91	5.23	1.49	1.88	9.62	23.19	2.92
MnO	0.09	0.12	0.09	0.16	0.08	<MDL	0.63	0.24	0.08
MgO	50.53	50.91	33.04	36.25	16.91	17.8	18.76	10.31	19.99
CaO	0.03	<MDL	2.18	0.16	22.93	19.89	4.8	0.06	10.9
Na_2O			0.8	<MDL	1.1	1.76	<MDL		3.32
NiO	0.43	0.44	0.1	<MDL	<MDL	<MDL	<MDL	0.14	0.11
ZnO								0.27	
K20									0.94
F									0.27
Cl									0.05
Total:	100.39	100.78	100.02	100.63	100.21	99.33	99.77	99.42	96.81
Si	1.002	0.995	1.928	1.979	1.993	1.921	2.964	<MDL	6.582
Ti			<MDL	<MDL	<MDL	0.001		0.002	0.006
Al	<MDL	<MDL	0.109	0.023	0.061	0.163	1.955	0.472	1.787
Cr	<MDL	<MDL	0.015	0.005	0.029	0.036	0.095	1.406	0.194
Fe(T)	0.161	0.164	0.142	0.149	0.045	0.057	0.578	0.647	0.351
Mn	0.001	0.002	0.003	0.005	0.003	<MDL	0.039	0.007	0.01
Mg	1.823	1.834	1.705	1.841	0.908	0.963	2.01	0.513	4.269
Ca	0	<MDL	0.081	0.006	0.886	0.774	0.37	0.002	1.673
Na			0.054	<MDL	0.077	0.124	<MDL		0.924
Ni	0.008	0.009	0.004	<MDL	<MDL	<MDL	<MDL	0.004	0.013
Zn								0.007	
K									0.172
Fe									0.121
Cl									0.012
Total:	2.997	3.004	4.04	4.007	4	4.039	8.01	3.055	16.107

Table C11 Major element chemistry of minerals from

Muskox coarse garnet peridotite MOX1 45.5

Phase:	OL*	OPX*	CPX*	GAR*	GAR
Description:	C=R	C=R	C=R	R	C
# Analyses Averaged:	8	4	4	6	2
SiO_2	40.6	57.54	54.9	41.38	41.3
TiO_2		0.11	0.24		
Al_2O_3	0.05	0.52	1.88	19.44	18.61
Cr_2O_3	0.05	0.27	1.82	4.97	6.99
FeO	9.77	5.8	3.1	8.75	7.58
MnO	0.12	0.15	0.12	0.41	0.29
MgO	49.47	35.26	17.13	19.33	19.72
CaO	0.04	0.56	18.67	5.13	5.25
Na_2O		0.17	1.92	0.16	<MDL
NiO	0.41	0.13	0.1	<MDL	<MDL
ZnO					
K20					
F					
Cl					
Total:	100.41	100.47	99.81	99.46	99.74
Si	0.992	1.974	1.987	3.008	2.997
Ti		0.003	0.007		
Al	0	0.021	0.08	1.665	1.591
Cr	0.001	0.007	0.052	0.286	0.401
Fe(T)	0.2	0.166	0.094	0.532	0.46
Mn	0.002	0.004	0.003	0.025	0.018
Mg	1.802	1.803	0.924	2.094	2.133
Ca	0.001	0.021	0.724	0.399	0.408
Na		0.011	0.135	0.013	<MDL
Ni	0.008	0.003	0.002	<MDL	<MDL
Zn					
K					
Fe					
Cl					
Total:	3.007	4.015	4.008	8.023	8.007

Muskox coarse garnet peridotite MOX31 224.5

Phase:	OL	OPX	OPX*	CPX*
Description:		C	R	
# Analyses Averaged:	4		3	4
SiO_2	40.54	57.15	57.7	54.85
TiO_2		<MDL	0.11	0.23
Al_2O_3	<MDL	2.2	0.71	1.81
Cr_2O_3	0.07	0.44	0.58	1.91
FeO	10.31	5.61	6.09	3.28

MnO	0.12	0.13	0.15	0.13
MgO	48.9	35.04	34.88	17.23
CaO	0.03	0.11	0.63	18.51
Na_2O		<MDL	0.22	1.94
NiO	0.34	<MDL	0.09	<MDL
ZnO				
K20				
F				
Cl				
Total:	100.25	100.68	101.17	99.89
Si	0.994	1.949	1.971	1.985
Ti		<MDL	0.003	0.006
Al	<MDL	0.089	0.029	0.077
Cr	0.001	0.012	0.016	0.055
Fe(T)	0.212	0.16	0.174	0.099
Mn	0.002	0.004	0.004	0.004
Mg	1.788	1.781	1.776	0.929
Ca	0.001	0.004	0.023	0.717
Na		<MDL	0.015	0.136
Ni	0.007	<MDL	0.003	<MDL
Zn				
K				
Fe				
Cl				
Total:	3.005	3.998	4.012	4.009

Table C13 Major element chemistry of minerals from of Muskox porphyroclastic peridotite DDH2 91.5

Phase:	CPX	CPX*	GAR*
Description:	Grain 1 C	Grain 2 C=R	C=R
# Analyses Averaged:		4	8
SiO_2	54.77	54.62	40.92
TiO_2	0.25	0.28	
Al_2O_3	1.36	1.4	19.46
Cr_2O_3	0.5	1.06	4.47
FeO	4.79	4.65	10.14
MnO	0.13	0.12	0.37
MgO	18.65	18.22	19.11

CaO	18.01	17.75	4.81
Na_2O	1.23	1.36	0.15
NiO	0.1	0.12	0.02
ZnO			
K20			
F			
Cl			
Total:	99.78	99.51	99.34
Si	1.987	1.987	2.993
Ti	0.007	0.008	
Al	0.058	0.06	1.677
Cr	0.014	0.031	0.259
Fe(T)	0.145	0.141	0.62
Mn	0.004	0.004	0.023
Mg	1.009	0.988	2.083
Ca	0.7	0.692	0.377
Na	0.086	0.096	0.01
Ni	0.003	0.002	0.001
Zn			
K			
Fe			
Cl			
Total:	4.013	4.008	8.044

Muskox porphyroclastic peridotite MOX11 162.1

Phase:	OL	OPX*	GAR
Description:	C=R	C=R	C=R
# Analyses Averaged:	8	4	5
SiO_2	41.24	57.42	40.7
TiO_2		0.06	
Al_2O_3	<MDL	0.39	15.7
Cr_2O_3	0.06	0.35	10.04
FeO	8.36	4.91	7.49
MnO	0.09	0.11	0.32
MgO	49.9	35.66	18.77
CaO	0.04	0.7	6.39
Na_2O		0.16	<MDL
NiO	0.4	0.16	<MDL
ZnO			
K20			
F			
Cl			
Total:	100.05	99.64	99.41
Si	1.004	1.976	3.006

Ti		0.001	
Al	<MDL	0.015	1.367
Cr	0.001	0.009	0.586
Fe(T)	0.17	0.141	0.463
Mn	0.002	0.003	0.02
Mg	1.81	1.829	2.066
Ca	0.001	0.026	0.506
Na		0.011	<MDL
Ni	0.008	0.004	<MDL
Zn			
K			
Fe			
Cl			
Total:	2.995	4.016	8.014

Muskox porphyroclastic peridotite MOX24 124.0A

Phase:	OL*	OPX*	CPX*	GAR*
Description:	C=R	C=R	C=R	C=R
# Analyses Averaged:	7	9	4	5
SiO_2	40.69	57.73	54.8	40.88
TiO_2		<MDL	<MDL	
Al_2O_3	<MDL	0.35	0.8	15.39
Cr_2O_3	0.06	0.3	1.32	10.67
FeO	8.23	4.86	2.57	7.39
MnO	0.11	0.13	0.12	0.35
MgO	50.65	35.74	18.87	18.63
CaO	0.04	0.71	20.09	6.73
Na_2O		0.13	0.89	<MDL
NiO	0.4	0.11	0.11	<MDL
ZnO				
K20				
F				
Cl				
Total:	100.12	99.96	99.48	100.04
Si	0.991	1.981	1.988	3.007
Ti		<MDL	<MDL	
Al	<MDL	0.014	0.034	1.335
Cr	0.001	0.008	0.038	0.621
Fe(T)	0.167	0.14	0.078	0.455
Mn	0.002	0.004	0.004	0.022
Mg	1.838	1.828	1.02	2.042
Ca	0.001	0.026	0.781	0.53
Na		0.005	0.063	<MDL
Ni	0.008	0.003	0.002	<MDL

Zn				
K				
Fe				
Cl				
Total:	3.008	4.01	4.007	8.011

Muskox porphyroclastic peridotite MOX25 124.8

Phase:	OL	CPX*	GAR*	GAR
Description:	C=R	C=R	R	C
# Analyses Averaged:	5	3		
SiO_2	41.03	55.1	41.69	40.96
TiO_2		0.06		
Al_2O_3	<MDL	1.39	19.65	17.27
Cr_2O_3	0.05	0.94	4.88	8.05
FeO	9.29	3.1	7.83	8.02
MnO	0.09	0.11	0.28	0.29
MgO	49.63	18.54	20.06	19.34
CaO	0.04	19.28	5.12	5.72
Na_2O		1.21	<MDL	<MDL
NiO	0.38	0.06	<MDL	<MDL
ZnO				
K20				
F				
Cl				
Total:	100.46	99.79	99.51	99.65
Si	0.999	1.991	3.01	2.998
Ti		0.002	NA	
Al	<MDL	0.059	1.672	1.49
Cr	0.001	0.027	0.279	0.466
Fe(T)	0.189	0.094	0.473	0.491
Mn	0.002	0.003	0.017	0.018
Mg	1.801	0.999	2.159	2.11
Ca	0.001	0.746	0.396	0.448
Na		0.085	<MDL	<MDL
Ni	0.007	0.002	<MDL	<MDL
Zn				
K				
Fe				
Cl				
Total:	3	4.007	8.006	8.02

Muskox porphyroclastic peridotite MOX28 320.1

Phase:	OL	CPX*	GAR	GAR*

Description:	C=R	C=R	C	R
# Analyses Averaged:	7	6	3	3
SiO_2	40.79	54.49	41.12	41.32
TiO_2		0.23		
Al_2O_3	0.05	1.86	19.57	20.19
Cr_2O_3	<MDL	1.41	4.55	3.87
FeO	10.54	3.26	9.21	9.23
MnO	0.11	0.12	0.43	0.41
MgO	48.76	17.15	18.73	19.01
CaO	0.04	19.41	5.77	5.5
Na_2O		1.8	0.13	<MDL
NiO	0.27	0.09	<MDL	<MDL
ZnO				
K20				
F				
Cl				
Total:	100.49	99.74	99.42	99.53
Si	0.998	1.979	3	3
Ti		0.006		
Al	0	0.079	1.683	1.727
Cr	<MDL	0.041	0.263	0.222
Fe(T)	0.216	0.099	0.562	0.561
Mn	0.002	0.004	0.027	0.025
Mg	1.778	0.928	2.037	2.058
Ca	0.001	0.755	0.451	0.428
Na		0.127	0.006	<MDL
Ni	0.005	0.001	<MDL	<MDL
Zn				
K				
Fe				
Cl				
Total:	3.001	4.018	8.029	8.021

Table C18 Major element chemistry of minerals from

Muskox websterite MOX0 157.45

Phase:	OL*	OPX*	CPX*	GAR*

Description:				
# Analyses Averaged:	4	2	3	4
SiO_2	40.11	56.9	53.96	41.11
TiO_2		0.13	0.21	
Al_2O_3	<MDL	0.76	1.81	20.18
Cr_2O_3	<MDL	0.64	1.72	4.03
FeO	10.72	6.09	3.04	9.47
MnO	0.12	0.11	0.12	0.42
MgO	48.91	34.99	17.23	18.87
CaO	0.04	0.52	18.74	5.47
Na_2O		0.22	1.94	<MDL
NiO	0.28	<MDL	<MDL	<MDL
ZnO				
K20				
F				
Cl				
Total:	100.18	100.37	98.75	99.57
Si	0.987	1.96	1.977	2.99
Ti		0.003	0.006	
Al	<MDL	0.031	0.078	1.73
Cr	<MDL	0.018	0.05	0.232
Fe(T)	0.221	0.175	0.093	0.576
Mn	0.002	0.003	0.004	0.026
Mg	1.794	1.796	0.941	2.046
Ca	0.001	0.019	0.736	0.427
Na		0.014	0.138	<MDL
Ni	0.006	<MDL	<MDL	<MDL
Zn				

K				
Fe				
Cl				
Total:	3.011	4.02	4.022	8.026

Table C19 Major element chemistry of minerals from

Muskox websterite MOX0 158.8A

Phase:	CPX*	GAR*
Description:		
# Analyses Averaged:	2	3
SiO_2	53.08	40.25
TiO_2	0.22	
Al_2O_3	1.89	20.39
Cr_2O_3	1.13	3.07
FeO	3.14	10.42
MnO	0.09	0.55
MgO	16.26	16.51
CaO	20.76	7.69
Na_2O	1.72	0.12
NiO	<MDL	<MDL

ZnO		
K20		
F		
Cl		
Total:	98.29	98.91
Si	1.966	2.975
Ti	0.006	
Al	0.082	1.777
Cr	0.033	0.18
Fe(T)	0.097	0.644
Mn	0.003	0.034
Mg	0.898	1.819
Ca	0.824	0.609
Na	0.124	0.016
Ni	<MDL	<MDL
Zn		
K		
Fe		
Cl		
Total:	4.032	8.054

Table C20 Major element chemistry of minerals from

Muskox websterite MOX0 162.8A

Phase:	OPX	OPX*	CPX*	GAR*	GAR
Description:	C	C=R	C=R	Grain 1 C=R	Grain 2 C=R
# Analyses Averaged:	3	2	2	5	5
SiO_2	57.1	57.17	54.16	40.83	40.46
TiO_2	0.12	0.13	0.26		
Al_2O_3	0.67	0.54	2.01	18.33	17.41
Cr_2O_3	0.51	0.32	2.83	6.11	7.38
FeO	5.91	5.89	3.23	9.18	9.13
MnO	0.15	0.15	0.1	0.45	0.43
MgO	34.69	35.06	16.46	18.86	18.51
CaO	0.56	0.56	17.82	5.44	5.6
Na_2O	0.23	0.16	2.37	0.21	0.17
NiO	0.11	0.09		<MDL	<MDL
ZnO					
K20					
F					
Cl					
Total:	99.97	100.06	99.25	99.26	98.97
Si	1.971	1.972	1.977	2.998	2.994
Ti	0.003	0.003	0.007		
Al	0.027	0.022	0.087	1.586	1.519
Cr	0.014	0.009	0.082	0.355	0.432
Fe(T)	0.171	0.17	0.099	0.564	0.565
Mn	0.004	0.004	0.003	0.028	0.027

Mg	1.785	1.802	0.896	2.064	2.042
Ca	0.021	0.021	0.697	0.428	0.444
Na	0.015	0.01	0.168	0.016	0.014
Ni	0.002	0.003	0.001	<MDL	<MDL
Zn					
K					
Fe					
Cl					
Total:	4.013	4.015	4.016	8.038	8.037

Table C21 Major element chemistry of minerals from

Muskox websterite MOX0 162.8B

Phase:	OPX*	CPX	CPX*	GAR	GAR*
Description:		Grain 1	Grain 2	Grain 1	Grain 2
# Analyses Averaged:	2		2		3
SiO_2	57.35	54.66	55.03	40.32	40.9
TiO_2	0.12	0.17	0.27		
Al_2O_3	0.7	1.67	1.94	17.85	18.71
Cr_2O_3	0.55	1.72	1.8	7.09	5.72
FeO	6.03	3.09	3.3	9.14	8.88

MnO	0.16	0.1	0.14	0.38	0.43
MgO	34.6	17.78	16.88	18.68	18.94
CaO	0.55	18.74	18.67	5.32	5.25
Na_2O	0.19	1.73	2.03	<MDL	0.17
NiO	0.13	0.09		<MDL	<MDL
ZnO					
K20					
F					
Cl					
Total:	100.34	99.75	100.05	98.79	98.89
Si	1.973	1.981	1.988	2.983	3.004
Ti	0.003	0.005	0.007		
Al	0.029	0.072	0.083	1.556	1.619
Cr	0.015	0.049	0.051	0.415	0.332
Fe(T)	0.174	0.094	0.1	0.566	0.545
Mn	0.005	0.003	0.004	0.024	0.027
Mg	1.774	0.96	0.909	2.06	2.073
Ca	0.02	0.728	0.723	0.422	0.413
Na	0.013	0.122	0.142	0.016	0.014
Ni	0.002	0.003	0.002	0	0
Zn					
K					
Fe					
Cl					
Total:	4.008	4.015	4.009	8.04	8.028

Table C22 Major element chemistry of minerals from

Muskox websterite MOX0 179.3

Phase:	OPX*	CPX*	GAR*	GAR
Description:	C=R	C=R	R	C
# Analyses Averaged:	4	6	4	2
SiO_2	57.64	54.95	41.03	40.56
TiO_2	0.12	0.21		
Al_2O_3	0.55	1.82	18.84	16.36
Cr_2O_3	0.35	1.9	5.72	8.43
FeO	6	3.09	8.87	9.06
MnO	0.14	0.12	0.38	0.43
MgO	35	17.19	19.02	17.81
CaO	0.58	18.62	5.29	6.44
Na_2O	0.19	2	0.15	<MDL
NiO	0.05		<MDL	<MDL
ZnO				
K20				
F				
Cl				
Total:	100.61	99.89	99.19	99.09
Si	1.976	1.987	3.002	3.014

Ti	0.003	0.006		
Al	0.022	0.078	1.624	1.432
Cr	0.009	0.054	0.331	0.495
Fe(T)	0.172	0.093	0.543	0.563
Mn	0.004	0.004	0.023	0.027
Mg	1.789	0.927	2.075	1.973
Ca	0.021	0.721	0.415	0.513
Na	0.012	0.14	0.012	<MDL
Ni	0.001	0.001	<MDL	<MDL
Zn				
K				
Fe				
Cl				
Total:	4.011	4.011	8.025	8.018

Table C23 Major element chemistry of minerals from

Muskox websterite MOX0 197.0

Phase:	OL*	OPX*	CPX*	GAR*
Description:				
# Analyses Averaged:	2		3	2

SiO_2	40.09	56.01	53.34	40.26
TiO_2		0.12	0.28	
Al_2O_3	<MDL	0.7	2.06	17.39
Cr_2O_3	0.04	0.53	1.91	7.17
FeO	10.81	6.34	3.4	9.62
MnO	0.15	0.11	0.12	0.46
MgO	48.97	34.62	16.58	18.09
CaO	0.03	0.9	18.34	5.61
Na_2O		0.18	2.17	0.12
NiO	0.27	0.1	<MDL	<MDL
ZnO				
K20				
F				
Cl				
Total:	100.33	99.62	98.2	98.67
Si	0.986	1.951	1.971	2.996
Ti		0.003	0.008	
Al	<MDL	0.029	0.09	1.525
Cr	0.001	0.015	0.056	0.422
Fe(T)	0.222	0.185	0.105	0.599
Mn	0.003	0.003	0.004	0.029
Mg	1.795	1.798	0.913	2.006
Ca	0.001	0.034	0.726	0.447
Na		0.012	0.155	0.015
Ni	0.005	0.004	<MDL	<MDL
Zn				
K				
Fe				

Cl				
Total:	3.014	4.033	4.027	8.039

Table C24 Major element chemistry of minerals from

Muskox websterite MOX0198.37

Phase:	OPX*	CPX*	GAR	GAR*
Description:	C=R	C=R	C	R
# Analyses Averaged:	7	6		5
SiO_2	57.57	54.81	39.98	40.57
TiO_2	0.12	0.26		
Al_2O_3	0.52	1.85	16.3	17.76
Cr_2O_3	0.34	2.01	8.35	6.88
FeO	5.84	3.19	9.04	9.01
MnO	0.12	0.1	0.41	0.42
MgO	35.05	16.94	17.39	18.56
CaO	0.54	18.74	6.6	5.55
Na_2O	0.19	2.12	<MDL	0.15
NiO	0.13	<MDL	<MDL	<MDL
ZnO				
K20				

F				
Cl				
Total:	100.3	99.98	98.08	98.79
Si	1.978	1.983	3.005	3
Ti	0.003	0.007		
Al	0.021	0.079	1.444	1.548
Cr	0.009	0.058	0.497	0.402
Fe(T)	0.168	0.096	0.569	0.557
Mn	0.003	0.003	0.026	0.026
Mg	1.794	0.914	1.949	2.045
Ca	0.02	0.726	0.531	0.44
Na	0.011	0.149	0.01	0.013
Ni	0.003	0.001	0	0
Zn				
K				
Fe				
Cl				
Total:	4.01	4.016	8.03	8.032

Table C25 Major element chemistry of minerals from

Muskox websterite MOX0 216.83

Phase:	OPX*	CPX	CPX*	GAR*
Description:		Grain 1	Grain 2	
# Analyses Averaged:	4			2
SiO_2	56.33	55.34	54.25	40.56
TiO_2	0.14	0.16	0.28	
Al_2O_3	0.61	1.63	2.05	18.04
Cr_2O_3	0.53	1.52	1.47	6.46
FeO	6.12	3.1	3.28	9.39
MnO	0.17	0.13	0.09	0.39
MgO	35.09	17.6	17.04	18.51
CaO	0.5	19.37	19.27	5.55
Na_2O	0.2	1.75	1.75	<MDL
NiO	0.09	0.04	0.03	<MDL
ZnO				
K20				
F				
Cl				
Total:	99.65	100.64	99.51	98.89
Si	1.955	1.988	1.974	2.996
Ti	0.004	0.004	0.008	
Al	0.025	0.069	0.088	1.571
Cr	0.014	0.043	0.042	0.377
Fe(T)	0.178	0.093	0.1	0.58
Mn	0.005	0.004	0.003	0.024
Mg	1.816	0.942	0.924	2.038
Ca	0.019	0.746	0.752	0.439
Na	0.012	0.122	0.123	<MDL

Ni	0.002	0.001	0.001	<MDL
Zn				
K				
Fe				
Cl				
Total:	4.03	4.013	4.015	8.025

Table C26 Major element chemistry of minerals from

Muskox websterite MOX0 233.5

Phase:	OL	CPX*	GAR*
Description:			
# Analyses Averaged:	4	4	
SiO_2	40.66	55.01	39.88
TiO_2		0.25	
Al_2O_3	<MDL	1.85	16.51
Cr_2O_3	<MDL	1.19	7.93
FeO	10.85	3.33	9.27
MnO	0.12	0.12	0.42
MgO	48.54	17.16	17.82
CaO	0.04	19.39	5.96

Na_2O		1.81	0.13
NiO	0.26	<MDL	<MDL
ZnO			
K20			
F			
Cl			
Total:	100.41	100.08	97.92
Si	0.997	1.988	2.999
Ti		0.007	
Al	<MDL	0.079	1.464
Cr	<MDL	0.034	0.472
Fe(T)	0.222	0.101	0.583
Mn	0.002	0.003	0.027
Mg	1.774	0.924	1.998
Ca	0.001	0.751	0.48
Na		0.127	0.018
Ni	0.005	<MDL	<MDL
Zn			
K			
Fe			
Cl			
Total:	3.002	4.013	8.041

Table C27 Major element chemistry of minerals from

Muskox websterite MOX1 59.0

Phase:	OL*	OPX*	CPX	CPX*	GAR*
Description:	C=R	C=R	C	R	C=R
# Analyses Averaged:	4	3			2
SiO_2	40.88	57.68	54.58	54.75	40.63
TiO_2		0.14	0.24	0.26	
Al_2O_3	<MDL	0.55	1.71	2.02	19.04
Cr_2O_3	<MDL	0.26	1.85	1.25	5.17
FeO	10.52	6.09	2.99	3.38	9.34
MnO	0.12	0.16	0.15	0.11	0.38
MgO	48.57	35.02	17.11	17.18	18.76
CaO	0.03	0.55	18.97	18.92	5.25
Na_2O		0.19	1.88	1.87	<MDL
NiO	0.28	<MDL	<MDL	<MDL	<MDL
ZnO					
K20					
F					
Cl					
Total:	100.38	100.57	99.47	99.73	98.58
Si	1.001	1.977	1.984	1.984	2.994
Ti		0.004	0.007	0.007	
Al	<MDL	0.022	0.073	0.086	1.653
Cr	<MDL	0.007	0.053	0.036	0.301
Fe(T)	0.216	0.175	0.091	0.102	0.576

Mn	0.003	0.005	0.005	0.004	0.024
Mg	1.773	1.789	0.927	0.928	2.06
Ca	0	0.02	0.739	0.734	0.415
Na		0.011	0.132	0.132	<MDL
Ni	0.006	<MDL	<MDL	<MDL	<MDL
Zn					
K					
Fe					
Cl					
Total:	2.998	4.009	4.0114	4.012	8.023

Table C28 Major element chemistry of minerals from

Muskox websterite MOX3 42.1

Phase:	OL*	OPX*	OPX	CPX	CPX*	GAR*	GAR
Description:	C=R	C=R	L	C	R	R	C
# Analyses Averaged:	2	2	2	2	2		2
SiO_2	40.69	57.6	57.41	54.74	54.59	41	41.13
TiO_2		0.14	0.13	0.25	0.29		
Al_2O_3	<MDL	0.51	0.5	1.79	1.89	18.73	19.13
Cr_2O_3	0.05	0.31	0.27	1.83	1.93	5.75	5.17

FeO	10.02	5.99	5.81	3.23	3.3	9.18	8.81
MnO	0.14	0.14	0.18	0.1	0.12	0.43	0.4
MgO	49.42	35.21	35.33	17.02	16.92	18.89	19.07
CaO	<MDL	0.55	0.54	18.89	18.69	5.19	5.19
Na_2O		0.2	0.16	2.01	2.11	0.13	0.13
NiO	0.36	0.14		<MDL	0.11	<MDL	<MDL
ZnO							
K20							
F							
Cl							
Total:	100.65	100.73	100.33	99.86	99.88	99.3	98.97
Si	1.489	1.973	1.972	1.984	1.98	3.004	3.009
Ti	0	0.004	0.003	0.007	0.008		
Al	<MDL	0.021	0.02	0.077	0.081	1.617	1.649
Cr	0.001	0.009	0.007	0.052	0.055	0.333	0.299
Fe(T)	0.307	0.172	0.167	0.098	0.1	0.562	0.539
Mn	0.004	0.004	0.005	0.003	0.004	0.027	0.025
Mg	2.696	1.798	1.809	0.919	0.915	2.062	2.079
Ca	<MDL	0.02	0.02	0.733	0.726	0.408	0.407
Na	0.001	0.013	0.01	0.141	0.149	0.018	0.017
Ni	0.011	0.003	0.002	<MDL	0.002	<MDL	<MDL
Zn							
K							
Fe							
Cl							
Total:	4.509	4.016	4.016	4.014	4.019	8.03	8.025

Table C29 Major element chemistry of minerals from

Muskox websterite MOX3 74.42

Phase:	OL	OPX*	CPX*
Description:			
# Analyses Averaged:	4	3	5
SiO_2	40.84	57.38	55.44
TiO_2		0.11	0.17
Al_2O_3	<MDL	0.63	1.73
Cr_2O_3	<MDL	0.5	1.72
FeO	10.55	6.25	2.99
MnO	0.12	0.15	0.12
MgO	49.16	34.71	17.57
CaO	0.04	0.58	18.84
Na_2O		0.2	1.77
NiO	0.27	<MDL	<MDL
ZnO			
K20			
F			
Cl			
Total:	100.96	100.53	100.35
Si	0.995	1.972	1.993

Ti		0.003	0.005
Al	<MDL	0.025	0.073
Cr	<MDL	0.014	0.049
Fe(T)	0.215	0.18	0.09
Mn	0.002	0.004	0.004
Mg	1.785	1.778	0.941
Ca	0.001	0.022	0.725
Na		0.014	0.123
Ni	0.005	<MDL	<MDL
Zn			
K			
Fe			
Cl			
Total:	3.004	4.012	4.003

Table C30 Major element chemistry of minerals from

Muskox websterite MOX3 78.85A

Phase:	OL	OPX*
Description:		
# Analyses Averaged:	6	3

SiO_2	41.88	57.73
TiO_2		
Al_2O_3	<MDL	1.40
Cr_2O_3	<MDL	0.43
FeO	6.69	4.36
MnO	0.08	0.11
MgO	51.59	36.32
CaO	<MDL	0.47
Na_2O		<MDL
NiO	0.44	0.09
ZnO		
K20		
F		
Cl		
Total:	100.66	100.85
Si	1.005	1.958
Ti		0.000
Al	<MDL	0.056
Cr	<MDL	0.012
Fe(T)	0.134	0.124
Mn	0.001	0.003
Mg	1.845	1.837
Ca	<MDL	0.017
Na		<MDL
Ni	0.008	0.003
Zn		
K		
Fe		

Cl		
Total:	2.995	4.011

Table C31 Major element chemistry of minerals from

Muskox websterite MOX3 78.85B

Phase:	OL	OL	OPX*	CPX*	CPX
Description:	Grain 1	Grain 2		Grain 1	Grain 2
# Analyses Averaged:	4	2	4	2	3
SiO_2	40.95	41.4	57.65	55.1	55.47
TiO_2			0.12	0.25	0.24
Al_2O_3	<MDL	<MDL	0.6	1.89	1.62
Cr_2O_3	0.05	<MDL	0.45	2.25	1.73
FeO	10.32	9.07	6.12	3.14	3.27
MnO	0.15	0.12	0.14	0.11	0.13
MgO	48.51	49.4	34.84	16.56	17.3
CaO	0.04	0.04	0.53	18.47	18.77
Na_2O			0.17	2.13	1.9
NiO	0.27	0.39	0.07	<MDL	<MDL
ZnO					

K20					
F					
Cl					
Total:	100.23	100.41	100.61	99.91	100.43
Si	1.003	1.007	1.977	1.993	1.996
Ti			0.003	0.007	0.006
Al	<MDL	<MDL	0.024	0.081	0.069
Cr	0	<MDL	0.012	0.064	0.049
Fe(T)	0.211	0.184	0.176	0.095	0.098
Mn	0.003	0.003	0.004	0.003	0.004
Mg	1.772	1.79	1.781	0.893	0.927
Ca	0.001	0.001	0.02	0.716	0.724
Na			0.01	0.149	0.132
Ni	0.005	0.008	0.003	<MDL	<MDL
Zn					
K					
Fe					
Cl					
Total:	2.996	2.992	4.009	4.002	4.005

Table C32 Major element chemistry of minerals from

Muskox websterite MOX7 30.0

Phase:	OL	OPX*	CPX*
Description:			
# Analyses Averaged:	2	2	2
SiO_2	41.06	57.58	54.91
TiO_2		0.12	0.29
Al_2O_3	<MDL	0.54	1.89
Cr_2O_3	<MDL	0.4	1.9
FeO	10.02	5.84	3.19
MnO	0.14	0.14	0.12
MgO	49.14	35.22	16.85
CaO	<MDL	0.48	18.86
Na_2O		0.23	2.25
NiO	0.3	0.1	<MDL
ZnO			
K20			
F			
Cl			
Total:	100.66	100.6	100.26
Si	1	1.974	1.983
Ti		0.003	0.008
Al	<MDL	0.022	0.08
Cr	<MDL	0.011	0.054
Fe(T)	0.204	0.167	0.096
Mn	0.003	0.004	0.004
Mg	1.785	1.799	0.907
Ca	<MDL	0.018	0.73

Na		0.015	0.158
Ni	0.006	0.002	<MDL
Zn			
K			
Fe			
Cl			
Total:	2.998	4.015	4.020

Table C33 Major element chemistry of minerals from

Muskox websterite MOX7 54.0

Phase:	OPX*	OPX	CPX*	CPX
Description:	Grain 1	Grain 2	Grain 1	Grain 2
# Analyses Averaged:			3	2
SiO_2	57.57	57.61	54.71	55.19
TiO_2	0.07	0.12	0.16	0.27
Al_2O_3	0.68	0.55	1.76	1.78
Cr_2O_3	0.57	0.48	1.86	2.04
FeO	5.65	5.97	3.17	3.1
MnO	0.09	0.15	0.1	0.11

MgO	35.13	35.17	17.16	16.95
CaO	0.5	0.49	18.85	18.74
Na_2O	<MDL	0.2	1.87	2.09
NiO	0.17	0.09	<MDL	0.11
ZnO				
K20				
F				
Cl				
Total:	100.44	100.83	99.62	100.32
Si	1.973	1.972	1.985	1.989
Ti	0.002	0.003	0.004	0.007
Al	0.028	0.022	0.075	0.076
Cr	0.016	0.013	0.054	0.058
Fe(T)	0.162	0.171	0.096	0.094
Mn	0.003	0.004	0.003	0.003
Mg	1.795	1.794	0.928	0.911
Ca	0.018	0.018	0.733	0.724
Na	<MDL	0.014	0.132	0.146
Ni	0.005	0.003	<MDL	0.002
Zn				
K				
Fe				
Cl				
Total:	4.000	4.014	4.01	4.01

Table C34 Major element chemistry of minerals from

Muskox websterite MOX11 122.2

Phase:	OPX*	CPX*	GAR	GAR*
Description:		C=R	Grain 1 R	Grain 2 C=R
# Analyses Averaged:	2	11		7
SiO_2	57.36	54.64	41.05	40.6
TiO_2	0.1	0.23		
Al_2O_3	0.57	1.86	18.84	17.25
Cr_2O_3	0.44	2.39	5.95	7.56
FeO	5.93	3.17	8.81	8.89
MnO	0.13	0.11	0.38	0.4
MgO	35.14	16.71	19.16	18.43
CaO	0.55	18.43	5.17	6
Na_2O	0.17	2.26	<MDL	0.18
NiO	<MDL	0.09	<MDL	<MDL
ZnO				
K20				
F				
Cl				
Total:	100.39	99.81	99.38	99.19
Si	1.971	1.982	2.998	2.999
Ti	0.003	0.006		
Al	0.023	0.079	1.622	1.502

Cr	0.012	0.069	0.344	0.441
Fe(T)	0.17	0.096	0.538	0.549
Mn	0.004	0.003	0.024	0.025
Mg	1.799	0.904	2.085	2.029
Ca	0.02	0.716	0.405	0.475
Na	0.011	0.159	<MDL	0.015
Ni	<MDL	0.002	<MDL	<MDL
Zn				
K				
Fe				
Cl				
Total:	4.013	4.017	8.016	8.036

Table C35 Major element chemistry of minerals from

Muskox websterite MOX11 200.5A

Phase:	OL*	OPX*	CPX*	GAR*
Description:				
# Analyses Averaged:	3	3	3	4
SiO_2	40.72	57.77	54.97	40.58
TiO_2		0.11	0.24	

Al_2O_3	<MDL	0.64	1.63	17.14
Cr_2O_3	<MDL	0.58	2.09	7.42
FeO	10.24	5.9	3.07	9.29
MnO	0.1	0.15	0.14	0.44
MgO	49.01	35.05	16.91	18.09
CaO	<MDL	0.52	18.88	6.02
Na_2O		0.15	2.11	0.13
NiO	0.24	0.12	<MDL	<MDL
ZnO				
K20				
F				
Cl				
Total:	100.28	100.96	99.98	99.03
Si	0.997	1.974	1.989	3.007
Ti		0.003	0.007	
Al	<MDL	0.026	0.07	1.497
Cr	<MDL	0.016	0.06	0.435
Fe(T)	0.21	0.169	0.093	0.576
Mn	0.002	0.004	0.003	0.028
Mg	1.789	1.785	0.912	1.999
Ca	<MDL	0.019	0.732	0.478
Na		0.01	0.148	0.012
Ni	0.005	0.003	<MDL	<MDL
Zn				
K				
Fe				
Cl				
Total:	3.002	4.008	4.013	8.031

Table C36 Major element chemistry of minerals from

Muskox websterite MOX11 287.67

Phase:	OL	CPX*	GAR*	GAR
Description:			Grain 1	Grain 2
# Analyses Averaged:	4	3	2	2
SiO_2	40.13	54.74	40.79	40.28
TiO_2		0.21		
Al_2O_3	<MDL	1.97	21.14	20.39
Cr_2O_3	0.05	0.85	2.46	3.02
FeO	12.08	3.14	10.15	10.6
MnO	0.18	0.1	0.55	0.57
MgO	47.77	16.27	16.79	16.52
CaO	0.04	21.24	7.24	7.61
Na_2O		1.65	<MDL	<MDL
NiO	0.14	0.03	<MDL	<MDL
ZnO				
K20				
F				
Cl				

Total:	100.34	100.2	99.13	98.97
Si	0.991	1.983	2.991	2.977
Ti		0.006		
Al	<MDL	0.084	1.826	1.776
Cr	0	0.024	0.142	0.176
Fe(T)	0.25	0.095	0.623	0.655
Mn	0.004	0.003	0.034	0.036
Mg	1.759	0.878	1.835	1.82
Ca	0.001	0.824	0.569	0.603
Na		0.116	<MDL	<MDL
Ni	0.003	0.001	<MDL	<MDL
Zn				
K				
Fe				
Cl				
Total:	3.008	4.015	8.02	8.043

Table C37 Major element chemistry of minerals from

Muskox websterite MOX24 42.6

Phase:	OL*	OPX*	OPX	CPX	CPX*	GAR*	GAR

Description:	C	Grain 1 C	Grain 2 W/L	L	C=R	Grain 1 C=R	Grain 2 C=R
# Analyses Averaged:			2		3	2	3
SiO_2	41.05	57.12	57.87	54.32	55.03	40.99	40.61
TiO_2		0.11	0.15	0.26	0.3		
Al_2O_3	<MDL	0.73	0.55	2.05	2.13	19.08	17.85
Cr_2O_3	<MDL	0.63	0.32	2.24	1.64	5.05	6.59
FeO	11.64	6.09	6.61	3.48	3.59	10.03	9.86
MnO	0.12	0.17	0.18	0.08	0.11	0.39	0.47
MgO	48.32	34.87	34.43	16.28	16.83	18.68	18.35
CaO	0.05	0.53	0.59	18.26	18.41	5.16	5.58
Na_2O		0.21	<MDL	2.41	2.11	0.12	0.08
NiO	0.21	0.09	0.06	0.03	0.05	0.02	0.01
ZnO							
K20							
F							
Cl							
Total:	101.39	100.55	100.82	99.4	100.2	99.52	99.41
Si	1	1.965	1.984	1.982	1.987	3.001	2.996
Ti		0.003	0.004	0.007	0.008		
Al	<MDL	0.03	0.022	0.088	0.091	1.647	1.552
Cr	<MDL	0.017	0.009	0.065	0.047	0.292	0.385
Fe(T)	0.237	0.175	0.19	0.106	0.108	0.614	0.608
Mn	0.003	0.005	0.005	0.002	0.003	0.024	0.03
Mg	1.755	1.788	1.76	0.885	0.906	2.038	2.018
Ca	0.001	0.02	0.022	0.714	0.712	0.405	0.441
Na		0.014	<MDL	0.171	0.147	0.017	0.012
Ni	0.004	0.003	0.002	0.001	0.002	0.001	0.001
Zn							
K							
Fe							

Cl							
Total:	3.000	4.019	4.001	4.021	4.012	8.038	8.042

Table C38 Major element chemistry of minerals from

Muskox websterite MOX24 43.35

Phase:	OPX *	OPX	CPX*	GAR*	GAR
Description:	R	C		Grain 1 C=R	Grain 2 C=R
# Analyses Averaged:	3			2	4
SiO_2	57.8	58.24	55.14	40.73	41.07
TiO_2	0.14		0.25		
Al_2O_3	0.57	0.74	1.73	17.75	18.73
Cr_2O_3	0.38	0.57	1.86	7.24	5.83
FeO	6.02	5.72	3.36	8.84	9.12
MnO	0.12	0.1	0.14	0.42	0.46
MgO	35.04	34.57	17.07	18.92	19.06
CaO	0.53	0.63	19.03	5.21	5.31
Na_2O	0.19	<MDL	1.88	<MDL	<MDL
NiO	0.12	0.12	<MDL	<MDL	<MDL
ZnO					
K20					

F					
Cl					
Total:	100.68	100.69	100.5	99.11	99.57
Si	1.979	1.99	1.987	2.998	2.999
Ti	0.004		0.007		
Al	0.023	0.03	0.074	1.54	1.612
Cr	0.01	0.015	0.053	0.421	0.336
Fe(T)	0.172	0.164	0.101	0.544	0.557
Mn	0.003	0.003	0.004	0.026	0.028
Mg	1.788	1.76	0.917	2.076	2.074
Ca	0.019	0.023	0.735	0.411	0.415
Na	0.008		0.131	<MDL	<MDL
Ni	0.002	0.003	<MDL	<MDL	<MDL
Zn					
K					
Fe					
Cl					
Total:	4.006	3.988	4.011	8.017	8.021

Table C39 Major element chemistry of minerals from

Muskox websterite MOX24 105.2

Phase:	OPX*	CPX*
Description:		
# Analyses Averaged:		2
SiO_2	57.84	55.46
TiO_2	0.12	0.22
Al_2O_3	0.54	1.78
Cr_2O_3	0.29	1.82
FeO	6.09	3.16
MnO	0.13	0.09
MgO	34.75	17.18
CaO	0.53	18.59
Na_2O	0.15	1.93
NiO	0.1	<MDL
ZnO		
K20		
F		
Cl		
Total:	100.52	100.23
Si	1.984	1.996
Ti	0.003	0.006
Al	0.022	0.076
Cr	0.008	0.052
Fe(T)	0.175	0.095
Mn	0.004	0.003
Mg	1.777	0.922
Ca	0.02	0.717
Na	0.01	0.134

Ni	0.003	<MDL
Zn		
K		
Fe		
Cl		
Total:	4.003	4.000

Table C40 Major element chemistry of minerals from

Muskox websterite MOX24 206.73

Phase:	OPX*	CPX*	GAR*	GAR
Description:			Grain 1	Grain 2
# Analyses Averaged:	3	4		
SiO_2	57.38	55.09	41.17	39.88
TiO_2	0.13	0.25		
Al_2O_3	0.5	1.88	18.32	16.69
Cr_2O_3	0.36	1.37	7.04	7.75
FeO	6.06	3.3	9.15	9.07
MnO	0.17	0.09	0.4	0.49
MgO	35.05	17.08	18.92	17.61
CaO	0.62	19.11	5.24	5.89

Na_2O	0.23	1.8	<MDL	<MDL
NiO	0.1	<MDL	<MDL	<MDL
ZnO				
K20				
F				
Cl				
Total:	100.6	99.94	100.24	97.39
Si	1.972	1.991	2.996	3.008
Ti	0.003	0.007		
Al	0.02	0.08	1.571	1.483
Cr	0.01	0.039	0.405	0.462
Fe(T)	0.174	0.1	0.557	0.572
Mn	0.005	0.002	0.025	0.031
Mg	1.795	0.92	2.052	1.98
Ca	0.023	0.74	0.408	0.476
Na	0.016	0.126	<MDL	<MDL
Ni	0.003	<MDL	<MDL	<MDL
Zn				
K				
Fe				
Cl				
Total:	4.021	4.006	8.014	8.013

Table C41 Major element chemistry of minerals from

Muskox websterite MOX24 240.0

Phase:	OL*	OL	OPX*	CPX*	GAR*
Description:	Grain 1	Grain 2			
# Analyses Averaged:		3	2	2	2
SiO_2	41.23	41.04	56.51	54.16	40.7
TiO_2			0.12	0.17	
Al_2O_3	<MDL	<MDL	0.54	1.65	18.46
Cr_2O_3	<MDL	<MDL	0.34	1.66	5.83
FeO	7.18	8.22	6.18	2.93	9.15
MnO	0.08	0.09	0.16	0.1	0.42
MgO	52	50.8	35.02	17.68	18.72
CaO	<MDL	<MDL	0.57	18.89	5.38
Na_2O			0.18	1.69	0.17
NiO	0.37	0.39	0.09	<MDL	<MDL
ZnO					
K20					
F					
Cl					
Total:	100.87	100.53	99.66	98.92	98.83
Si	0.991	0.994	1.962	1.979	3
Ti			0.003	0.005	
Al	<MDL	<MDL	0.022	0.071	1.604
Cr	<MDL	<MDL	0.009	0.048	0.34

Fe(T)	0.144	0.167	0.18	0.09	0.564
Mn	0.002	0.002	0.005	0.003	0.026
Mg	1.863	1.835	1.812	0.963	2.057
Ca	<MDL	<MDL	0.021	0.74	0.425
Na			0.012	0.119	0.025
Ni	0.007	0.008	0.003	<MDL	<MDL
Zn					
K					
Fe					
Cl					
Total:	3.008	3.005	4.029	4.017	8.04

Table C42 Major element chemistry of minerals from

Muskox websterite MOX24 255.45

Phase:	OL	OL	CPX*	GAR*
Description:	Grain 1	Grain 2		
# Analyses Averaged:	2	4	4	3
SiO_2	39.98	40.76	54.99	41.09
TiO_2			0.25	

Al_2O_3	<MDL	<MDL	1.94	19.73
Cr_2O_3	<MDL	0.07	1.53	4.39
FeO	10.99	8.26	3.55	9.41
MnO	0.15	0.1	0.13	0.42
MgO	48.59	50.86	16.99	18.88
CaO	0.03	0.04	18.88	5.27
Na_2O			1.9	<MDL
NiO	0.2	0.42	0.04	<MDL
ZnO				
K20				
F				
Cl				
Total:	99.93	100.44	100.19	99.2
Si	0.988	0.99	1.986	3
Ti			0.007	
Al	<MDL	<MDL	0.083	1.698
Cr	<MDL	0.001	0.044	0.254
Fe(T)	0.227	0.168	0.107	0.574
Mn	0.003	0.002	0.004	0.026
Mg	1.789	1.841	0.915	2.055
Ca	0.001	0.001	0.731	0.412
Na			0.133	<MDL
Ni	0.004	0.008	0.001	<MDL
Zn				
K				
Fe				
Cl				
Total:	3.011	3.01	4.01	8.02

Table C43 Major element chemistry of minerals from of

Muskox websterite MOX25 120.6A

Phase:	OL	OPX*	CPX
Description:			
# Analyses Averaged:	4	3	6
SiO_2	40.44	57.74	54.81
TiO_2		0.12	0.27
Al_2O_3	<MDL	0.4	1.77
Cr_2O_3	<MDL	0.15	1.3
FeO	11.47	6.9	3.66
MnO	0.14	0.19	0.16
MgO	48.2	34.58	16.76
CaO	0.03	0.54	18.74
Na_2O		0.13	1.91
NiO	0.24	0.09	0.03
ZnO			
K20			
F			
Cl			

Total:	100.51	100.76	99.41
Si	0.994	1.982	1.995
Ti		0.003	0.007
Al	<MDL	0.016	0.076
Cr	<MDL	0.004	0.037
Fe(T)	0.236	0.198	0.112
Mn	0.003	0.006	0.005
Mg	1.766	1.769	0.909
Ca	0.001	0.02	0.731
Na		0.008	0.135
Ni	0.005	0.003	0.001
Zn			
K			
Fe			
Cl			
Total:	3.005	4.004	4.008

Table C44 Major element chemistry of minerals from

Muskox websterite MOX25 161.5C

Phase:	OL	OL	OPX*	CPX*
Description:	Grain 1	Grain 2		
# Analyses Averaged:				4
SiO_2	41.14	41.39	58.43	54.93
TiO_2			0.12	0.22
Al_2O_3	<MDL	<MDL	0.56	1.71
Cr_2O_3	<MDL	<MDL	0.36	1.92
FeO	11.92	9.92	5.94	3.08
MnO	0.14	0.13	0.12	0.12
MgO	48.03	49.29	35.02	17.37
CaO	0.03	<MDL	0.57	18.69
Na_2O				1.9
NiO	0.18	0.35	0.09	
ZnO				
K20				
F				
Cl				
Total:	101.44	101.09	101.21	99.94
Si	1.002	1.003	1.987	1.986
Ti			0.003	0.005
Al	0	0	0.022	0.072
Cr	0	0	0.009	0.054
Fe(T)	0.242	0.201	0.168	0.093
Mn	0.002	0.002	0.003	0.003
Mg	1.744	1.781	1.775	0.936
Ca	0	<MDL	0.02	0.723
Na			0.007	0.133
Ni	0.004	0.0068	0.003	0.001

Zn				
K				
Fe				
Cl				
Total:	2.997	2.996	4	4.012

Table C45 Major element chemistry of minerals from

Muskox websterite MOX25 246.19

Phase:	OL	CPX*	GAR*
Description:			
# Analyses Averaged:	4	4	2
SiO_2	41.19	55.14	41.56
TiO_2	<MDL	0.24	
Al_2O_3	<MDL	1.83	19.37
Cr_2O_3	0.05	1.86	5.37
FeO	9.9	3.15	8.96
MnO	0.1	0.11	0.42
MgO	48.71	17.04	19.22
CaO	0.03	18.65	5.23
Na_2O	<MDL	2	

NiO	0.32		
ZnO			
K20			
F			
Cl			
Total:	100.28	100.02	100.14
Si	1.006	1.991	3.006
Ti		0.007	
Al	0	0.078	1.651
Cr	0.001	0.053	0.307
Fe(T)	0.202	0.095	0.542
Mn	0.002	0.003	0.026
Mg	1.774	0.917	2.072
Ca	0.001	0.722	0.405
Na	<MDL	0.14	0.013
Ni	0.006	0.001	0.001
Zn			
K			
Fe			
Cl			
Total:	2.993	4.008	8.022

Table C46 Major element chemistry of minerals from

Muskox websterite MOX31 230.74

Phase:	OL*	OL	OPX*	CPX*	GAR*
Description:	Grain 1	Grain 2			
# Analyses Averaged:	4	2	2	3	4
SiO_2	40.09	40.92	56.88	53.62	41.23
TiO_2			0.12	0.27	
Al_2O_3	<MDL	<MDL	0.57	2.02	20.01
Cr_2O_3	<MDL	<MDL	0.4	1.6	4.35
FeO	10.72	8.7	6.41	3.36	9.68
MnO	0.12	0.13	0.12	0.13	0.45
MgO	48.82	50.51	34.76	16.95	18.99
CaO	0.05	<MDL	0.54	18.71	5.02
Na_2O			0.16	1.96	0.14
NiO	0.37	0.38	0.1	<MDL	<MDL
ZnO					
K20					
F					
Cl					
Total:	100.14	100.64	99.92	98.62	99.78
Si	0.987	0.993	1.968	1.971	2.994
Ti			0.003	0.007	
Al	<MDL	<MDL	0.023	0.088	1.713
Cr	<MDL	<MDL	0.011	0.046	0.25
Fe(T)	0.221	0.177	0.186	0.103	0.588

Mn	0.003	0.003	0.004	0.004	0.028
Mg	1.792	1.827	1.793	0.928	2.056
Ca	0.001	<MDL	0.02	0.737	0.391
Na			0.009	0.14	0.012
Ni	0.007	0.007	0.003	0.002	<MDL
Zn					
K					
Fe					
Cl					
Total:	3.011	3.006	4.019	4.026	8.03

Table C47 Major element chemistry of minerals from

Muskox websterite MOX31 242.5

Phase:	OL	OPX*	CPX*
Description:			
# Analyses Averaged:	5	4	2
SiO_2	40.11	56.71	53.47
TiO_2		0.14	0.28
Al_2O_3	<MDL	0.52	1.83
Cr_2O_3	<MDL	0.34	1.56

FeO	11	6.29	3.42
MnO	0.15	0.15	0.12
MgO	48.74	35.19	17.11
CaO	0.04	0.55	18.95
Na_2O		0.18	1.93
NiO	0.28	0.1	<MDL
ZnO			
K20			
F			
Cl			
Total:	100.3	100.09	98.67
Si	0.987	1.96	1.967
Ti		0.004	0.008
Al	0	0.021	0.079
Cr	0	0.009	0.045
Fe(T)	0.226	0.182	0.105
Mn	0.003	0.004	0.004
Mg	1.788	1.813	0.938
Ca	0.001	0.02	0.747
Na		0.012	0.138
Ni	0.006	0.002	<MDL
Zn			
K			
Fe			
Cl			
Total:	3.012	4.029	4.032

Table C48 Major element chemistry of minerals from

Muskox websterite MOX31 242.6

Phase:	OPX*	CPX*	ILM
Description:			
# Analyses Averaged:	3	3	3
SiO_2	57.78	54.86	<MDL
TiO_2	0.13	0.23	52.28
Al_2O_3	0.54	1.79	0.15
Cr_2O_3	0.24	1.43	2.58
FeO	6.23	3.38	31.16
MnO	0.14	0.15	0.27
MgO	34.86	17.24	12.65
CaO	0.63	18.73	<MDL
Na_2O	0.16	1.7	
NiO	0.1	<MDL	0.12
ZnO			<MDL
K20			
F			
Cl			
Total:	100.8	99.51	99.22
Si	1.979	1.991	0.001

Ti	0.003	0.006	1.235
Al	0.022	0.077	0.005
Cr	0.007	0.041	0.064
Fe(T)	0.178	0.103	0.819
Mn	0.004	0.004	0.007
Mg	1.78	0.933	0.593
Ca	0.023	0.728	0.001
Na	0.011	0.12	
Ni	0.003	<MDL	0.003
Zn			0.001
K			
Fe			
Cl			
Total:	4.009	4.003	2.729

Table C49 Major element chemistry of minerals from

Muskox websterite MOX31 281.2

Phase:	OL*	OPX*	CPX*	GAR*
Description:				
# Analyses Averaged:		3	5	

SiO_2	41.21	57.37	55.37	41.62
TiO_2		0.11	0.27	
Al_2O_3	<MDL	0.66	1.94	19.41
Cr_2O_3	0.05	0.5	1.6	4.78
FeO	8.5	6.05	3.27	9.24
MnO	0.08	0.14	0.11	0.41
MgO	50.42	34.78	17.11	19.3
CaO	0.06	0.61	18.61	5.06
Na_2O		0.22	1.98	<MDL
NiO	0.44	0.1	<MDL	<MDL
ZnO				
K20				
F				
Cl				
Total:	100.75	100.51	100.25	99.83
Si	0.998	1.972	1.993	3.017
Ti		0.003	0.007	
Al	<MDL	0.027	0.082	1.658
Cr	0.001	0.014	0.045	0.274
Fe(T)	0.172	0.174	0.099	0.56
Mn	0.002	0.004	0.003	0.025
Mg	1.819	1.782	0.918	2.085
Ca	0.002	0.022	0.718	0.393
Na		0.015	0.138	<MDL
Ni	0.009	0.003	<MDL	<MDL
Zn				
K				
Fe				

Cl				
Total:	3.002	4.015	4.005	8.013

Table C50 Major element chemistry of minerals from

Muskox orthopyroxenite MOX1 48.6

Phase:	OL	OPX*	CPX*
Description:			
# Analyses Averaged:	2	3	1
SiO_2	41.03	56.85	53.78
TiO_2		0.06	0.29
Al_2O_3	<MDL	0.67	1.87
Cr_2O_3	<MDL	0.89	1.85
FeO	7.84	5.4	3.23
MnO	0.09	0.15	0.14
MgO	51.08	34.91	16.96
CaO	<MDL	0.92	18.51
Na_2O		0.2	1.84
NiO	0.39	0.09	<MDL
ZnO			
K20			
F			
Cl			
Total:	100.39	100.09	98.48
Si	0.994	1.962	1.977

Ti		0.002	0.008	
Al	<MDL	0.027	0.081	
Cr	<MDL	0.024	0.054	
Fe(T)	0.159	0.156	0.099	
Mn	0.001	0.005	0.005	
Mg	1.844	1.796	0.929	
Ca	<MDL	0.034	0.729	
Na		0.014	0.131	
Ni	0.008	0.003	<MDL	
Zn				
K				
Fe				
Cl				
Total:	3.006	4.02	4.013	

Table C51 Major element chemistry of minerals from

Muskox orthopyroxenite MOX24 31.1B

Phase:	OPX	OPX*	CPX*	GAR*

Description:	Grain 1	Grain 2		
# Analyses Averaged:		7	5	4
SiO_2	57.36	57.79	55.1	40.72
TiO_2	0.06	0.14	0.26	
Al_2O_3	0.82	0.5	1.83	17.3
Cr_2O_3	1.04	0.31	2.16	7.32
FeO	5.45	5.77	3.13	8.83
MnO	0.11	0.13	0.13	0.43
MgO	33.97	35.15	16.82	18.39
CaO	1.01	0.52	18.4	5.66
Na_2O	0.24	0.14	2.08	<MDL
NiO	0.11	0.11	<MDL	<MDL
ZnO				
K20				
F				
Cl				
Total:	100.16	100.46	99.89	98.67
Si	1.976	1.98	1.992	3.016
Ti	0.002	0.004	0.007	
Al	0.033	0.02	0.078	1.51
Cr	0.028	0.008	0.062	0.429
Fe(T)	0.157	0.165	0.095	0.547
Mn	0.003	0.004	0.004	0.027
Mg	1.744	1.795	0.907	2.03
Ca	0.037	0.019	0.713	0.449
Na	0.016	0.009	0.145	<MDL
Ni	0.003	0.003		<MDL
Zn				

K				
Fe				
Cl				
Total:	4	4.002	4.002	8.00895

Table C52 Major element chemistry of minerals from

Muskox orthopyroxenite MOX25 120.6B

Phase:	OPX*	OPX	OPX
Description:	Grain 1	Grain 2 C	Grain 3
# Analyses Averaged:			2
SiO_2	57.2	57.15	56.25
TiO_2	<MDL	0.06	0.09
Al_2O_3	0.61	0.83	1.28
Cr_2O_3	0.85	0.77	1.29
FeO	5.37	5.27	5.43
MnO	0.11	0.17	0.13
MgO	34.8	34.28	33.48
CaO	1.02	0.79	1.21
Na_2O	0.26	0.32	0.36
NiO	0.15	0.13	0.12

ZnO			
K20			
F			
Cl			
Total:	100.35	99.76	99.64
Si	1.967	1.974	1.954
Ti	0.001	0.002	0.002
Al	0.025	0.034	0.052
Cr	0.023	0.021	0.035
Fe(T)	0.154	0.152	0.158
Mn	0.003	0.005	0.004
Mg	1.784	1.765	1.733
Ca	0.038	0.029	0.045
Na	0.017	0.022	0.024
Ni	0.004	0.004	0.003
Zn			
K			
Fe			
Cl			
Total:	4.016	4.007	4.012

Table C53 Major element chemistry of minerals from

Muskox orthopyroxenite MOX28 269.6

Phase:	OPX*	CPX*
Description:		
# Analyses Averaged:	3	3
SiO_2	57.58	54.66
TiO_2	0.08	0.27
Al_2O_3	0.78	1.88
Cr_2O_3	0.76	1.29
FeO	5.54	3.42
MnO	0.14	0.11
MgO	34.72	16.93
CaO	0.88	19.71
Na_2O	0.16	1.8
NiO	0.12	0.09
ZnO		
K20		
F		
Cl		
Total:	100.69	100.1
Si	1.972	1.98
Ti	0.002	0.007
Al	0.031	0.08
Cr	0.021	0.037
Fe(T)	0.159	0.103
Mn	0.004	0.003

Mg	1.772	0.914
Ca	0.032	0.765
Na	0.011	0.127
Ni	0.002	0.002
Zn		
K		
Fe		
Cl		
Total:	4.006	4.018